Title
Rules of Engagement Enabling Leukocyte Rolling and Adhesion: An In Silico Model Study

Permalink
https://escholarship.org/uc/item/9238m4j8

Author
Tang, Jonathan

Publication Date
2010

Peer reviewed|Thesis/dissertation

Rules of Engagement Enabling Leukocyte Rolling and Adhesion:
An In Silico Model Study

By

Jonathan Tang

A dissertation submitted in partial satisfaction of the

requirements for the degree of

Joint Doctor of Philosophy
With University of California, San Francisco

In

Bioengineering

in the

Graduate Division

of the

University of California, Berkeley

Committee in charge:

Professor C. Anthony Hunt, Chair
Professor Robert C. Spear
Professor Donna Hudson
Professor Lee Schruben

Spring 2010

Rules of Engagement Enabling Leukocyte Rolling and Adhesion:
An In Silico Model Study

Copyright 2010

by

Jonathan Tang

Abstract

Rules of Engagement Enabling Leukocyte Rolling and Adhesion:
An In Silico Model Study

by

Jonathan Tang

Joint Doctor of Philosophy with University of California, San Francisco

in Bioengineering

University of California, Berkeley

Professor C. Anthony Hunt, Chair

Rolling, activation, and adhesion on endothelial surfaces are necessary steps for the proper recruitment of leukocytes from circulating blood to sites of inflammation. Once at the target site, leukocytes help destroy pathogens and decompose damaged tissue. Inflammatory mechanisms, when uncontrolled, are also associated with diseases such as asthma, rheumatoid arthritis, and atherosclerosis. Improved therapeutics can be developed with a better understanding of the molecular-level events that mediate this process.

This dissertation reports the development of a synthetic, in silico model for use as an experimental system for testing the plausibility of mechanistic hypotheses of how molecular components may interact to cause leukocyte behaviors during rolling, activation, and adhesion to endothelial surfaces. Object-oriented software components were designed, instantiated, verified, plugged together, and then operated in ways that can map concretely to mechanisms and processes believed responsible for leukocyte rolling, activation, and adhesion. The result is an in silico analogue of the wet-lab experimental systems to study leukocyte rolling and adhesion; the experimentally measured phenotypic attributes of the analogue can be compared and contrasted to those of leukocytes from the referent systems.

We first demonstrate that the in silico devices can generate behaviors similar to those observed in vitro at the cell-level and population-level, by comparing simulation results with data from three different in vitro experimental conditions. The validated model was then used to test the hypothesized mechanism of LFA-1 integrin clustering in adhesion. The in silico device showed that clustering was not necessary to achieve adhesion as long as densities of LFA-1 and its ligand ICAM-1 were above a critical level. Importantly, at low densities LFA-1 clustering enabled improved efficiency: adhesion exhibited measurable, cell level positive cooperativity.

Our results provide convincing evidence for the feasibility of using synthetic in silico systems to improve our understanding of the molecular- and cellular-level events mediating leukocyte rolling, activation, and adhesion during inflammation. This work represents early, but important advances for future in silico research into plausible causal links between molecular-level events and the variety of systems-level behaviors that distinguish normal leukocyte adhesion from disease-associated adhesion.

Table of Contents

List of Figures

List of Tables

List of Abbreviations

CVS	Concurrent Versions Systems
CXCL1	CXC Chemokine Ligand 1
CXCR-2	CXC Chemokine Receptor 2
FRET	Fluorescence resonance energy transfer
GFP	Green Fluorescent Protein
GRO-α	Human CXCL1
ICAM-1	Intercellular adhesion molecule 1 (CD54)
ISWBC	In silico white blood cell
KC	Murine CXCL1
KO	Knockout
LFA-1	Lymphocyte function associated antigen-1 ($\alpha_L\beta_2$, CD11a/CD18)
Mac-1	Macrophage antigen 1, ($\alpha_M\beta_2$, CD11b/CD18)
PI3K	Phosphoinositide 3-kinase
PI3Kγ	Class IB Phosphoinositide 3-kinase
PI3Kγ-/-	Class IB Phosphoinositide 3-kinase Knockout
PMA	Phorbol myristate acetate
PSGL-1	P-selectin glycoprotein ligand 1
VCAM-1	Vascular cell adhesion molecule 1
VLA-4	Very late antigen 4 ($\alpha_4\beta_1$, CD49d/CD29)
WT	Wild type

Acknowledgements

There are many people I would like to acknowledge for their contribution to this work. I would like to first thank my advisor, Tony Hunt, for giving me the freedom to independently explore and develop my own research project, while at the same time providing crucial intellectual support when it was needed. In addition to Tony, many other faculty, grad students, and postdocs of the UC Berkeley and UC San Francisco communities have provided help and guidance with my PhD. Specifically, I would like to express my gratitude to the members of my dissertation committee, Robert Spear, Donna Hudson, and Lee Schruben for their invaluable assistance in reviewing the proposals and drafts that led up to this final dissertation. A special thanks goes to Glen Ropella, Jesse Engelberg, Sean Kim, Sunwoo Park, Mark Grant, Amina Qutub, and other current and former members of the Biosystems Lab. They have been of tremendous help in covering many technical and theoretical issues. This dissertation would not have been possible without their help.

I am truly grateful for my family. My parents, Jerry and Kitty, have always been supportive throughout my academic career. My older brother, Ken, has offered me never-ending encouragement and moral support. I cannot imagine completing this degree without their guidance and support.

My gratitude also goes out to all my friends who were near me during all these years. I would especially like to thank Jeffrey Jacobi who has been there supporting me, comforting me, cheering for me, in happy and in the most stressful times.

1. Introduction

Rolling, activation, and adhesion are necessary steps for the proper recruitment of leukocytes from the circulating blood to a site of inflammation. Once at the target site, leukocytes help to destroy pathogens and decompose damaged tissue from wounds. However, inflammatory mechanisms are also associated with diseases such as asthma, rheumatoid arthritis, multiple sclerosis, and atherosclerosis. Such diseases can be characterized by inappropriate leukocyte recruitment and the misdirected actions of leukocytes towards healthy host-tissue [1]. Discovery of new and improved therapeutics will be facilitated by having a better understanding of how this process works and by being able to predict the consequences of interventions. Making such predictions requires having a model with a large, explorable behavior space. Traditional mathematical models are insufficient for the task.

Leukocyte adhesion has been studied experimentally in vivo using intravital microscopy of animal tissue, as well as in vitro and ex vivo using flow chamber assays, which has helped to uncover many of the components and basic mechanisms involved. However, it has become evident that the interactions between leukocytes and endothelial cells during rolling, activation, and adhesion exhibit a number of properties of complex biological systems. It involves a cascade of molecular, mechanical, and biochemical signaling events that are spatially and temporally coordinated [2, 3]. This complexity, along with the current limitations in available experimental techniques to visualize the dynamics of in vivo tissues with sub-cellular resolution, has greatly hindered progress towards understanding this process in its entirety. This further merits the use of new models to help understand the underlying mechanisms mediating this process.

A goal in systems biology research is to understand linkages from molecular level events to system phenotype: link genotype to phenotype. That task requires having plausible, adequately detailed design plans for how components (single and composite) at various system levels are thought to fit and function together. Ideas about such plans can be induced from the results of experiments. Experimentation is then used to reconcile different design plan hypotheses. More is needed, however, to actually demonstrate that a design plan is functionally plausible, which is very different than demonstrating that it is consistent with measured behaviors. The former requires that one assemble individual components according to a design, and then show that the constructed device, an analogue—on its own—exhibits behaviors that match those observed in the original experiment. Building such analogues in silico is now feasible. To make it practicable, we need multilevel modeling and simulation methods that make it easy to test, reject, and refine many candidate design plans.

This dissertation describes the development and usage of a new class of models that can meet those needs. Using the synthetic modeling approach, we have developed a novel in silico model that can be used as an experimental system for testing hypothesized design plans of the molecular-level events that mediate leukocyte rolling, activation, and adhesion. In this work, we focus on the possible role of LFA-1 clustering events on the leukocyte membrane and spatial configurations of its ligand, ICAM-1, on the endothelial surface during rolling, activation, and adhesion. How important could these hypothesized mechanisms be for leukocyte adhesion? Answers to this question will help us to gain a better understanding of the spatiotemporal events and key rules of engagement that may determine when and how leukocytes are able to adhere to endothelial cell surfaces during inflammatory conditions.

1.1 Leukocyte Rolling, Activation, and Adhesion

The initial interactions between leukocytes and endothelial surfaces are primarily mediated by the selectin family of receptors, consisting of L-selectin, P-selectin, and E-selectin. P-selectin is largely responsible for leukocyte rolling, and is expressed on the surface of inflamed endothelial cells. All three selectins bind to glycosylated carbohydrates, with PSGL-1 being the predominant ligand for all three selectins. These selectin-ligand interactions are transient, which can be attributed to their fast rates of bond formation and dissociation, and thus enables the leukocyte to roll along the endothelium as it experiences shear from the blood flow in the venules [3].

The transition from rolling to adhesion is exclusively mediated by the integrin receptors. They are a family of heterodimeric molecules consisting of an α and a β subunit, that can exist in multiple molecular conformational states each having different ligand binding properties. So far, a low-, an intermediate-, and a high-affinity state have been identified. When in their high-affinity conformation state, integrin bonds can enable the leukocytes to resist the force from the blood flow and firmly adhere to the vessel wall or flow chamber surface [4]. In addition, clustering of integrins on the membrane is thought to help increase adhesion under certain conditions. Natively, these integrins exist in non-adhesive, low-affinity states to prevent leukocytes from sticking non-specifically to blood vessels. As leukocytes roll along the venular surface, their chemokine receptors can detect immobilized chemokines, such as CXCL1, on activated endothelial cells. Upon detection, intracellular signaling events can trigger these conformational changes. Engagement of selectins and some integrins have also been shown to initiate various activation signals that enhance adhesion [5, 6].
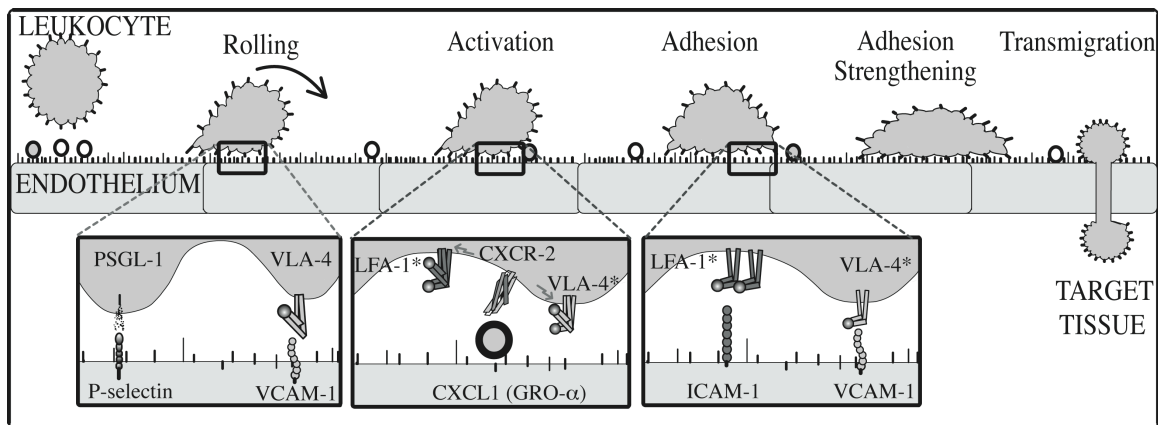
Figure 1.1. The relevant receptor-ligand pairs during leukocyte rolling, activation, and adhesion on inflamed murine cremaster muscle venules. The selectin family of receptors mediates the initial rolling interactions. The most important is P-selectin, which bind to carbohydrate ligands, such as PSGL-1. VLA-4 and LFA-1 are the predominant integrins involved in initial adhesion. VLA-4, unique among the integrins, in its low affinity state can also support rolling interactions. Upon detection of chemokine, integrins undergo conformational changes, such that they are able to form strong high-affinity bonds with their ligands. LFA-1 integrin might also undergo clustering events. After the leukocyte polarizes, it crawls toward a site of transmigration and through the endothelial layer [3]. Integrins labeled with asterisks, as in LFA-1* and VLA-4*, indicate integrins in a high-affinity conformational state.

The low-, intermediate-, and high-affinity integrins most likely represent discrete states in a continuum of integrin conformational changes. It is observed that leukocyte activation by chemokines only induces a small fraction of integrins to change conformational states. Therefore, even though the average affinity of an integrin population may increase, the individual integrins assume a range of conformations at any time [3].

The major integrins for leukocyte rolling and adhesion are $\alpha_4\beta_1$ (VLA-4), $\alpha_L\beta_2$ (lymphocyte function associated antigen-1, LFA-1), and $\alpha_M\beta_2$ (Mac-1). The cellular adhesion molecule VCAM-1 is the major ligand for VLA-4, while ICAM-1 is the major ligand for LFA-1 and Mac-1. The integrins primarily mediate adhesion, however some can also participate in rolling. For example, VLA-4 in its low affinity state is able to support rolling interactions.

It is important to emphasize that expression of the adhesion molecules, chemokines, and chemokine receptors are dependent upon the cell or tissue type and activation state. For example, neutrophils only express VLA-4 integrin under special conditions whereas it is basally expressed in other leukocyte types, such as lymphocytes and monocytes. This differential expression in leukocyte and endothelial cell receptors is thought to help regulate which leukocyte types get recruited to a specific inflamed tissue type [3].

1.2 Expectations: What We Hope To Learn

1.2.1 Synthetic Modeling

With their Adhesive Dynamics simulations, Hammer and co-workers have elegantly demonstrated how challenging it can be to generate similar rolling characteristics in silico when using physical and mechanical representations combined with traditional modeling formalisms [7-10]. In their models, leukocytes are represented as solid spheres decorated with rod-like "microvilli" containing receptors at their tips. Using a Monte Carlo algorithm for the determination of receptor-ligand interactions, they have successfully produced a jerky stop-and-go pattern similar to that observed for rolling leukocytes. Such models can be fragile to context. When they target specific phenomena and constrain their use to account for specific sets of data, it becomes difficult to extend the model to different experimental circumstances or to help explain different phenomena or particular examples of individual behavior. It becomes difficult to explore potential mechanistic differences between individual cell behaviors, for example. Are there alternative modeling and simulation approaches that are less susceptible to such problems? The multilevel approach described here was selected in part to help circumvent those problems.

Most often, hypotheses about detailed biological mechanisms are induced from the data. Fitting inductive mathematical models to data is often used as evidence in support of particular mechanistic hypotheses. To date, designing and conducting new wet-lab experiments has been the only practicable means to experimentally falsify those hypothesized, conceptual mechanisms. Experimenting on synthetic analogues provides a powerful new means of discovering and testing the plausibility of mechanistic details. Synthetic models provide an independent, scientific means to challenge, explore, better understand, and improve any inductive mechanism and, importantly, the assumptions on which it rests [11].

1.2.1.1 Phenotypic Overlap

The in silico white blood cell (ISWBC) system we have constructed is designed to map to and be an experimentally useful analogue of the wet-lab experimental systems used to study leukocyte rolling and adhesion. We have used the synthetic modeling methodology, an example of what has been referred to as executable biology [12, 13]. Object-oriented software components were designed, instantiated, verified, plugged together, and then operated in ways that can map concretely to mechanisms and processes believed responsible for leukocyte rolling and adhesion.

The envisioned in silico leukocytes, functioning within an analogue of the wet-lab context, will have many behaviors, properties, and characteristics that mimic those of referent in vitro, ex vivo, and in vivo systems. A measure of a particular behavior, property, or characteristic is a phenotypic attribute. Table 1.1 lists several targetable attributes. The greater the similarity between the measured behaviors of our in silico white blood cells and the referent model attributes of interest, the more useful that in silico system will become as a research tool and as an expression of the coalesced, relevant leukocyte knowledge. A goal has therefore been to produce increasing overlap between ISWBC behaviors, properties, and characteristics, and the referent model properties listed in Table 1.1.

Our approach is based on the theory that when two model systems— a wet lab model of leukocyte rolling and adhesion and an in silico analogue—are composed of components for which similarities can be established, and the two systems exhibit multiple attributes that are similar, then there may also be similarities in the generative mechanisms responsible for those attributes (Figure 1.2). Those similarities can be explored by iterative testing and refinement of the in silico analogue coupled with related wet-lab experiments. An example: distance traveled by an in silico leukocyte (or a leukocyte in vitro) under various simulated (or actual) shear stress. We cannot expect these measurements to overlap completely or even have the same units. Observations on behavior similarity can be used simultaneously to eliminate invalid model features and identify gaps in our knowledge of the experimental referent system.

Phenotypic Attribute	Reference
Characteristic jerky stop and go movement during rolling on P-Selectin in vitro	[14]
Highly fluctuating rolling velocities on P-Selectin in vitro	[15]
Larger rolling velocities observed at higher shear rates in vitro	[16]
Smaller rolling velocities at higher ligand substrate densities in vitro	[16]
In silico rolling velocities on simulated P-Selectin match values reported in literature	[16]
Small number of bonds within the contact zone, e.g., within 2-20	[17]
Distance-time and velocity-time data for in silico rolling on simulated P-Selectin or VCAM-1 are indistinguishable from data reported in literature	[14, 15, 18]
Chemokines induce adhesion within seconds	[19]
Leukocyte spreading during firm adhesion	[20]
LFA-1 and ICAM-1 lateral mobility and diffusion	[21]
LFA-1 nanocluster formation upon binding multivalent ligand	[22]
ICAM-1 spatial configurations in vivo	[23-27]
Effect of phosphoinositide 3-kinase inhibitors on adhesion ex vitro	[28]
Effect of phosphoinositide 3-kinase inhibitors on adhesion in vivo	[28]
Induction of LFA-1-dependent neutrophil rolling on ICAM-1 by engagement of E-selectin	[29]
Synergistic effect observed during neutrophil rolling on P- and E-selectin	[30]
Effect of knocking out VAV1/3 guanine nucleotide exchange factors on neutrophil rolling	[31]
Effect of inhibitors to signaling molecules on cell arrest (pertussis toxin (PTx)-sensitive G proteins, p38 mitogen-activated protein kinase)	[29]

Table 1.1 Potentially Targetable Phenotypic Attributes of Leukocytes from Wet-lab Models of Rolling and Adhesion
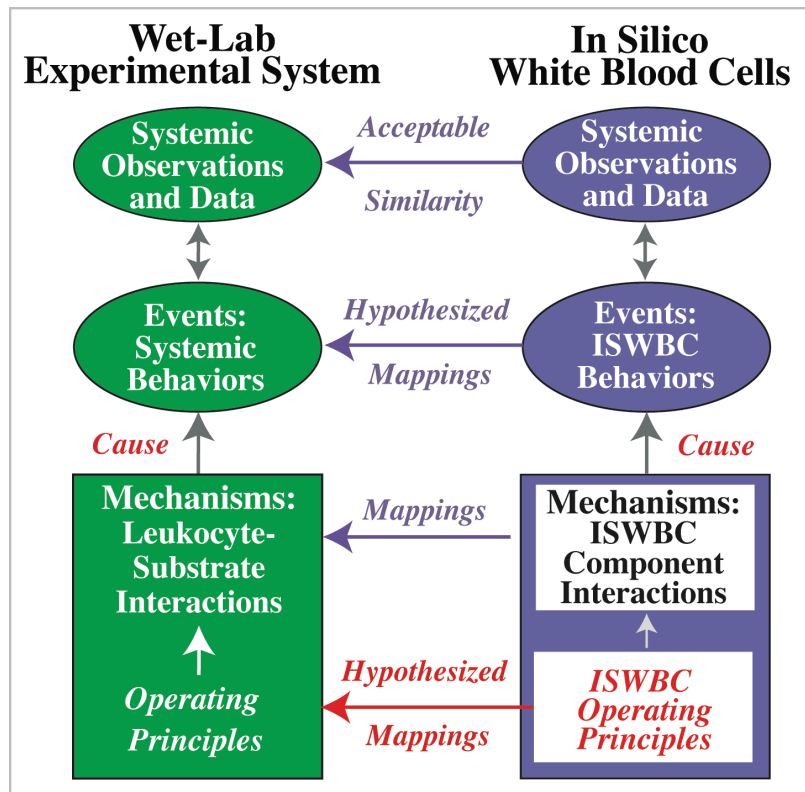
Figure 1.2. Relationships between In Silico White Blood Cell Analogues and Wet-lab Experimental Systems for Studying Leukocyte Rolling and Adhesion. To avoid confusion and clearly distinguish model components, features, measurements, and events from their wet-lab counterparts, we use SMALL CAPS when referring to those of the ISWBC analogue. An ISWBC consists of autonomous LEUKOCYTES that use their LIGANDS to interact and form BONDS with the SUBSTRATE-COATED SURFACE. Interactions are determined by a set of operating principles. There is a clear mapping between in silico components and wet-lab counterparts. Following execution, interacting components cause local behaviors (BOND FORMATION, BOND DISSOCIATION, CHEMOKINE DETECTION, and INTEGRIN ACTIVATION) and systemic behaviors (LEUKOCYTE ROLLING and ADHESION). A level of validation is achieved when a pre-specified set of in silico attributes is measurably similar to a corresponding set of wet-lab attributes. Upon validation, one can hypothesize that a semi-quantitative mapping exists between in silico events and wet-lab events, and that the set of in silico operating principles has a biological counterpart.

6

1.2.1.2 Ten Capabilities

To achieve the phenotypic overlap described above, we need to enable ISWBCs to mimic an expanding variety of leukocyte attributes.   We arrived at ten capabilities that the envisioned ISWBCs should exhibit.

1. *Individual behavior*: the models need to be capable of accurately representing the unique individual behavior patterns typical of leukocytes observed in vitro and in vivo.

2. *Multilevel*: it needs to be easy to increase or decrease the number of model levels and alter communications between levels.

3. *Mapping:* there are clear mappings between leukocyte and ISWBC components and their interactions because in silico observables have been designed to be consistent with those of the referent in vitro flow chambers or in vivo systems.

4. *Turing test:* when an ISWBC and the simulated flow chamber are each endowed with a specified set of ligands, the measures of ISWBC behaviors during simulations should be, to a domain expert (in a type of Turing test), experimentally indistinguishable from in vitro flow chamber measurements; this requires that an ISWBC and its framework must be suitable for experimentation.

5. *Transparent*: ISWBCs must be transparent.   The details of components and their interactions as the simulation progresses need to be visualizable, measurable, and accessible to intervention.

6. *Articulate:* the components articulate. It must be easy to join, disconnect, and replace ISWBC components within and between levels, including the simulated experimental context.

7. *Granular*: because of how ISWBCs are componentized, it should be relatively simple to change usage and assumptions, or increase or decrease detail in order to meet the particular needs of an experiment, without requiring significant re-engineering of the in silico system.

8. *Reusable:* an ISWBC (and its components) must be reusable for simulating behaviors in different experimental conditions, in vitro and in vivo, and when different sets of ligands, chemokines, and chemical reagents (e.g., antibodies) are considered.

9. *Embeddable*: ISWBCs must be constructed so that they can function as components of larger, whole organism or tissue models, and eventually represent the full range of trafficking attributes.

10. *Discrete interactions:* to enable the above capabilities, an ISWBC and its framework must use discrete interactions that explicitly show the relation between components.

In this dissertation, we describe significant progress in building and experimenting with ISWBCs designed to exhibit these capabilities. Having these ten capabilities, will allow us to

continually refine our models without having to reengineer the whole system, and without having to compromise already validated features and behaviors.

1.2.2 LFA-1 Clustering and Phosphoinositide-3 Kinase in Leukocyte Biology

The mechanisms allowing stabilization of leukocyte adhesion after initial adhesion are not fully understood. One mechanism that has been hypothesized is LFA-1 clustering on the leukocyte membrane. However, the nature of integrin clustering remains unclear. With fluorescence microscopy, clustering has been reported in the form of large, dot-like unevenly distributed clusters [32, 33], polarized patches on one side of the cell surface [34, 35], and differential concentrations of LFA-1 to the leading and trailing portions of a polarized or migrating cell [36]. In addition to these inconsistent and imprecise definitions of clustering, the experimental issues with studying clustering in vitro make it difficult to determine what drives the formation of clusters. For example, leukocytes contain both LFA-1 integrin and its ligand ICAM-1 on their membrane surface. Activation of LFA-1 on leukocytes in vitro often leads to formation of homotypic cell aggregations, which itself may drive the redistribution of integrins into clusters that can persist for several minutes after cells are separated by vortexing [36]. Therefore clustering may not be a direct consequence of LFA-1 activation factors, but instead may be an artifact of cell aggregation observed from studying cells in vitro.

Kim et al. used fluorescence resonance energy transfer (FRET) to analyze LFA-1 distributions on lymphocytes in vitro. They activated cells at low cell densities to prevent formation of aggregates of homotypically adherent cells. They observed that binding to monomeric ICAM-1 induced profound conformational changes of LFA-1, but did not alter clustering. In contrast, binding to ICAM-1 oligomers induced significant microclustering in the forms of dot-like clusters [22].

Class IB phosphoinositide-3 kinase (PI3Kγ) is a signal transduction molecule that has been linked to numerous leukocyte functions including movement, contraction, chemotaxis, and secretion. PI3Kγ also appears to play an important role in regulating inflammation. Many studies have shown that recruitment of leukocytes lacking PI3Kγ is impaired in several animal models of inflammation. However, the molecular details of how PI3Kγ regulates recruitment have not been determined [38, 39].

To gain insight into the role of murine PI3Kγ on leukocyte rolling and adhesion under flow conditions, Smith et al. compared the behaviors of leukocytes from PI3K knockout mice (PI3Kγ-/-) and wild type (WT) mice in flow chambers coated with the endothelial cell substrate molecules P-selectin (substrate for rolling), ICAM-1 (substrate for adhesion), and CXCL1 (chemokine for leukocyte activation and subsequent induction of PI3Kγ signaling) [28]. In their study, they observed that leukocytes from the PI3Kγ-/- mice had a reduced ability to adhere to these substrate-coated surfaces in comparison to leukocytes from WT mice. This experiment was also done in vivo in exteriorized cremaster muscle venules of PI3Kγ-/- and WT mice injected with CXCL1. They observed a similarly reduced ability of leukocytes from PI3Kγ-/- mice to adhere to the CXCL1-treated venular surfaces in comparison to those from WT leukocytes. Interestingly, most leukocytes from PI3Kγ-/- mice that were able to adhere to the CXCL1-coated endothelium were only able to do so for short periods of time in comparison to leukocytes in WT mice. Using antibodies, they determined that the main leukocyte receptor being used for adhesion in these CXCL1-treated venules was LFA-1 (the receptor for endothelial cell ICAM-1). Smith et al. hypothesized that LFA-1 clustering (or something similar) following

multivalent binding to multivalent ICAM-1, as was observed by Kim et al., [22], might be the PI3Kγ-mediated mechanism that is responsible for the defect in adhesion. Can we create an in silico device to test this hypothesis.

Earlier studies have provided some evidence that LFA-1 clustering is mediated by PI3K, and more importantly that this clustering process is important for leukocyte adhesion. However, at best a correlation rather than a causal relationship between LFA-1 clustering with increased adhesiveness can be demonstrated using current wet-lab methods [37].

Constantin et al. showed that chemokines triggered a rapid increase in LFA-1 affinity on lymphocytes. Using immunofluorescently labeled LFA-1 with confocal microscopy, they observed that chemokines also stimulated LFA-1 movement into clusters and large polar patches [34]. Inhibiting PI3K activity blocked LFA-1 mobility but had no effect on LFA-1 affinity change. In separate experiments, PI3K inhibitors prevented lymphocytes from adhering to low densities of immobilized ICAM-1 substrate. At high ICAM-1 densities, inhibiting PI3K had no effect on lymphocyte adhesion.

Lum et al. used sophisticated in vitro methods to study murine neutrophils after stimulation with IL-8 chemokine [40]. They correlated the dynamics of adhesion with the increased expression of high affinity LFA-1 and membrane redistribution. Using fluorescence microscopy, they observed redistribution of high affinity LFA-1 into small punctate submicron clusters and large polar caps several μm^2 in area within 30 s of IL-8 stimulation. Within 2 min of chemokine stimulation, the polar caps dissipated into numerous smaller clusters. By 10 min, practically all clusters had dispersed and the number of active LFA-1 was observed to have dropped by ~50%. Inhibition of PI3K activity by treatment with wortmannin did not affect the expression of high affinity LFA-1, but significantly inhibited the amount of LFA-1 clustering and formation of polar caps. Treatment with wortmannin after IL-8 stimulation also significantly decreased the amount of adhesion to fluorescent microbeads coated with ICAM-1 in a flow cytometric based assay.

1.3 Hypotheses and Specific Aims

The goal of this project is to develop a novel in silico model that can be used as an experimental system for testing hypothesized design plans of the molecular-level events that mediate leukocyte rolling, activation, and adhesion. In this work, we focus on the possible role of LFA-1 clustering events on the leukocyte membrane and ICAM-1 spatial configurations on the endothelial cell membrane during rolling and adhesion. How important could these hypothesized mechanisms be for leukocyte adhesion? Could these molecular-level mechanisms be responsible for the observations made from the ex vivo and in vivo experiments comparing leukocyte rolling and adhesion in WT and PI3Kγ-/- mice? Answers to these questions will help us to gain a better understanding of the spatiotemporal events and key rules of engagement that may determine when and how leukocytes are able to adhere to endothelial cell surfaces during inflammatory conditions.

This dissertation is organized as follows. We begin in Chapter 2 with a discussion of the different modeling approaches used in biomedical research to study leukocyte rolling, activation, and adhesion. This will include constructive in vivo, in vitro, and ex vivo wet lab models. Inductive mathematical models will also be discussed. Each of their advantages and disadvantages will be addressed. Then we focus on the synthetic in silico modeling approach and explore its merit to study leukocyte rolling, activation, and adhesion.

One specific aim is to construct a simple in silico synthetic analogue of the in vitro parallel plate flow chamber system for studying leukocyte rolling and adhesion, and demonstrate that the in silico device can generate behaviors similar to those observed in vitro at the individual cell level as well as at the population level. Chapter 3, reports the development and use of such a synthetic in silico device. The leukocyte membrane is discretized into abstract patches that contain leukocyte receptors objects that can detect, bind, and dissociate with their respective substrate ligand. Leukocyte movement is a function of the number and type of bonds, and location of the bond-containing patches at the interface. We first demonstrate that the in silico device can generate behaviors similar to those observed in vitro at the individual cell level as well as at the population level, by comparing simulation results with data from three different in vitro experiments using in vitro flow chambers coated with different combinations of P-selectin, VCAM-1, and GRO-α chemokine [14, 15, 18, 19]. This combination of substrate molecules was chosen because it represents a minimal set of endothelial substrate molecules sufficient for allowing leukocytes to roll, become activated, and adhere without undergoing significant receptor-clustering behaviors under these conditions. PSGL-1, VLA-4, and CXCR-2 (the leukocyte receptors for the endothelial cell substrates P-selectin, VCAM-1, and GRO-α, respectively) are all located on microvilli of leukocytes.

A second aim will be to use the model to explore the hypothesized mechanism of LFA-1 integrin clusering on adhesion and to test the hypothesis that in silico LFA-1 integrin clustering is needed for leukocyte adhesion on simulated ICAM-1 substrate-coated flow chamber surfaces. Chapter 4 describes how we expanded and iteratively revised the model such that lateral movement and clustering of LFA-1 and its inhibition can be represented in order to test this hypothesis. This entailed increasing the resolution of the functional membrane patches on the leukocyte membrane such that it contains another high-resolution grid to represent the cell body membrane surface, the space between microvilli, where LFA-1 integrin molecules are located. We then simulated the ex vivo experiments that used leukocytes from PI3Kγ-/- and wild type mice in flow chambers coated with P-selectin, ICAM-1, and CXCL-1, and determined that the inclusion of an LFA-1 clustering mechanism and its inhibition allows the in silico model to reproduce the defect in adhesion observed from these experiments [28].

The final specific aim is to expand and iteratively refine the model further to represent the endothelial cell surface in order to test the hypothesis that in silico LFA-1 clustering on the leukocyte membrane in combination with a multimeric ICAM-1 configuration on the simulated endothelial cell surface allows for robust and sustained adhesion. In Chapter 5, we describe how we iteratively refined the model such that different hypothesized ICAM-1 spatial configurations observed in vivo can be tested. We simulated the in vivo experiments of leukocyte rolling and adhesion on the exteriorized CXCL1-treated mouse cremaster muscle venules of PI3Kγ-/- and WT mice, and determined that the addition of these hypothesized mechanisms enables the in silico model to mimic the observations from these in vivo experiments.

Finally, Chapter 5 provides an overview of the project and a discussion of the relevance of this study. The future research direction is also addressed.

2 Models of Leukocyte Rolling, Activation, and Adhesion

2.1 In Vivo Models

Transillumination intravital microscopy has been used for more than 150 years to study leukocyte rolling in the microcirculation. In this setup, an organ is exteriorized and the tissue is spread over a transparent platform for transillumination and viewing. It is the oldest and still the most widely used technique for studying leukocyte-endothelial interactions in vivo during acute inflammation because of its ease of operation and image quality. However, it is only effective when viewing tissues less than 100 μm thick. Intravital microscopy of the murine cremaster muscle has become a frequently used in vivo model because it is relatively thin, transparent, and is sufficiently vascularized. Inflammation can be induced by surgical trauma, or intravenous or intrascrotal injection of pro-inflammatory cytokines [41].

Fluorescence intravital microscopy, which makes use of fluorescently labeled cells, has been used effectively to observe leukocyte recruitment in less transparent tissue such as Peyer's patches [42], the liver [43], lung [44], peripheral lymph nodes [45], and many more. Leukocytes are isolated in vitro by various techniques, including density gradient (Percoll, Ficoll), magnetic bead selection, and flow cytometric cell sorting. After labeling with dyes such as acridine orange and rhodamine 6G, they are injected during an in vivo experiment [41]. Alternatively, transgenic and gene knockin mice that express green fluorescent protein (GFP) in specific leukocyte types are available and have been used [30]. The use of fluorescent labeling often makes fluorescence intravital microscopy a very difficult procedure. Photobleaching can be very quick, and it is not uncommon to observe the fluorescent label completely disappear within seconds. Additionally, there is increasing evidence that fluorescence labeling can seriously distort the genuine cell properties by causing tissue injury, structural changes, unintentional cell activation, and yield experimental results that are uninterpretable [41, 46]. New techniques are being developed to address the latter issue by limiting the phototoxicity of fluorescent dyes [41].

The main advantage of using intravital microscopy is the ability for direct, real-time, in situ observation of leukocytes as they interact with endothelial cells. The level of resolution permits quantification of the number of leukocytes that tether, roll, adhere, and transmigrate when observing population-level dynamics [47]. Calculation of cell displacements can also be determined when observing single cell dynamics [48]. Some of the major findings from experiments using intravital microscopy would have been difficult to make using in vitro models. For example, the use of intravital microscopy has enabled us to observe that there are spatially segregated regions on Peyer's patch high endothelial cells for T and B lymphocyte recruitment [49]. In addition, the use of fluorescence intravital microscopy has been helpful in revealing that leukocytes behave differently in different tissue, indicating functional differences in endothelial cells between vessel types and other tissues [50]. This is most likely the result of differing cytokines and adhesion molecules involved as well as the time course for upregulation of these molecules between the different endothelial cell types [51].

While these in vivo models allow for observation of the system in physiological conditions, its major disadvantage is that it offers the entire complexity of the living system. Observations from such studies can sometimes be unexpected and difficult to interpret. Many in vivo studies try to reduce the complexity of the system with the use of biological tools, such as antibodies, recombinant proteins, small molecule inhibitors and genetically engineered cells and

animals. The function of one or more components is inhibited and its effects on individual leukocyte behavior or on the total number of leukocytes that roll, adhere, or transmigrate are observed [47]. However, the complexity and the simultaneous presence of multiple elements of interest (leukocytes, endothelium, adhesion molecules, signaling molecules, extracellular matrix proteins, and other blood components) limit the amount of reduction achievable in vivo. For example, there are multiple adhesion molecules on the leukocyte and endothelial surface, many of which have overlapping and sometimes collaborative functions. Some molecules also participate in multiple stages of the leukocyte adhesion cascade, and play different functions within each [52]. Further adding to the complexity is the presence of unknown factors with in vivo system, such as unknown adhesion molecules. For example, not all of the physiological ligands for E-selectin have been identified [53, 54]. This overwhelming complexity makes it difficult and sometimes impossible to pinpoint the role, and in some cases multiple roles, of a single molecule.

The inability of experimental techniques to dynamically visualize leukocytes as they interact with venules in vivo with sub-cellular resolution has also greatly hindered progress towards understanding this process. Because the in vivo system lacks complete transparency, an abstract design plan of how the molecular components interact to give rise to systems-level behaviors can only be induced from such experiments. Further experiments may help to reconcile differing or competing hypothesized design plans by identifying those that are consistent with the experimental data. However more is needed to actually demonstrate that a design plan is functionally plausible.

Another notable limitation of in vivo models is that the use of animals makes them expensive, resource intensive, and time-consuming. Additionally, the analysis of leukocyte motion from the resulting video images is not an easy task. These limitations preclude their use for large-scale drug screening experiments.

2.2 In Vitro Models

In vitro models have allowed researchers to study leukocyte rolling and adhesion in more simplified, defined, and reproducible environments. The in vitro assays for studying cell adhesion can be broadly divided into static or dynamic models. Static models use cell adhesion assays that allow cells to settle and adhere without any flow-related dynamics. In contrast, dynamic models are performed in the presence of shear [55].

The main advantage of using static adhesion assays is their quickness and ease of use. They are particularly attractive when quantification of large series of samples is required, such as in large-scale drug screening experiments. The setup involves allowing leukocytes to settle to plates coated with substrate molecules or endothelial cells. Forces such as simple fluid flushing, the application of buoyance or rotating motions, or centrifugation are then applied to the bound cells. The number of cells that remain attached after the application of force is then quantified [55]. These static models have become less used since it has been discovered that shear provides a necessary stimulus for certain behaviors. For example, transient adhesive interactions mediated by the selections, occur only in the presence of shear [16, 56].

Dynamic models offer a more physiological environment than static models with the generation of shear conditions similar to that those that are found in the vasculature. The in vitro parallel plate flow chamber is the most commonly used apparatus for studying leukocyte adhesion under flow conditions. This setup consists of two surfaces arranged in parallel: one

lower plate coated with an immobilized adhesive substrate and one upper plate that serves as the top of the chamber. A gasket separates the two plates and maintains a defined distance between them. Using a device such as a syringe pump, isolated leukocytes or cell suspensions are perfused through a chamber, while their interactions with immobilized substrate or cells are recorded using time-lapse videomicroscopy [57, 58].

A key advantage of using the parallel plate flow chamber is that it allows the experimentalist to define the environment as the system is reconstructed. The adhesive surface can consist of activating factors with isolated adhesion molecules, a lipid bilayer containing isolated adhesion molecules, or even a monolayer of endothelial cells. Whole blood, isolated primary cells, suspension cell line, ligand-coated latex beads, or antibody-coated latex beads can be perfused through the flow chamber, while the individual steps of adhesion including rolling, firm arrest, adhesion strengthening, spreading, and migration are recorded [57].

Similar to in vivo models, disadvantages of in vitro parallel plate flow chambers include the limited number of samples that can be simultaneously tested and the time-consuming analysis of the resulting video images. The continuous chamber perfusion also makes it difficult to pharmacologically manipulate the system in real-time. These limitations preclude their use for large-scale drug screening experiments [58].

Both static and dynamic in vitro models attempt to reconstruct the in vivo system and thus can be considered as synthetic models, however they sacrifice physiological fidelity. Limitations with current biological experimental techniques combined with an incomplete knowledge of the system make it impossible to completely reconstruct a biological system from animate organic components with biological realism. At best, a parallel plate flow chamber coated with a monolayer of confluent endothelial cells can be used. However, growing endothelial cells to confluence is time-consuming, and they are not entirely phenotypically representative of in vivo endothelial monolayers. Thus, their presence in the model may introduce further complexity into the in vitro model without improving its physiological relevance [58]. In vitro setups also require a sufficiently large number of leukocytes. Procedures for isolating leukocyte subtypes are not efficient and are also time-consuming. It has been shown that neutrophils become unintentionally modified or activated because of the large number of steps required. Therefore, it is questionable whether the observed behaviors of isolated murine neutrophils in vitro are relevant to those native cells in the circulation under physiologic conditions [59]. For example, in vitro isolated and stained neutrophils do not show normal rolling behavior when injected back in mice [41].

Similar to in vivo models, the current in vitro models of leukocyte adhesion are not completely transparent. The details of the molecular components and their interactions as the experiment progresses cannot be visualized and measured. Thus design plans of how the components interact and operate to yield their systems level properties can only be induced.
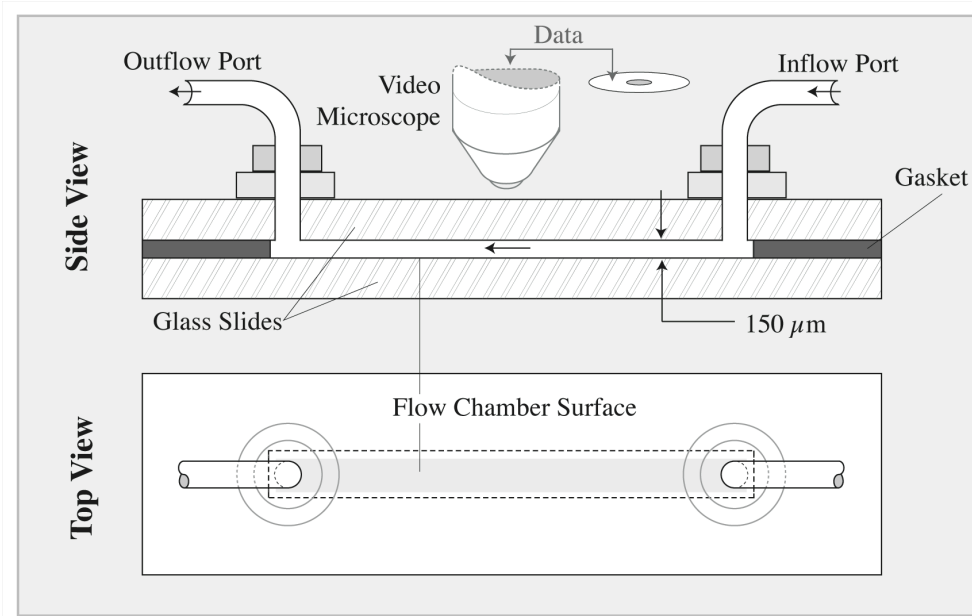
Figure 2.1 Illustration of a typical parallel plate flow chamber used for in vitro studies of leukocyte rolling and adhesion under shear flow conditions. This setup consists of two flat surfaces arranged in parallel: one lower plate coated with cells or an immobilized adhesive substrate and one upper plate that serves as the top of the chamber. The two plates are separated by a gasket, which maintains a defined distance between them. Isolated leukocytes or cell suspensions are perfused from the inflow port, through a chamber, and out through the outflow port. The leukocytes are recorded using timelapse videomicroscopy as they interact with cells or the immobilized substrate.

2.3 Ex Vivo Models

The ex vivo flow chamber was recently developed to combine the strengths of in vitro and in vivo models for studying leukocyte adhesion. It consists of a similar chamber apparatus as the in vitro parallel plate flow chamber, and thus allows for a higher level of reduction than in vivo systems. However, it uses the extracorporeal flow of murine blood from the carotid artery to perfuse the flow chamber, and thus offers a more physiological flow environment than conventional in vitro systems [59]. This experimental setup has been used to identify a synergism between E- and P-selectin during rolling. Rolling neutrophils on coimmobilized P- and E-selectin was sixfold and fourfold higher than on P- or E-selectin alone [30].

The ex vivo flow chamber system shares the same advantages and disadvantages as the in vitro flow chamber. The only additional advantage is that cells do not need to be isolated, minimizing the likelihood of contamination or unintentional activation of leukocytes. Thus, they have more physiological relevance than typical in vitro models.

2.4 Mathematical Models of Leukocyte Rolling and Adhesion

The discrete-time models used in the Adhesive Dynamics simulations by Hammer and co-workers are currently the most developed mathematical models used to study leukocyte rolling and adhesion [7-10]. Leukocytes in their models are idealized as solid spheres decorated with rod-like microvilli containing receptors at their tips. Their simulations have allowed them to explore the molecular and biophysical properties of adhesion molecules, such as reaction rates and bond elasticity, and how these properties may relate to macroscopic behavior such as rolling and adhesion [8, 9].

In their simulations, the position of the cell is determined at each time step from the net force and torque on the cell using a hydrodynamic mobility function for a sphere near a plane wall in a viscous fluid. The net force and torque acting on the cell from bonds, fluid shear, steric repulsion, and gravity are calculated. When calculating the forces on the sphere due to fluid shear, their model uses the Goldman equation [60]: the amount of force a sphere experiences from an applied shear force is calculated by assuming that the sphere is solid. At each time step in the Adhesive Dynamics simulation, positions of bonds on the spherical particle are tracked enabling the authors to calculate the forces that each bond experiences.

To account for the effect of an applied force on the kinetics of bond dissociation, Hammer and co-workers have employed both the Bell model and Dembo Hookean Spring model [61]. The Bell Model predicts the bond dissociation rate as a function of applied force, whereas the Dembo model treats bonds as Hookean springs and relates bond dissociation rate to the length of the stretched bond.

Their Adhesive Dynamics model has allowed them to simulate and analyze data from cell-free experiments using sialyl Lewis^x-coated microspheres rolling over E-selectin-coated surfaces under hydrodynamic flow [8]. However, recent experiments have shown that leukocyte rolling on substrate-coated, flow chamber surfaces is significantly slower and smoother than that of ligand-coated microspheres [15, 62]. It has been hypothesized that the deformability of leukocytes can influence rolling by increasing the contact area. In vivo, leukocytes rolling at blood wall shear rates of 800 s^{-1} elongate in the direction of flow to 140% of their estimated undeformed diameter and have a 3.6-fold increased contact area with the endothelium than at blood wall shear rates of 50 s^{-1} [63]. These experiments have influenced other modelers to explore the mechanical and rheological properties that influence leukocyte morphology and

15

deformation. The 2-D elastic ring model [64] and the 2-D compound drop [65] model offer an account for the deformability of leukocytes during rolling. However, because of the way receptor-ligand interactions are treated deterministically, these models do not produce the characteristic jerky stop-and-go behavior of rolling leukocytes.

More recently, Jadhav et al. created a 3-D mathematical model that provides a representation of leukocyte deformability: it can mimic the stochastic nature of receptor-ligand interactions [66]. Their model uses a mathematical formulation called the Immersed Boundary Method to simulate the measured motion of a leukocyte by representing it as an elastic capsule in a linear shear field. They use a Monte Carlo method for simulating receptor-ligand interactions, enabling them to simulate the jerky stop-and-go movement of rolling leukocytes. Their model explored the effects of membrane stiffness on cell deformation and leukocyte rolling. It is believed that the contact area between the surface and the leukocyte membrane would increase for leukocytes under increasing shear rates. By introducing deformation in their model, they are able to observe this change in contact area. Much knowledge has been gained from these different models of leukocyte rolling and adhesion. They have brought insight into how molecular and biophysical parameters of adhesion molecules or cell deformability may influence leukocyte rolling and adhesion.

Models such as these can generally be characterized as inductive. They describe relationships between variables using equations that use measurable data points as inputs. They are often good at using data to make predictions. However, such models can be difficult to construct and analyze if the number of interdependent variables grows and if the relationships depend on qualitative events, such as variables that change over time, depending on certain events. It can also be extremely difficult to construct if precise quantitative data is lacking. Additionally, mathematical models are not flexible and can be difficult to expand when trying to adapt to different experimental circumstances or to help explain different phenomena or particular examples of individual behavior. All of these issues are relevant to leukocyte rolling, activation, and adhesion.

2.5 Synthetic Models

Bailey et al. constructed a multi-cell, tissue-level, agent-oriented analogue of human adipose-derived stromal cell trafficking through a microvasculature structure within skeletal muscle following acute ischemia [67]. A goal was to identify potential bottlenecks that may limit the efficiency of administered therapeutic cells being recruited into the site of ischemic injury after intravenous injection. They used confocal microscopy images to manually construct an image of the morphology of a characteristic microvascular network. ENDOTHELIAL CELLS lining the VESSEL SURFACE, TISSUE RESIDENT MACROPHAGES, CIRCULATING MONOCYTES, and therapeutic STEM CELLS were individual agents. The agent-oriented model was coupled with a network blood flow analysis program that calculated BLOOD PRESSURE, FLOW VELOCITIES, and SHEAR STRESSES throughout the MICROVASCULAR NETWORK.

Each ENDOTHELIAL CELL, MONOCYTE, and counterpart to a human, adipose-derived, stromal cell (HASC) could be either positive or negative in expression of each of several ADHESION MOLECULES. Similarly, EACH ENDOTHELIAL CELL, MONOCYTE, and TISSUE RESIDENT MACROPHAGE could be either positive or negative for SECRETION of each of the CHEMOKINES and CYTOKINES. Whether a circulating MONOCYTE or HASC rolled or adhered depended on whether they experienced a specified combination of ADHESION MOLECULE states and CHEMOKINE

SECRETION states from a nearby ENDOTHELIAL CELL, and whether they experienced a WALL SHEAR STRESS below a certain threshold level. If the CELL adhered for more than a specified number of simulation cycles, it transmigrated into the TISSUE space.

They observed that introduction of an additional ADHESION MOLECULE, with properties similar to PSGL-1, enabled the model to more closely mimic in vivo experimental results. They showed that small fractions of hASC's are able to roll on P-selectin even though they do not express PSGL-1. They proposed that the additional ADHESION MOLECULE might map to the cellular adhesion molecule CD24. This new knowledge gained reinforces the merit of investigating the complex mechanisms mediating leukocyte adhesion using a synthetic modeling and simulation approach.

While ISWBCs were constructed using similar methods and components, there are notable differences. The Bailey et al. model focused on leukocyte trafficking events at the tissue level. They explicitly represent in silico counterparts of differing blood pressures, flow velocities, and shear stresses throughout a microvascular network. LEUKOCYTES ROLLING and ADHERING on a substrate coated surface within an ISWBC system is a small aspect of leukocyte trafficking through microvascular tissue. ISWBCs focus more on the molecular and cellular level interactions, and have concrete counterparts to the molecular interactions between leukocyte and endothelial cell adhesion molecules.

3 Dynamics of In Silico Leukocyte Rolling, Activation, and Adhesion[1]

3.1 Introduction

What molecular-level events determine the behavioral outcome of individual leukocytes during the processes of rolling, activation, and adhesion to venular surfaces? Rolling and adhesion following attachment are two of the least complicated of many individual leukocyte behaviors that have been studied using wet-lab experimental models. Those behaviors are by no means deterministic. A striking feature of such studies is that cell behavior is heterogeneous: individual cell behaviors under identical conditions can be quite different. No two cells behave the same, yet collective behaviors are robust and fall reliably within narrow ranges. Rolling, for example, exhibits an irregular, jerky stop-and-go pattern along with highly fluctuating rolling velocities [14, 15, 61]. Additionally, in the presence of chemokine, only a fraction of a leukocyte population will adhere firmly [19].

A goal in systems biology research is to understand how molecular level interactions give rise to system level behaviors and properties. That task requires having plausible, adequately detailed design plans for how components at various system levels are thought to fit and function together. Advanced modeling and simulation methods are needed that can be used to test the plausibility of candidate ideas and design plans. Demonstrating that a design plan is functionally plausible requires assembling individual components according to that design plan, and then showing that the constructed device, an analogue – on its own – exhibits behaviors that match those observed in the original biological system. This can be done in silico using the synthetic modeling method [68-71] in which object-oriented software components are designed, verified, plugged together, and operated in ways that represent the mechanisms and processes according to the design plan.

Here we describe the development and usage of an in silico model that can be used as an experimental system for testing hypothesized design plans of the molecular-level events that are thought to mediate leukocyte rolling, activation, and adhesion to endothelial substrate during inflammation. We have used the synthetic modeling method. Object-oriented software components were designed, instantiated, verified, plugged together, and then operated in ways that can map concretely to mechanisms believed responsible for leukocyte rolling, activation, and adhesion. The result is a discrete event, discrete space, and discrete time analogue of the in vitro parallel plate flow chamber system for studying leukocyte rolling and adhesion; the experimentally measured phenotypic attributes can be compared and contrasted to those of leukocytes from referent systems. The expectation is that increasing behavioral similarity between actual leukocytes in context and our analogue systems will require, and can be achieved in part through, similarities in design plans and in generative mechanisms.

We investigated the ISWBC's ability to represent in vitro measures of rolling and adhesion by comparing simulation results with data from three different flow chamber experiments:

(1) Smith et al. [14] and Park et al. [15] observed human neutrophils rolling on various densities of P-selectin and under varying wall shear rates.

---

[1] This chapter was published in large part in [92]

(2) Alon et al. [18] recorded human lymphocyte-rolling trajectories on VCAM-1 in the presence of increasing wall shear rates at fixed time intervals.

(3) Monocyte rolling and adhesion on P-selectin and/or VCAM-1 in the presence or absence of GRO-α chemokine was studied by Smith et al. [19].

The individual in silico dynamics of rolling on simulated P-selectin, and separately on simulated VCAM-1, were an acceptable match to individual in vitro distance-time and velocity-time measurements. The analogues are also able to represent the transition from rolling to adhesion on P-selectin and VCAM-1 in the presence of GRO-α chemokine. The individual in silico and in vitro behavioral similarities translated successfully to population level measures. These behavioral similarities were enabled in part by subdividing the functionality of the analogue's surface into 600 independent, "cell"-controlled, equally capable modules of comparable functionality. The overlap in phenotypic attributes of our analogue with those of leukocytes in vitro confirm the considerable potential of our model for studying the key events that determine the behavioral outcome of individual leukocytes during rolling, activation, and adhesion.

3.2 Methods

3.2.1 Creating the Analogue

Our approach to designing and building the envisioned analogues is motivated by aspect-oriented software development and the middle-out approach first suggested by Brenner [72] and later detailed by Noble [73] for building models of complex biological systems. We adapted and merged these ideas in arriving at our working definition of middle-out modeling. First, specify the biological features under study (e.g., cell rolling and attachment to a surface). Each feature becomes an aspect of a software device – an archetype model. That archetype is iteratively transformed into a functioning analogue of the referent biological system. It is then validated and improved iteratively using the iterative refinement method described below.

Following this approach, our first task is to pick a set of properties, p_1, p_2, ... p_d (within a hyperspace of mechanistic properties) – around leukocyte rolling and adhesion in vitro, ex vivo, and in vivo. For example, we can pick the properties designated as Set A from Table 3.1. We next ask what software device could we implement to realize p_1? How can we realize p_2, etc.? We then ask, how can we realize p_1- p_d, all at the same time, using the same software device? Getting answers to those questions require exploratory modeling and simulation, occasionally using different modeling and simulation support packages. The in silico properties and the device we create to realize p_1-p_d form a foundational analogue, or archetype, from which we intend to expand outward (up, down, and even sideways) to establish a reductive hierarchy of components that could be used to identify important systems biology principles.

Phenotypic Attribute	Reference
Set A: initially targeted attributes	
Jerky stop and go movement	[14]
Highly fluctuating rolling velocities	[15]
Larger rolling velocities observed at higher shear rates	[16]
Smaller rolling velocities at higher ligand substrate densities	[16]
Set B: additional attributes added to targeted set	
In silico rolling velocities on simulated P-Selectin match values reported in literature	[16]
Small number of bonds within the contact zone, e.g., within 2-20	[17]
Distance-time and velocity-time data for in silico rolling on simulated P-Selectin or VCAM-1 are indistinguishable from data reported in literature	[14, 15, 18]
Chemokines induce adhesion within seconds	[19]
Leukocyte spreading during firm adhesion	[20]
Set C: future, targetable attributes	
LFA-1 and ICAM-1 lateral mobility and diffusion	[21]
LFA-1 nanocluster formation upon binding multivalent ligand	[22]
ICAM-1 spatial configurations in vivo	[23-27]
Effect of phosphoinositide 3-kinase inhibitors on adhesion ex vitro	[28]
Effect of phosphoinositide 3-kinase inhibitors on adhesion in vivo	[28]
Induction of LFA-1-dependent neutrophil rolling on ICAM-1 by engagement of E-selectin	[29]
Synergistic effect observed during neutrophil rolling on P- and E-selectin	[30]
Effect of inhibitors to signaling molecules on cell arrest (pertussis toxin (PTx)-sensitive G proteins, p38 mitogen-activated protein kinase)	[29]

Table 3.1 – Targeted Phenotypic Attributes of Leukocytes.

During early development of the ISWBCs attention focused primarily on Set A. Once satisfactory simulations began to be achieved, the targeted attributes were expanded to those in Set B. Final validations focused on the combined set.

3.2.2 Iterative Refinement Method

The first step in transitioning from an archetype to an improved in silico leukocyte is to thoroughly document the in silico properties and characteristics of the former. By doing so, we improve insight into its strengths and weaknesses. The next step is to obtain increasing overlap with measures of phenotypic attributes from the referent system. That is done systematically by iteratively revising together the hypothesis and the analogue by following the five steps below, also illustrated in Figure 3.1A-B. An example hypothesis: the current analogue can acceptably simulate the attributes listed as Set A [p_1, p_2, ... p_d] in Table 3.1. We begin the next iterative cycle with step 1.

1) Select an additional in vitro property or characteristic that is related to those already in the target set, and for which wet-lab experimental observations are available, such as the third property in Table 3.1. Identify the additional property as p_e.

2) Add p_e to the targeted set, yielding an expanded set [p_1, p_2, ... p_e], as illustrated by 2 in Figure 3.1B.

3) Determine if addition of the new attribute invalidates the current analogue, and if so, why. If not, repeat step 2.

4) Revise the model iteratively, possibly by adding mechanistic detail, until the measured phenotypic attributes of the revised analogue are sufficiently similar to [p_1, $p_{2,}$... p_e].

5) The next iterative cycle repeats steps 1–4 with p_f, etc.
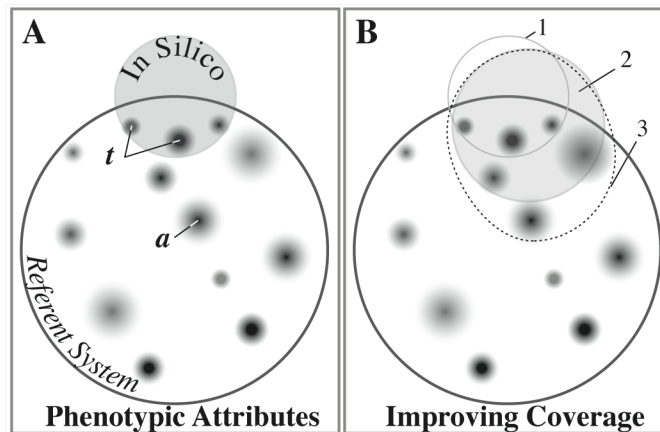
Figure 3.1 An illustration of similarities of in silico and the referent model system. An abstract, Venn-like diagram depicts overlapping sets of similar features of in silico systems and their referent models. The larger circle is a set of observable, measurable, phenotypic attributes. Attention is focused on selected aspects of the referent system, e.g., leukocyte interactions with the flow chamber surface. (A) a: each small shaded domain represents experimental measures of a specific characteristic or property such as distance rolled. The degree of shading illustrates different levels of experimental and measurement uncertainty. T: these are members of the set of targeted referent model attributes that the in silico model is expected mimic. The shaded circle contains the much smaller set of observable, measurable attributes of a foundational in silico analogue, such as the ISWBC. (B) The sketch illustrates the systematic, sequential extension of the foundational analogue's attributes to improve model-referent phenotype overlap. Circle #1: The set of attributes targeted by the ISWBC in A (the foundational analogue). Circle #2 (shaded): The targeted attributes (represented by circle #1) have been expanded to include two new attributes; however, ISWBC #1 fails to generate behaviors similar to the two newly targeted attributes, resulting in its invalidation. A copy of the ISWBC is iteratively refined (without losing or breaking the original behaviors) by adding new detail only as needed (or by replacing an atomic component with a composite component) until successful coverage of the expanded set of targeted attributes is achieved. Oval #3 (dotted): The analogue represented by circle #2 is to be improved: one new attribute is added to the set of targeted attributes in 2, and the process just described is repeated.

3.2.3 Model components

To avoid confusion hereafter and clearly distinguish in silico components, features, measurements, and events from their in vitro counterparts, such as leukocyte, adhesion, bond, etc., we use SMALL CAPS when referring to the in silico components. Examples are provided in Table 3.2.

The system described below is the product of iterative refinement of predecessor analogues that focused initially on Set A in Table 3.1 and later on Sets A and B. Refinement followed the process described above. The referent behaviors, properties, and characteristics that we chose to designate as targeted phenotypic attributes focused on leukocyte ligands PSGL-1, VLA-4 integrin, and CXCR-2 chemokine receptor in addition to their respective substrate ligands P-selectin, VCAM-1, and GRO-α chemokine. This group represents a minimal set of ligand-binding pairs sufficient for allowing leukocytes to roll, become activated, and firmly adhere in parallel plate flow chambers [14, 15, 18, 29, 74]. Table 3.3 lists the leukocyte receptors represented, their corresponding ligands, and the behaviors they support.

Ligand Molecule	In Silico Model Component	Object Class	Location
PSGL-1	PSGL1	ADHESION MOLECULE	MEMBRANE
P-selectin	PSELECTIN	ADHESION MOLECULE	SURFACE
VLA-4	VLA4	INTEGRIN	MEMBRANE
VCAM-1	VCAM1	ADHESION MOLECULE	SURFACE
CXCR-2	CXCR2	CHEMOKINE RECEPTOR	MEMBRANE
GRO-a	GROA	CHEMOKINE	SURFACE

Table 3.2 – In vitro and in silico ligand counterparts, their class types, and their locations within the ISWBC.

Leukocyte Receptor	Surface Receptor-Ligand	Behaviors
PSGL-1	P-Selectin	Rolling
VLA-4 Integrin	VCAM-1	Rolling, Firm Adhesion
CXCR-2 Chemokine Receptor	GRO-a Chemokine	Activation

Table 3.3 – Leukocyte receptors, their Corresponding Ligands, and the Leukocyte Behaviors they Mediate. These three receptor-ligand pairs were chosen because together they are sufficient for enabling leukocytes to roll, become activated, and firmly adhere in vitro.
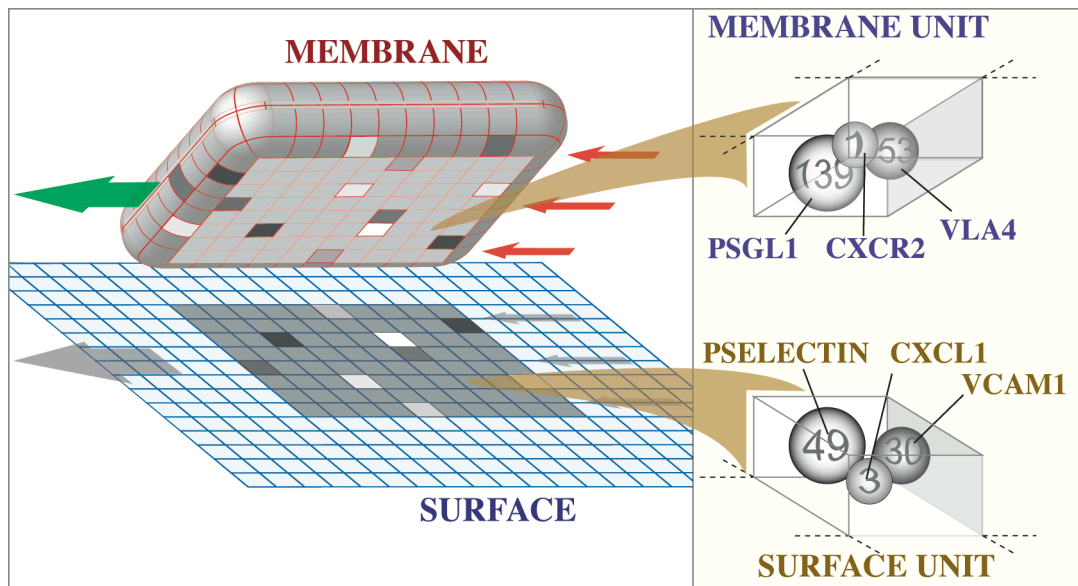
Fig 3.2 Sketches of the in silico experimental system components. (A) A LEUKOCYTE object is shown pulled away from the simulated flow chamber surface to which it was attached. The left arrow indicates ROLL direction; the three right arrows indicate SHEAR resulting from the simulated flow. The simulated flow chamber surface is discretized into independent units of function called SURFACE UNITS. The LEUKOCYTE'S MEMBRANE is similarly discretized into matching units of function called MEMBRANE UNITS: 600 total (20 × 30). The 8 × 10-shaded region on the SURFACE and on the underside of the LEUKOCYTE identifies the CONTACT ZONE. The UNITS within the CONTACT ZONE that are shaded differently indicate different numbers of BONDS had formed between LIGAND- LIGAND pairs in overlapping UNITS; otherwise, no BONDS formed. ROLLING is the result of a sequence of forward ratchet events. One ratchet event is the result of one row of MEMBRANE UNITS being released at the rear of the CONTACT ZONE along with engagement of a new row of at the front of the CONTACT ZONE. One ratchet event maps to a leukocyte rolling 1 μm (relative to the flow chamber surface). (Insert) MEMBRANE UNITS are illustrated. Each MEMBRANE UNIT is simulated using a software object functioning as a container. All leukocyte membrane functionality (relevant to these studies) within each UNIT is represented by three objects functioning as agents: PSGL1, VLA4 and CXCR2 (illustrated as spheres). The number of leukocyte ligands being represented by each is typically different from UNIT to UNIT, as illustrated by the numbers on the spheres.

Each LEUKOCYTE is represented by an object (Figure 3.2). Models of leukocyte adhesion often assume that the molecular interactions within the area of contact between leukocytes and the substrate-coated surface are the only relevant interactions during rolling and adhesion. We do the same. We assume that, because of the required, locally fast reaction times, all required intracellular processes occur quickly, or are localized close to the membrane. We assume that during rolling and adhesion, intracellular processes work together to enable behaviors. Consequently, for the attributes targeted, we treat intracellular processes as being constant and MEMBRANE UNIT processes (defined below) as being autonomous.

24

We refer to that portion of a leukocyte membrane in contact with the surface as the contact zone. Leukocyte membrane functionality within the contact zone is heterogeneously distributed. Some receptor types are confined to microvilli tips, whereas others are found in the spaces between. We discretized the leukocyte membrane by subdividing the contact zone into arbitrary units of functionality (hereafter, membrane unit). All of the functionality within a membrane unit (signaling to and from the cell interior, endocytosis, secretion, etc.) is aggregated, and represented by the behavior of a MEMBRANE UNIT. That behavior is an emergent property of the objects (or agents) contained within (see Figure 3.2). The granularity of that subdivision need only be fine enough to represent the targeted behaviors (Table 3.1). Because of having specified the articulate and granular capabilities (5 and 6: Introduction), it was easy to increase or decrease subdivision granularity.

Because the targeted attributes involve only the contact zone, only events that specifically influence those behaviors are represented. Other aspects of membrane dynamics and molecular biology are not ignored. They are simply not among the system aspects on which we have focused in this project. Any of them can be brought into focus when needed by adding one or more new components to each MEMBRANE UNIT, and that can be done without having to completely reengineer the ISWBC. There are currently only three objects within each MEMBRANE UNIT: one to represent the functionality of each of the three different leukocyte membrane ligands: PSGL-1 ligand, VLA-4 integrin, and CXCR-2 chemokine receptor. Each of these objects is an agent.

For convenience and simplicity, we represent the contact zone using an arrangement of MEMBRANE UNITS in a uniform grid (Figure 3.2), and refer to it as the CONTACT ZONE. A MEMBRANE UNIT within the CONTACT ZONE maps to an arbitrary portion of membrane that is in contact with the surface, and may include the tethers that are known to form between rolling leukocytes and surfaces [75]. Leukocytes have stretchy microvilli and are highly irregular in shape [75-77]. Consequently, the precise area of membrane-surface contact during rolling is uncertain. We reflect that uncertainty by specifying that MEMBRANE UNITS are changeable, and by not specifying a mapping between a MEMBRANE UNIT and a precise amount of membrane area. However, the mapping between MEMBRANE UNIT and distance rolled is important: that is discussed below. The LEUKOCYTE'S SURFACE outside the CONTACT ZONE is assumed a reservoir of MEMBRANE UNITS. For programming convenience, we represented that reservoir as an extension of the CONTACT ZONE, as illustrated in Figure 3.2, that has grid dimensions 5–10 times that of the size of CONTACT ZONE. Hereafter, we refer to the entire grid as the MEMBRANE. To accommodate MEMBRANE mobility relative to the SURFACE, the MEMBRANE at the software level is a 2D toroidal lattice.

The number of MEMBRANE UNITS within the CONTACT ZONE can be easily increased or decreased. The observed ratio of length to width of rolling rat leukocytes in vivo is approximately 1.25-1.5 [76] over a range of shear values. We assumed that rat and human leukocytes deform similarly, and therefore represented the contact zone using a rectangular grid with width-to-length dimensions having a similar ratio. All simulations in this report represent the CONTACT ZONE using an 8 × 10 arrangement of MEMBRANE UNITS. That resolution (level of granularity) was selected after experimenting with coarser and finer representations. Larger granularities failed to exhibit the targeted behaviors (within a factor of two or better). Smaller granularities failed to improve simulation results. For two reasons, we did not optimize CONTACT ZONE size. First, we have not yet developed a means of determining precisely which of two similar behaving but differently parameterized simulations is the closer match over a range of in

25

vitro measures. Second, LEUKOCYTE behavior also depends on the nature and specification of the components within (discussed below).

A portion of the bottom flow chamber surface is represented by the SURFACE SPACE (hereafter simply SURFACE). SURFACE functionality was also subdivided. In each simulation, its granularity matches that of the MEMBRANE, as illustrated in Figure 3.2: one unit of SURFACE corresponds to about 1 μm2. That grid is also a 2D toroidal lattice. As with the MEMBRANE, each unit of SURFACE function is represented by a container object, called a SURFACE UNIT, one per grid space. Contained within each SURFACE UNIT are agents representing the substrate molecules (P-selectin, VCAM-1, and GRO-α chemokine) for the three leukocyte membrane ligands listed in Tables 3.2 and 3.3.

Agents contained within MEMBRANE UNITS and SURFACE UNITS are of the class type LIGAND. A LIGAND agent represents a group of binding molecules of the same type that may be found within a portion of the membrane or flow chamber surface. For example, a PSGL1 represents several PSGL-1 adhesion molecules. The number represented is illustrated by the numbers assigned to the objects within each MEMBRANE UNIT in Figure 3.2. The actual number represented is determined by the parameter *TotalNumber*. At the beginning of each simulation, its value is uniquely determined according to the values of *DensityMean* and *DensitySTDev*. The targeted behaviors were achieved using random assignment of values to each PSGL1 and VLA4 agent. Particular patterns of ligands within the contact zone, such as regions of high and low PSGL-1 densities can also be implemented when required by targeted behaviors.

Table 3.3 shows LIGANDS sub-classed as ADHESION MOLECULES, CHEMOKINE RECEPTORS, and CHEMOKINES, corresponding to adhesion molecules, chemokine receptors, and chemokines, respectively. In addition, there is a sub-class of ADHESION MOLECULES called INTEGRINS. INTEGRINS are different from the other LIGANDS in that they have two sets of parameters, one represents a low, and another represents a high affinity state. All INTEGRINS are initially in the low affinity state. Events within the CONTACT ZONE (see below) determine if, and when, an INTEGRIN is converted to the high affinity state.

For each ligand type, on either the chamber surface or leukocyte membrane, there can be a corresponding LIGAND agent within the container object at each SURFACE and MEMBRANE grid location. We have set a maximum value of one LIGAND of each type at all locations. Table 3.2 lists each of the ligands in the model, the LIGAND objects that represent them, their LIGAND class type, and their location within the ISWBC.

3.2.4 Behaviors

During each simulation, the CONTACT ZONE portion of the MEMBRANE is positioned "above" the SURFACE so that LIGANDS in overlapping MEMBRANE and SURFACE UNITS can "see" and interact with each other (Figure 3.2) and form BONDS.

When the bonds on tethers and other points of contact are broken at the rear of a rolling leukocyte under the influence of shear, the leukocyte ratchets forward some distance (until sufficient new bonds are formed, as discussed below). The ISWBC works analogously. If there are no BONDS within the rear row of the CONTACT ZONE, the LEUKOCYTE ratchets forward (north) until the rear row contains at least one BOND during the simulation cycle. Ratcheting involves removing a row of MEMBRANE UNITS from the rear of the CONTACT ZONE while a new row is placed at the front. Thus, the location of the CONTACT ZONE on the MEMBRANE and its position "over" the SURFACE changes whereas CONTACT ZONE dimensions are kept constant. During a

single simulation cycle, a ratchet movement can be repeated up to nine times (for a LEUKOCYTE with a CONTACT ZONE length of 10 MEMBRANE UNITS). Currently, only forward (north) movement is permitted. However, we can enable east or west rolling-like movements when that is needed. We have also implemented SURFACE boundary conditions in order to reduce the number of simulated SURFACE UNITS. A LEUKOCYTE ROLLING off any edge will continue ROLLING at the opposite edge. This feature has reduced computational time and simplified visualization.

We specify that each ratchet movement maps, on average, to a leukocyte having moved 1 μm. If the data were available to support doing so, the mapping between each forward ratchet and relative distance moved could be drawn from a distribution having a mean of ~1 μm and some specified variance. By so doing, we may represent some of the real uncertainty associated with in vitro measures. However, the data are not yet available. For simplicity, we fixed the mapping to be 1 μm. If the mapping between a simulation cycle and in vitro time is changed, then this distance mapping too must change.

Components have been designed to facilitate changing CONTACT ZONE dimensions dynamically during a simulation. It is believed that leukocyte deformation supports firm adhesion by increasing the zone of contact, thereby allowing formation of more adhesive bonds. If a LEUKOCYTE remains ADHERENT for at least 100 simulation cycles, an extra row is added at the front and an extra column is added along one side (selected randomly) of the CONTACT ZONE allowing additional BONDS to form. This process mimics spreading and helps stabilize ADHESION.

During each simulation cycle, each LIGAND within the CONTACT ZONE has one opportunity to form and break BONDS. However, only BONDS at the rear row of the CONTACT ZONE experience the effects of the SHEAR (described below). Only when all BONDS at the rear have been BROKEN can a LEUKOCYTE ROLL. If at any time (during any simulation cycle), there are no intact BONDS within the CONTACT ZONE, the LEUKOCYTE removes itself from the SURFACE and the simulation ends, mimicking a leukocyte detaching and being swept away by the fluid flowing through the chamber. Figure 3.3 outlines the programmed decisional processes that determine the flow of events within each simulation cycle.
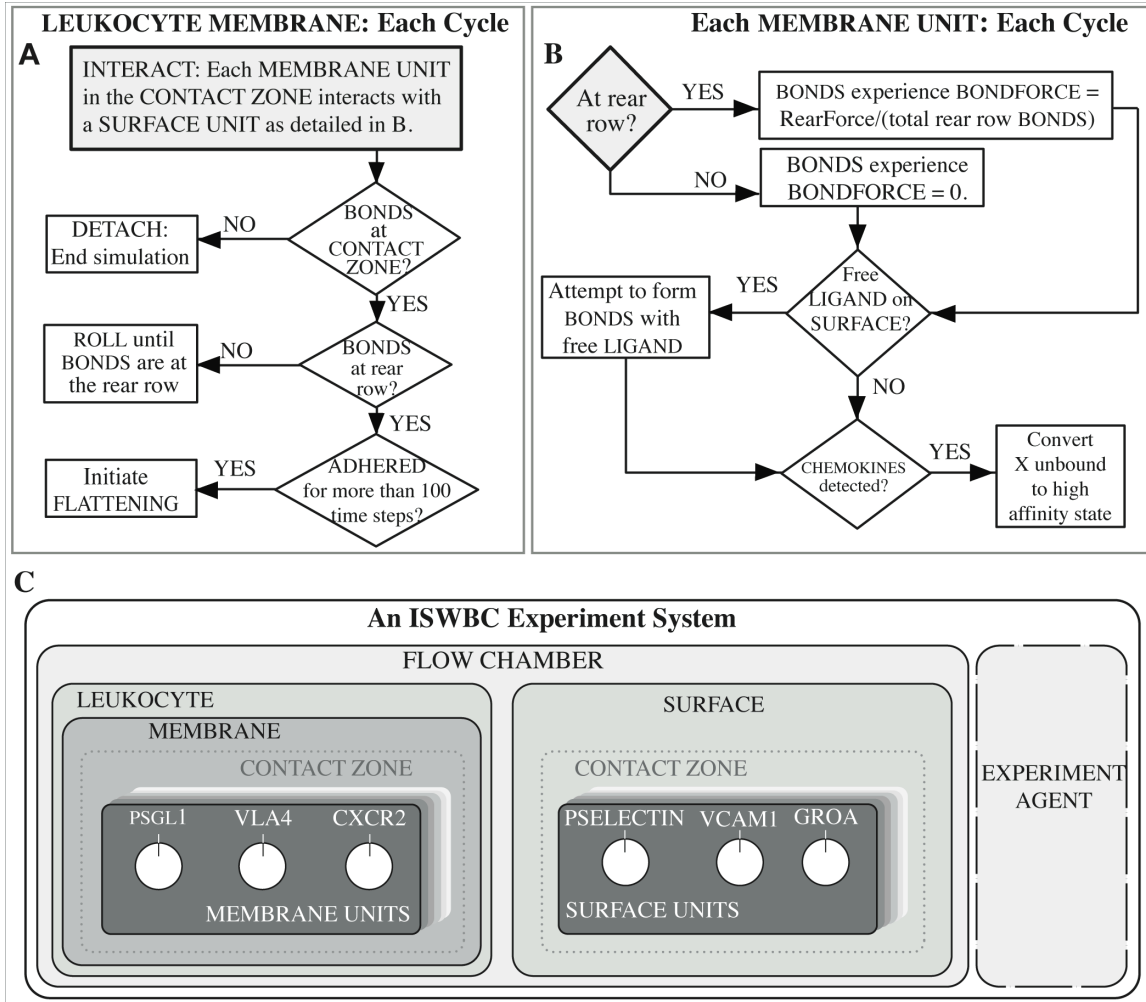
Figure 3.3 The decisional process for the LEUKOCYTE MEMBRANE and each MEMBRANE UNIT during a simulation cycle. (A) The LEUKOCYTE steps through its decisional process only once during a simulation cycle. At the start of the cycle, the MEMBRANE instructs all MEMBRANE UNITS within the CONTACT ZONE to follow the decisional process in B. Once that process is complete, the MEMBRANE completes its process by selecting and following the one applicable action option. (B) The state of each MEMBRANE UNIT depends on the properties of the three LIGAND objects contained within. During each simulation cycle, each MEMBRANE UNIT, selected at random, uses this decisional process to update its status relative to the SURFACE UNIT over which it is positioned. (C) The hierarchical organization of the ISWBC system is illustrated. There are six levels. An Experiment Agent exists within the system, but separate from the FLOW CHAMBER and LEUKOCYTE. It represents a researcher conducting wet-lab experiments: it measures and records events and behaviors during each simulation.

28

3.2.4.1 Forming and Breaking BONDS Between ADHESION MOLECULES

When a LEUKOCYTE LIGAND encounters its binding partner on an overlapped SURFACE UNIT, it first determines the theoretical maximum number of BONDS that can be formed (defined below). A Monte Carlo algorithm is then used to determine the actual number of BONDS that form. Each simulated adhesion molecule type uses the values of three parameters to determine BONDS-formation with its binding partner: 1) *TotalNumber* specifies the number of receptors. The smaller of the two *TotalNumber* parameters is used during calculations of the theoretical maximum. 2) *BondNumber* specifies the number of BONDS that already have been formed between the LIGAND pair. The theoretical maximum number of BONDS is simply the difference between these two values. 3) Pon is the probability of bond formation for each binding pair. Pon was fixed at 0.001, 0.001, and 0.005 for PSGL1-PSELECTIN, low affinity VLA4-VCAM1, and high affinity VLA4-VCAM1BONDS, respectively.

For each potential BOND, P_{on} is compared to a pseudo-random number between 0 and 1 to determine if the BOND is actualized. P_{on} is fixed for the duration of a simulation. For the INTEGRINS that represent ligands with high affinity states, this process is repeated separately using parameter values corresponding to the higher affinity state.

The effect of shear on the rear of a leukocyte is represented by the variable *RearForce*. BONDS experience a *bondforce* that is calculated each simulation cycle by dividing the *RearForce* by the total number of BONDS in the rear row of the CONTACT ZONE. BONDS within the rest of the CONTACT ZONE experience no *bondforce*. Drawing from the in vitro data discussed below, we have assumed the simple linear relationship between *bondforce* and the probability of BOND dissociation shown in Figure 3.4A. It is calculated as (probability of dissociation) = b0 + (*bondforce*) × b1, where b1 and b0 are the slope and intercept, respectively, of the line segment associated with a specific *bondforce*. Each type of simulated adhesion molecule pair uses a unique set of b0 and b1 values obtained from Figure 3.4A. Each relationship is intended to be an analogue of the force dependence of dissociation rates for P-selectin/PSGL-1 bonds reported by Park et al. [15], and those of high affinity VLA-4/VCAM-1 bonds reported by Zhang et al. [78] (Figure 3.4B). The *bondforce* relationships in Figure 3.4A are not intended to match or precisely fit in vitro data. Doing so would require that we specify the relationship between wet-lab measures of bond force and our in silico parameter *bondforce*. There is neither need nor reason to do so at this early stage of analogue development.

Park et al. calculated PSGL-1/P-selectin dissociation rates as a function of force experienced by the bond by observing PSGL-1 covered microbeads rolling on P-selectin substrate in a parallel plate flow chamber. For the range of dissociation rate constants relevant to this report (K_{off} values < 10/s), the in vitro data, as shown in Figure 3.4B, is close to linear (the values in Figure 3.4B were calculated from the reported, best fit values [15]). The unstressed dissociation constant, K0off, for PSGL-1/P-selectin bonds were calculated to be 1.6/s.

Zhang et al. used single-molecule dynamic force spectroscopy to investigate the strength of the VLA-4/VCAM-1 complex. The experimental conditions were not the same as in vitro. Nevertheless, the relative behavior of the VLA-4/VCAM-1 complex is expected to be similar to that in the flow chamber. The dissociation of the VLA-4/VCAM-1 complex was determined to involve overcoming two activation energy barriers. Under pulling forces < ~50 pN, dissociation rates were governed principally by the properties of the outer activation energy barrier. The K^0_{off} values for the outer energy barriers for the low- and high-affinity complexes were 1.4/s and 0.0035/s, respectively. The high affinity data in Figure 3.4B were converted from the reported

semi-log plots [78]. The force dependence of dissociation rate for low affinity VLA-4/VCAM-1 was not reported. Competitive binding experiments determined that native state VLA-4 has affinity constant values similar to those of the selectins [79]. We assumed that it is similar to PSGL-1/P-selectin, and represented it so in Figure 3.4A.
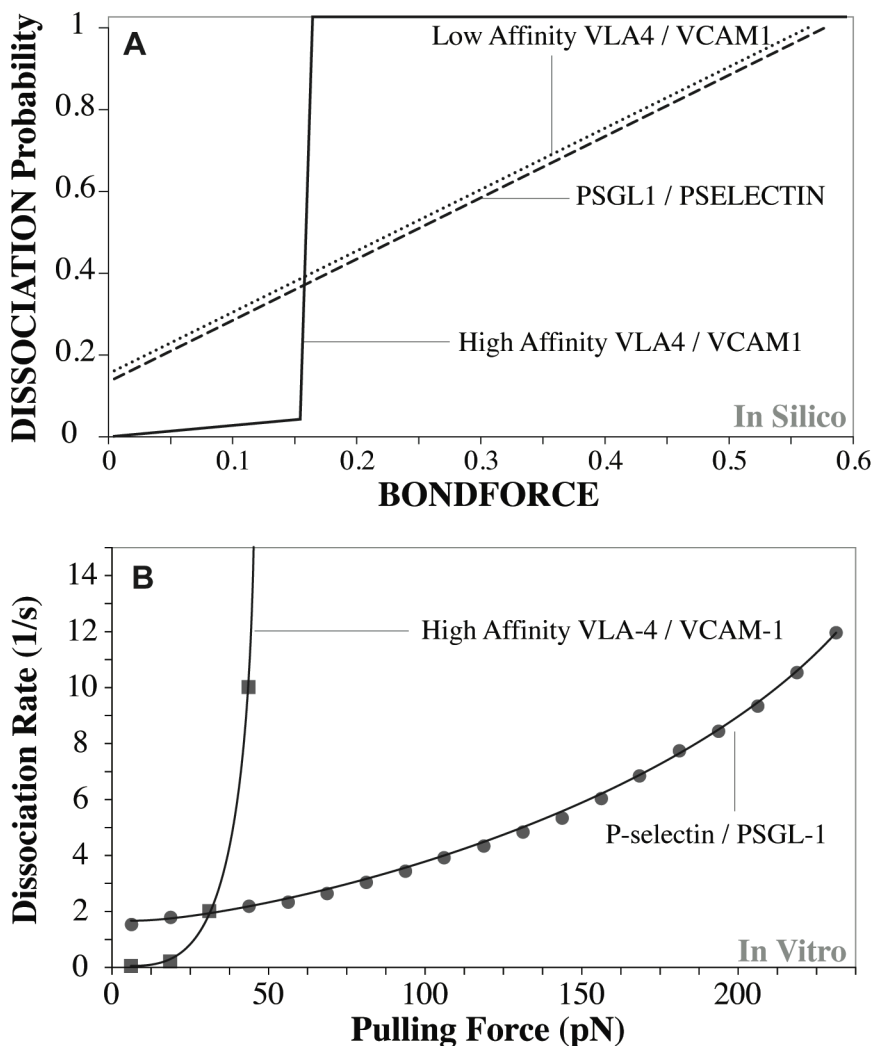
Figure 3.4 **FORCE dependence on BOND DISSOCIATION probability and force dependence on bond dissociation rates.** (A) Shown is the relationship between *bondforce* and probability of BOND DISSOCIATION for each of the three LIGAND pairs within the CONTACT ZONE. The effects of shear on the ligand-ligand bonds that form at the rear of the leukocyte are simulated using *bondforce*. BONDS within the rear row of the CONTACT ZONE experience a *bondforce* that is calculated by dividing the *RearForce*, a unitless parameter representing the effects of shear, by the total number of BONDS within the rear row. During a simulation cycle, each MEMBRANE UNIT in the rear row uses the current value of bondforce and the graphed relationship to calculate a probability that each BOND will be broken during that cycle. All BONDS elsewhere within the CONTACT ZONE experience a *bondforce* value of 0. UNSTRESSED (*bondforce* value of 0)

30

DISSOCIATION probabilities for PSGL1/PSELECTIN, LOW-AFFINITY VLA4/VCAM1, and HIGH-AFFINITY VLA4/VCAM1 were chosen to be 0.14, 0.16, and 0.0035, respectively. (B) The in vitro force dependence of dissociation rates for P-selectin/PSGL-1 bonds (as reported in [15]) and the high affinity VLA-4/VCAM-1 bonds (as reported in [78]) are plotted for comparison to the analogue relationships in A. The plotted values were taken from the fitted in vitro data: see Methods for details. The relationships in A are analogues of these experimentally determined relationships and are not meant to either match or fit that data. The dissociation rates of the PSGL-1/P-selectin bonds as a function of force were determined by experiments using PSGL-1-coated microbeads rolling on a P-selectin substrate in a parallel plate flow chamber [15]. The dissociation rates for the VLA-4/VCAM-1 complex, described in Methods, were calculated from data obtained using single-molecule dynamic force spectroscopy [78]. The force dependence of dissociation rates for low affinity VLA-4/VCAM-1 data was not reported. We assumed that it is similar to PSGL-1/P-selectin relationship in A.

3.2.4.2 Activation

A LEUKOCYTE that is interacting with the SURFACE uses CHEMOKINE RECEPTORS to detect any CHEMOKINE object that may be present. As a simplification (and because each simulation cycle is long compared to chemokine binding and dissociation), we specified P_{on} and P_{off} values of 1.0 for CHEMOKINE RECEPTORS such that each detected CHEMOKINE can BIND and DISSOCIATE (i.e., the events are registered as having been detected) within the same simulation cycle. Consequently, CHEMOKINES can be detected by the same RECEPTOR during different simulation cycles. For each CHEMOKINE detected, a message is sent to the INTEGRIN within that MEMBRANE UNIT to decrement the low affinity *TotalNumber* parameter and increment the high affinity *TotalNumber* parameter. If low affinity *TotalNumber* reaches 0, then the activation mechanism for that INTEGRIN is turned off.

A maximum of approximately 10% of β-2 integrins on a leukocyte membrane become induced into high affinity states when exposed to chemokines [80]. We have assumed that the VLA-4 integrin has similar properties. When the sum of the *TotalNumber* high affinity state parameters from all INTEGRINS within the MEMBRANE exceeds 12.5% of the sum of the *TotalNumber* high and low affinity values from all the INTEGRINS, the activation mechanism is turned off for all INTEGRINS. The above representation of the chemokine dynamics is a simple, abstract metaphor for a complex phenomenon. Future ISWBC descendants will include representations of chemokine binding and signaling dynamics that are more realistic.

3.2.5 ISWBC development

We have used the Recursive Porous Agent Simulation Toolkit (RePAST) as our modeling and simulation framework. It is a java-based software toolkit developed at the University of Chicago for creating and exercising agent-based models. The libraries provided are used to create, run, display, and collect data. From within the RePAST framework, the system described below can operate in ways that represent the hypothesized mechanisms and processes at the level of detail and resolution needed simulate the targeted attributes (Sets A and B) in Table 3.1.

31

Code is managed using Concurrent Versions Systems software (CVS) with a single HEAD branch and ChangeLogs for each commit. Experiments are conducted using the last stable version of the HEAD branch. As an experiment runs, simulation data is kept in memory until the end of the experiment, at which time it is written to comma separated files indexed by filename.

Development follows a loose and iterative specification, implementation, test, and commit process. Each specific change is documented in the ChangeLog. The changes are then committed to CVS; there is one CVS module for the entire framework.

3.2.6 The In Silico Experimental Method

An in silico experiment consists of building the software into an executable, creating and editing the parameter vector, and beginning the simulation. An experiment on an individual leukocyte consists of a single run with the output representing the results of the experiment. An experiment on a population of leukocytes can also be executed by performing a batch run. Depending on the experiment type, simulation output can consist of LEUKOCYTE positions, BONDS and RECEPTOR information at each time step. At the end of the experiment, one of several data reduction scripts may be run to process and analyze the simulation results. Microsoft Excel was used to examine and process data from simulations.

3.3 Results

3.3.1 Simulating Neutrophil Rolling on P-Selectin

The in vitro data suggests that leukocyte rolling is mediated by small numbers of receptor-ligand bonds formed within the contact zone. Mathematical model estimates of this number range between two and twenty [17]. Single bond events are believed to cause rolling behaviors similar to what one might expect of a stochastic process. There are two easily recognized manifestations: jerky stop-and-go patterns and highly fluctuating rolling velocities [61]. Given the importance of single bond events, each ISWBC BOND maps to a single ligand-ligand bond. However, a LIGAND can map to more than one ligand molecule.

The first of the targeted attributes was pause time measurements made over a small range of shear values as reported by Smith et al. [14] for human neutrophils rolling on a P-selectin–coated surface. Using high-speed videomicroscopy with a smallest resolvable step size of 0.5 μm, average pause times were in the range of 0.1 to 0.16 seconds for shear stress values of 0.5, 1.0, and 2.0 dyn/cm^2. Higher wall shear stress values caused shorter average pause times.

We defined LEUKOCYTE ROLLING as a sequence of at least 10 simulation cycles during which the LEUKOCYTE remained non-stationary on the SURFACE. Simulations using early LEUKOCYTE versions failed to exhibit any acceptable behaviors. Following the sequence of iterative refinements described in Methods, we arrived at the ISWBC used. We specified that each simulation cycle corresponds to about a tenth of a second of in vitro time. When parameterized according to Table 3.4, using the values listed in Table 3.5 (part I-A), the simulation's smallest forward movement (ratcheting forward by one MEMBRANE UNIT) maps to 1 μm, twice that of the videomicroscope used by Smith et al. To be acceptably similar, given the difference in time resolution, the magnitude of the average simulated pauses should be within 1 to 2 times the in vitro values of 0.1 to 0.16 seconds, or between 0.1 and 0.32. Figure 3.5 shows that at *RearForce* values of 0.2 through 0.5, the median PAUSE TIMES fell within that range. We judged these results to be acceptable. At a *RearForce* value of 0.1, the median PAUSE TIME

appeared to deviate slightly from this range. Future studies using a finer time resolution may yield results closer to the in vitro data, should that be needed.

Parameter Name	Description		Model Parameter Value	Experimental Value	Ref.
Leuk *TotalWidth*	LEUKOCYTE MEMBRANE width (in the *y* [east-west] dimension)		20 MEMBRANE UNITS	Avg. Human Leukocyte Diameters (μm): Lymphocyte: 6.2; Neutrophil: 7; Monocyte: 7.5	[77]
Leuk *TotalLength*	LEUKOCYTE MEMBRANE length (in the *x* [north-south] dimension)		30 MEMBRANE UNITS		
Leuk *ExposedWidth*	CONTACT ZONE width (in the *y* dimension)		8 MEMBRANE UNITS	NA	NA
Leuk *ExposedLength*	CONTACT ZONE length (in the *x* dimension)		10 MEMBRANE UNITS	NA	NA
PSGL1 *DensityMean* ± PSGL1 *DensitySTDev*	Mean number of PSGL-1 molecules (± standard deviation) represented by each PSGL1 agent	Experiment 1: Neutrophils	150 ± 5^a molecules	~18,000/Human Neutrophil	[81]
		Experiment 3: Monocytes	150 ± 5^b molecules	N/A	N/A
VLA4 *DensityMean* ± VLA4 *DensitySTDev*	Mean number of VLA-4 molecules (± standard deviation) represented by each VLA4 agent	Experiment 2: T-lymphocytes	45 ± 5 molecules	3,000/Human T-Lymphocyte	[82]
		Experiment 3: Monocytes	60 ± 5 molecules	6,000/Human Monocyte	
CXCR2 *DensityMean* ± CXCR2 *DensitySTDev*	Number of CXCR-2 molecules (± standard deviation) represented by each CXCR2 agent		1 ± 0 molecules	NA	NA
VLA4 *MaxPercHighAff*	Maximum percent of VLA-4 integrins on the leukocyte membrane that can be induced		12.5%	10%	[80]

33

	into a high affinity state [c]			
Pon (PSGL1-PSELECTIN1)	Probability of forming a PSGL1-PSELECTIN BOND	0.001	NA [d]	[83]
Pon (LOW AFFINITY VLA4-VCAM1)	Probability of forming a LOW AFFINITY VLA4-VCAM1 BOND	0.001	NA [d]	[82]
Pon (HIGH AFFINITY VLA4-VCAM1)	Probability of forming a HIGH AFFINITY VLA4-VCAM1 BOND	0.005	NA [d]	[82]
Pon (CXCR2-GROA)	Probability of forming a CXCR2-GROA BOND	1.0 [c]	NA	NA
Poff (CXCR2-GROA)	Probability of breaking a CXCR2-GROA BOND	1.0 [c]	NA	NA

Table 3.4 – Model Parameter Values for the LEUKOCYTE MEMBRANE and LIGANDS along with Corresponding In Vitro Values

[a] PSGL1*DensityMean* ± PSGL1*DensitySTDev* parameter values used for simulating Experiment 1, neutrophil rolling, were originally 25 ± 5. They were changed to the values currently listed to more closely reflect the experimental values of PSGL-1 density reported in the literature. No significant differences were observed when using these new parameter values.

[b] Values for PSGL-1 sites/human monocyte were not found in the literature and were assumed to be similar to values reported for human neutrophils.

[c] See Methods.

[d] *Pon* and *Kon* are intended to map to aspects of the same in vitro phenomena. However, there is no direct mapping between these parameters because the parent models belong to fundamentally different classes.

	In Vitro Values				*ISWBC Values*		
Experiment	**Shear (dyn/cm^2)**	**Substrate Molecule**	**Site Density / Plating Conc.**	*Rear Force*	LIGAND	LIGAND Density
I. Neutrophil Rolling on P –Selectin						
A. Pause Time	0.5, 1.0, 2.0	P-selectin	9 sites/μm^2	0.1 – 0.5	PSELECTIN	15 ± 5
B. Distance-Time	2	P-selectin	25 sites/μm^2	0.5	PSELECTIN	25 ± 5
C. Velocity-Time	0.5	P-selectin	9 sites/μm^2	0.1	PSELECTIN	15 ± 5
II. T-Lymphocyte Rolling on VCAM-1						
Distance-Time	0.73 – 7.3	VCAM-1	15 μg/mL	0.15 – 1.6	VCAM1	45 ± 5
III. Monocyte Rolling on P-selectin/VCAM-1/GRO-a						
		VCAM-1	100 ng/mL		VCAM1	13 ± 5
Rolling and Adhesion	1	P-Selectin	10 μg/mL	1	PSELECTIN	25 ± 5
		GRO-a	5 μg/mL		GROA	3 ± 2

Table 3.5 Experimental Values for the Three In Vitro Flow Chamber Environments and the Corresponding Parameter Values used for each of the Three Simulated Experimental Conditions. The FLOW CHAMBER SURFACE dimensions were fixed at 100 x 60 SURFACE UNITS. Each SURFACE grid space maps to approximately 1 μm^2 of effective flow chamber surface area.
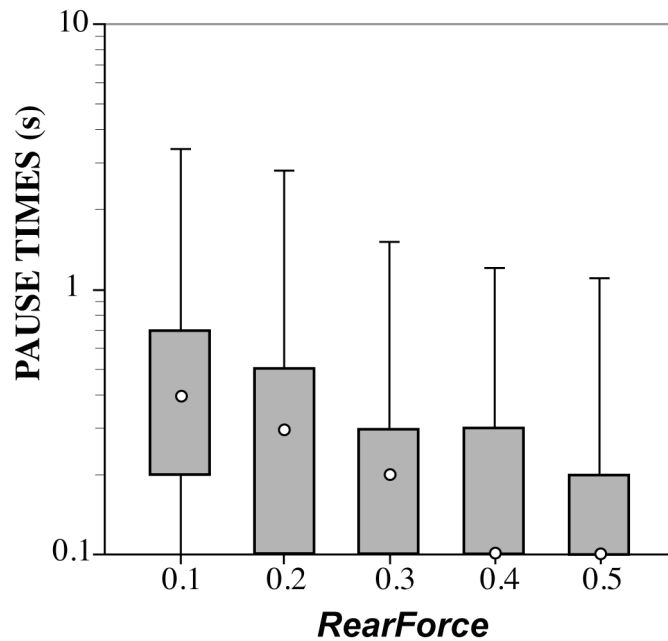
Figure 3.5 Boxplot of measured PAUSE TIMES for LEUKOCYTES ROLLING ON PSELECTIN at various *RearForce* values. At each *RearForce* value, average PAUSE TIME was recorded from 60 simulations that had at least 10 INTERACTIONS (pauses). In vitro, higher values of wall shear stress lead to shorter pause times. This data shows that higher *RearForce* values also lead to shorter LEUKOCYTE pause times. White circles: median pause time value. Box: lower and upper quartiles. Whiskers: minimum and maximum pause time values.

Simulated distance-time measures of LEUKOCYTES for each *RearForce* condition exhibited the characteristic jerky stop-and-go movement (Figure 3.6A). Smith et al. reported trajectories of human neutrophils rolling on P-selectin at a density of 25 sites/μm^2 while under a wall shear stress of 2.0 dyn/cm^2 [14]. When using the ENVIRONMENT parameter values from Table 3.5 (part I-B), simulations produced LEUKOCYTE trajectories that were experimentally similar to data obtained in vitro (Figure 3.6B).
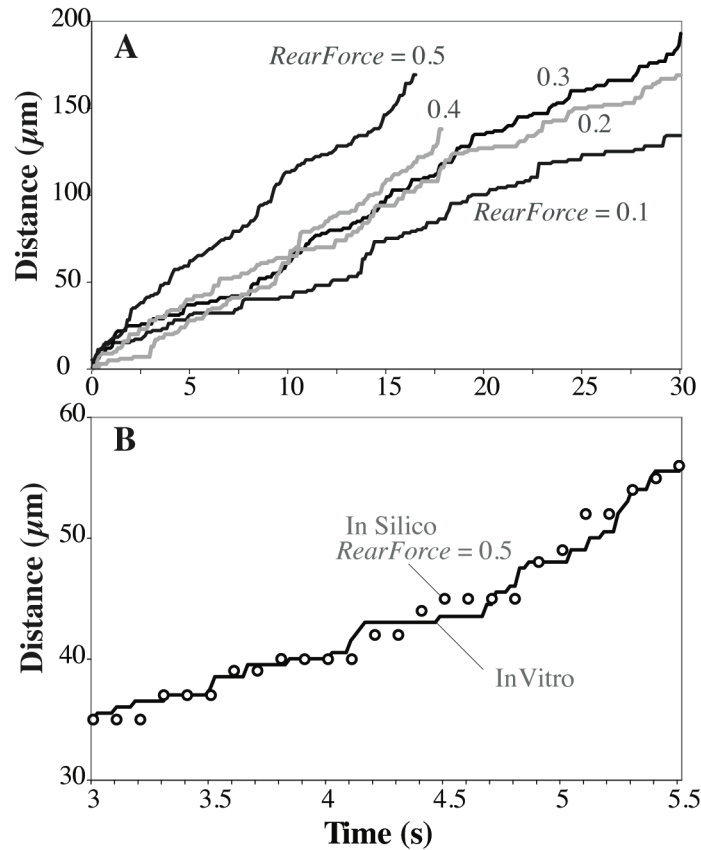
Figure 3.6 – LEUKOCYTES ROLLING on PSELECTIN exhibit the characteristic jerky stop-and-go pattern of leukocyte rolling in vitro

(A) Examples are graphed for distance-time plots for a single ROLLING LEUKOCYTE studied in each of the indicated five *RearForce* conditions using the ENVIRONMENT parameter values in Table 3.5 (part I-A). (B) Solid line: values of a single leukocyte trajectory as reported in [14]. Open circles: an example LEUKOCYTE trajectory from simulations that used the ENVIRONMENT parameter values in Table 3.5 (part I-B).

Simulated velocity-time measures also showed that LEUKOCYTES exhibited fluctuating velocities similar to those reported in the literature. Park et al. [15] observed human neutrophils rolling on P-selectin at a density of 9 sites/μm^2 under a wall shear rate of 0.5 dyn/cm^2. When we ran simulations using ENVIRONMENT parameter values from Table 3.5 (part I-C), we observed similar behavior: the range of both LEUKOCYTE ROLLING velocity values and distance values plotted in Figure 3.7 are similar to those reported in [15]. The results clearly exhibit the essential jerky stop-and-go movement and highly variable ROLLING velocities that are characteristic of leukocytes rolling in vivo and in vitro.
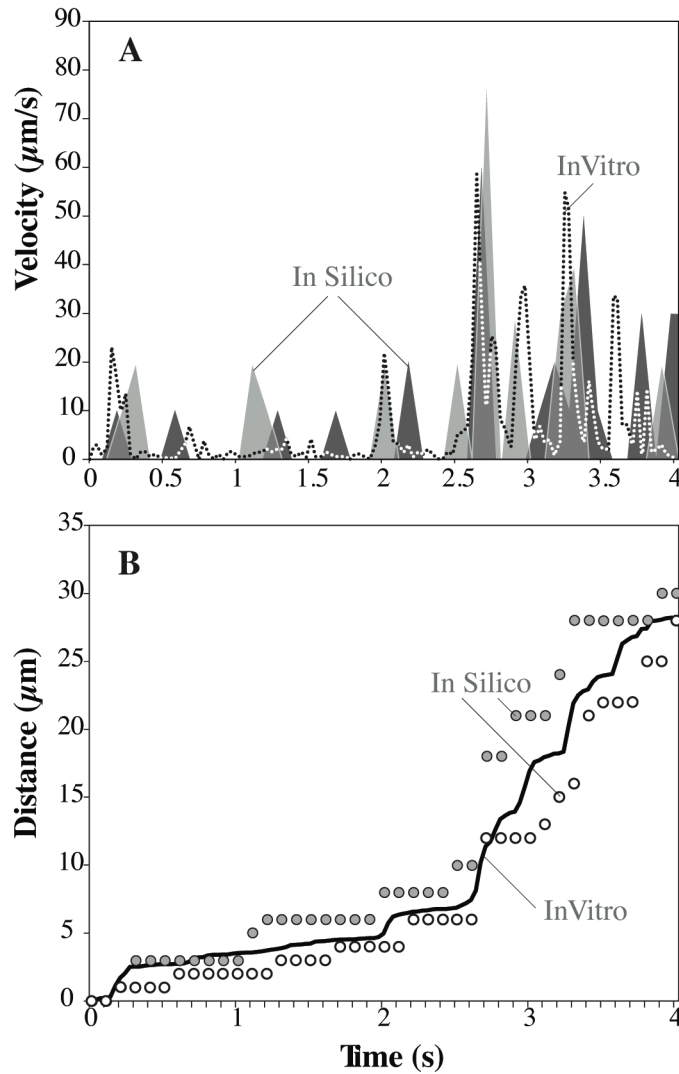
Figure 3.7. **Comparison of in silico and in vitro instantaneous velocity data** (A) Dotted trace: a leukocyte rolling on P-selectin in vitro as reported in [15]. Gray, shaded traces: two simulations of a LEUKOCYTE ROLLING on PSELECTIN using ENVIRONMENT parameter values from Table 3.5 (part I-C). Both traces show fluctuating rolling velocities similar to the dotted trace. (B) Distance-time plots from the experiments in A; solid line: in vitro leukocyte (calculated from the reported instantaneous velocity data); circles: the two in silico LEUKOCYTES from A.

To further evaluate and validate simulated leukocyte rolling, we determined the average ROLLING velocity, the average number of BONDS within the contact area along with the average number of BONDS at the rear of the LEUKOCYTE. Table 3.6 shows results. Average ROLLING velocities fell within ranges that have been reported for rolling on P-selectin. In addition, consistent with in vitro experimental data, average LEUKOCYTE ROLLING velocity increased with increasing *RearForce* values. The average number of BONDS within the contact area and the average number at the rear of the LEUKOCYTES under all three *RearForce* conditions were consistent with the estimated numbers stated above.

	RearForce				
	0.1	0.2	0.3	0.4	0.5
Average ROLLING velocity (µm/s)	3.42	5.19	7.98	10.68	14.16
Average number of BONDS in CONTACT ZONE	7.26	6.42	5.45	4.87	4.29
Average number of BONDS in the rear row of LEUKOCYTES' CONTACT ZONE	1.5	1.46	1.40	1.38	1.33

Table 3.6 Calculated Average ROLLING Velocities, BONDS in the Contact Zone, and BONDS in the Trailing Row of the LEUKOCYTES' CONTACT ZONE. Averages are from 60 simulations that had at least 10 INTERACTIONS (pauses). ROLLING velocities fall within ranges reported in the literature. Average number of BONDS in the CONTACT ZONE is in agreement with values estimated by mathematical models, which range from two to twenty bonds.

3.3.2 Experiments That Simulate Leukocyte Rolling on VCAM-1

VLA-4 is unique among the integrins, as it has been shown to support leukocyte tethering and rolling. In flow chambers coated with VCAM-1, a ligand for VLA-4, leukocytes roll even in the absence of selectins or chemokines [18, 19]. The goal of the second set of simulation experiments was to show that ISWBC ROLLING behaviors are similar to those of leukocytes rolling on VCAM-1 in the absence of chemokine. Alon et al. observed human T-lymphocytes rolling on different densities of purified VCAM-1 in flow chambers [18] under increasing shear stress. Shear was increased at fixed intervals resulting in increased leukocyte rolling velocities. Using parameter values from Table 3.4 and Table 3.5 (part II), simulations generated LEUKOCYTE ROLLING trajectories that appeared to be indistinguishable to those reported by Alon et al (Figure 3.8). Average ROLLING VELOCITIES were calculated for each *RearForce* value. They were within the range of in vitro rolling velocities at each reported shear stress value (Figure 3.8, Insert).
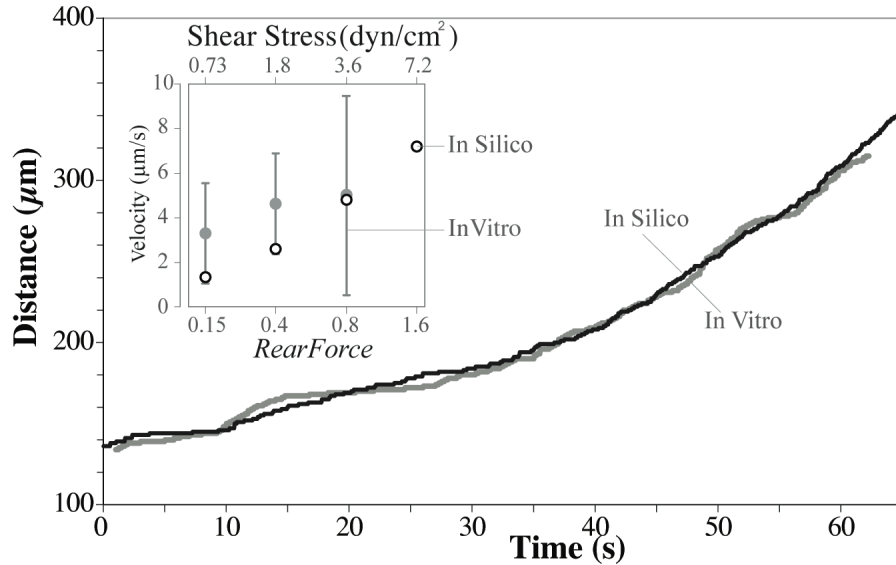
Figure 3.8. **Simulating experimental condition 2: rolling on VCAM-1 with shear increased at fixed intervals.** Alon et al. [18] observed T-lymphocytes rolling on VCAM-1 in the absence of chemokine under increasing wall shear stress; wall shear stress was increased at fixed intervals causing increased leukocyte rolling velocities. Black line: a leukocyte trajectory reported in [18]. Gray line: an example LEUKOCYTE trajectory when using ENVIRONMENT parameter values from Table 3.5 (part II). Insert: in vitro measures of leukocyte velocity for different values of shear (upper axis); the standard deviations (vertical bars) were conservatively estimated using the standard errors reported in [18]. Circles: average ROLLING velocities of LEUKOCYTES (n = 60) for different *RearForce* values (lower axis) fall within the in vitro ranges. The original published distance-time plots begin at ~140 microns.

3.3.3 Simulating Leukocyte Rolling, Activation, and Adhesion on P-selectin and/or VCAM-1 in the Presence or Absence of GRO-α Chemokine

Smith et al. [19] used a flow chamber to observe human monocytes rolling and adhering on P-selectin and VCAM-1 with or without immobilized GRO-α chemokine: six different conditions. During perfusion of leukocytes through the flow chamber, 30-second recordings of five fields of view were taken along the chamber length. The average number of rolling and arrested cells was determined. Cells that did not roll for at least 20 seconds were considered arrested. Using that same combination of in silico substrate analogues, the ISWBC parameter space, constrained by the already established parameter values in Table 3.5 (parts I and II), was searched empirically for parameter sets that would provide acceptable matches for all six experimental conditions. The LEUKOCYTE parameters from Table 3.4 and the ENVIRONMENT parameters from Table 3.5 (part III) represents such a set; it produced the in silico results in Figure 3.9: the results are averages from 20 sets of in silico experiments containing 30 LEUKOCYTES each, with the duration of each run being 300 simulation cycles (equivalent to about

40

30 seconds). The number of ROLLING and adhering LEUKOCYTES for each batch were counted and averaged. LEUKOCYTES that remained stationary on the SURFACE for at least 200 simulation cycles (about 20 seconds) were classified as ADHERED. Figure 3.9 shows that for all ligand combinations simulated, the data matched that from in vitro fairly well. There was even a similar significant increase in the number of ADHERENT LEUKOCYTES on PSELECTIN and VCAM1 due to the presence of GROA CHEMOKINE, as was observed in vitro.
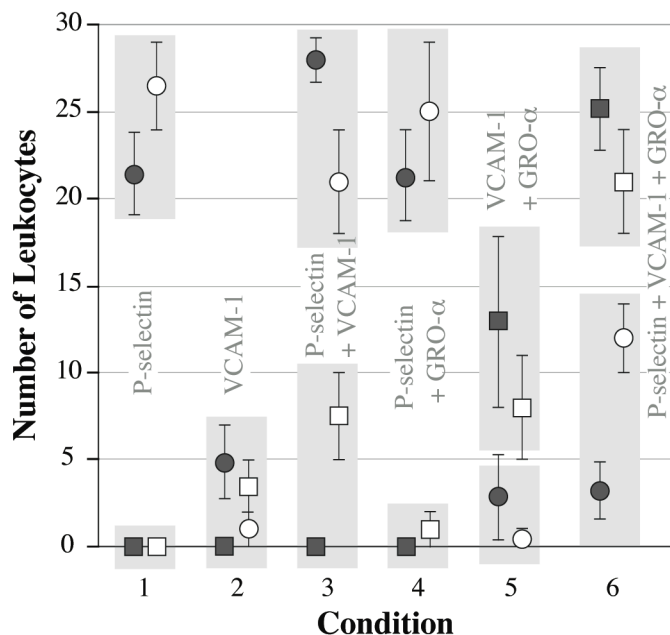
Figure 3.9. Comparison of in vitro and in silico results for rolling and adhesion for six different experimental conditions. The in vitro conditions (from [19]): the flow chamber surface was coated with P-selectin and/or VCAM-1 with or without immobilized GRO-α chemokine. The number of leukocytes that rolled and adhered within each of five fields of view were recorded for a 30-second observation interval. In vitro: white circles: average number of leukocytes that rolled; white squares: average number of leukocytes that adhered; error bars: ± 1 SD. The data are clustered and plotted for each of six conditions, as labeled. By using the parameter values in Table 3.5 (part III), the in silico experiments mimicked the in vitro experimental conditions and also the results: the results are averages from 20 sets containing 30 LEUKOCYTES each; each simulation ran for 300 simulation cycles (equivalent to about 30 seconds). In silico: dark circles: average LEUKOCYTES that ROLLED; dark squares: average LEUKOCYTES that ADHERED; error bars: ± 1 SD. Each light gray box contains the two sets of observations (in vitro and in silico) that should be compared.

There are some notable discrepancies between the in silico and in vitro data that are most likely a consequence of the ISWBC being an abstract simplification of the more complex reality. For example, in the absence of GRO-α chemokine, Smith et al. observed a small fraction of cells

that were able to adhere when rolling on VCAM-1 alone or when VCAM-1 was co-immobilized with P-selectin. This small fraction of adhering cells may be attributable to the pre-activation of monocytes during cell isolation procedures. We do not include any pre-activation effects, and consequently do not observe any ADHERING LEUKOCYTES in the absence of GROA CHEMOKINE. By affecting adhesion, the pre-activation of monocytes may additionally affect the number of rolling leukocytes on VCAM-1 substrate. We had such considerations in mind when we adjusted parameter values, and so did not seek the best possible match for any one condition. Instead, we focused on similarities in leukocyte behavior under different conditions. By adjusting parameter values to bring in silico and in vitro observations closer together for one condition, we typically amplified discrepancies for other conditions. If narrowing these discrepancies is deemed among the important issues to be addressed next, then our approach would be to include that specification within the targeted attribute list in Set C of Table 3.1. To achieve that goal, additional ISWBC detail would likely be required. Literature guided, exploratory simulations would be needed to identify candidate details. Fortunately, because ISWBC design and construction are being guided by the ten capabilities listed in the Introduction, such exploratory simulations are relatively easy to pursue.

Smith et al. also tracked individual monocytes under flow to obtain rolling and arrest profiles [19]. They observed that with P-selectin and VCAM-1 co-immobilized with GRO-α chemokines, monocyte arrest occurred within a few seconds. We simulated their protocol: we tracked individual LEUKOCYTES that were able to transition from ROLLING to FIRM ADHESION. We also observed that FIRM ADHESION on PSELECTIN and VCAM1 in the presence of GROA CHEMOKINE was primarily mediated by high affinity VLA4 and that it occurred within SECONDS. Figure 3.10 shows an example LEUKOCYTE that is able to ADHERE after ROLLING.
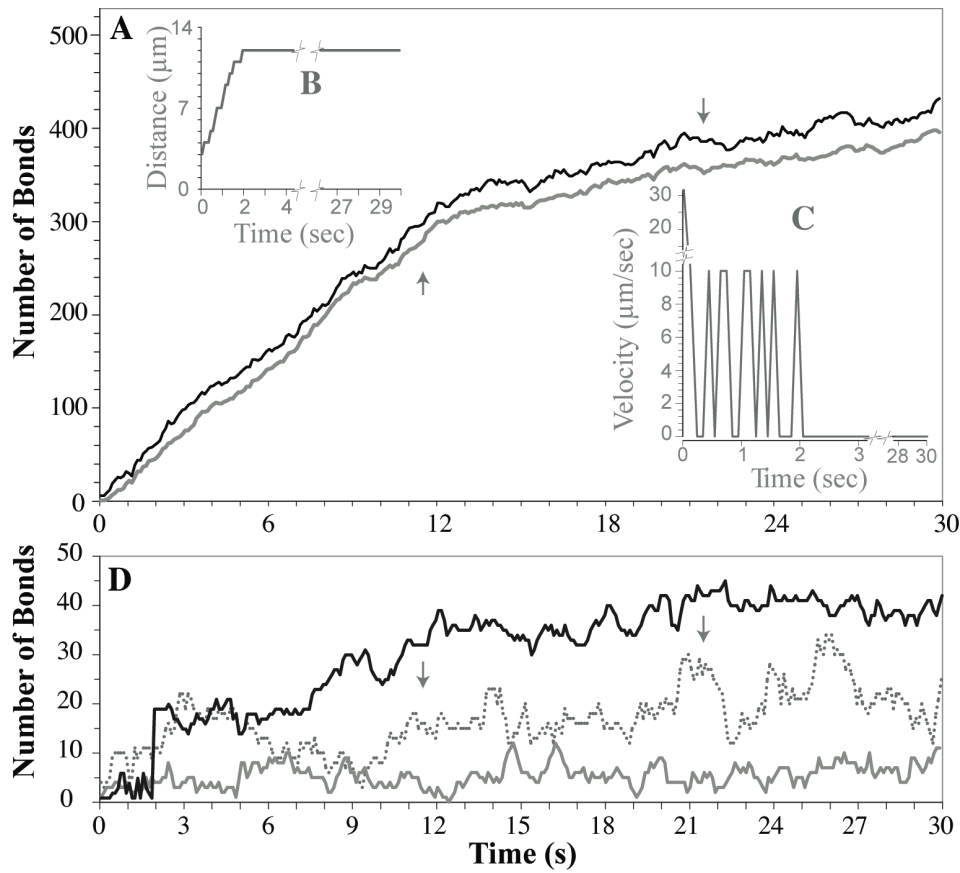
Figure 3.10 – Measurements from a LEUKOCYTE that ROLLED and ADHERED to PSELECTIN and VCAM1 after activation by GROA CHEMOKINE

Smith et al. [19] observed that when the flow chamber surface is coated with P-selectin and VCAM-1 co-immobilized with GRO-α chemokines, monocyte arrest occurred within a few seconds. The data graphed is from an in silico experiment that simulated that protocol and is for an individual LEUKOCYTE that transitioned from ROLLING to FIRM ADHESION (Table 3.5, part III). (A) Dark line: total number of BONDS formed within the CONTACT ZONE between LEUKOCYTE MEMBRANE and SURFACE. Light gray line: number of high affinity VLA4-VCAM1 BONDS formed: these results show that ADHESION is mediated primarily by the high affinity VLA4-VCAM1 BONDS. (B) DISTANCE-TIME plot and (C) VELOCITY-TIME plot: they show that the LEUKOCYTE rolled for less than a few simulated seconds before firmly adhering to the SURFACE, consistent with leukocyte adhesions observed in vitro. (D) For the same experiment, the number of low affinity VLA4-VCAM1 BONDS and PSELECTIN-PSGL1 BONDS are small and so are plotted here at a smaller scale. Dotted trace: number of low affinity VLA4-VCAM1 BONDS. Lower solid gray trace: number of BONDS formed between PSELECTIN and PSGL1. The black trace is a separate plot of the total number of BONDS formed at each time in the rear row of this CONTACT ZONE; these data show that for the ISWBC, the LOW AFFINITY VLA4/VCAM1 AND PSELECTIN/PSGL1 BONDS play only a minor role in supporting ADHESION. Arrows indicate when a LEUKOCYTE MEMBRANE SPREADING event occurred.

43

3.4 Discussion

3.4.1 Design

The conceptual model of the referent system is fundamental in the design of the in silico model, and therefore should be stated: from the perspective of an external observer, the functionalities within the leukocyte membrane are grouped into a large number of similarly capable modular, functional units. Leukocyte rolling in vitro involves a balance between the hydrodynamic force exerted by fluid flow and the resistant forces resulting in part from transient bonds being formed between the leukocyte and the substrate. Shear force coupled with random events causes bonds to break at the rear of the contact zone. Bonds formed within the contact zone are by nature transient and will dissociate even in the absence of a tensile force. Only a few bonds need to be present at any time in order to maintain a rolling interaction. In order to maintain that interaction, broken bonds must be replaced by new ones formed elsewhere within the contact zone.

The transition from rolling to adhesion is mediated by the integrin receptors that, when induced into a high affinity state, are capable of forming effective ligand interactions that are sufficiently stable to withstand the hydrodynamic fluid force. However, they exist natively in a low affinity state and can only aid in supporting rolling interactions. There are many hypothesized mechanisms of integrin activation. We explored one of the simplest: a chemokine receptor, upon binding to its chemokine ligand, induces a local VLA-4 integrin molecule into a high affinity state. The resulting high affinity integrins form stronger and longer-lasting bonds with VCAM-1. Diffusion and clustering of VLA-4 integrins is also hypothesized to play a role in firm adhesion. However, to keep things relatively simple at this early stage, we have not simulated those events.

3.4.2 Achievements

The ISWBC components have been verified, plugged together, and operated in ways that may represent (at a relatively high level) mechanisms and processes that influence leukocyte rolling and adhesion. This approach has allowed us to represent the spatial and discrete event phenomena that are thought to occur during leukocyte rolling, activation, and adhesion. It has allowed us to represent apparently stochastic elements within the system that may play a vital role in determining leukocyte behavior *in vivo* and *in vitro*. Our earliest archetype had a CONTACT ZONE comprised of 2 x 3 MEMBRANE UNITS (48 for the total MEMBRANE of the LEUKOCYTE). With it, we failed to even approach the first two targeted attributes in Set A, Table 3.1; we were unable to simulate the stochastic fine structure present in the in vitro data because the discretization was too coarse. It is common in simulation that such artifacts show up when the discretization (granularity) is too coarse. To better achieve the targeted behaviors, we decreased the relative MEMBRANE UNIT size (decreased granularity) to represent the CONTACT ZONE by 3 x 6 units and then in steps to the current size of 8 x 10 units (600 UNITS for the total MEMBRANE). With each increase in granularity, simulated results more closely mimicked the in vitro data, as judged by inspection. We also explored even finer grained CONTACT ZONES, up to 20 x 30, without further apparent gains in similarity. Taken together, these results suggest that membrane functionality within and adjacent to the contact zone is distributed into many (from our results, about 80) equally capable units.

Though the ISWBCs are relatively simple, we have demonstrated that they can generate the targeted attributes under three different experimental conditions. Traditional models typically focus on just one condition. ISWBCs mimic the dynamics of leukocytes rolling separately on a P-selectin or VCAM-1 substrate under simulated flow conditions. In addition, they mimic the transition from rolling to adhesion on P-selectin and VCAM-1 in the presence of GRO-α chemokine. Importantly, when simulating populations of leukocytes under different experimental conditions (combinations of substrate molecules), the in silico system generates quantitative population-level data that are similar to data from in vitro experiments.

One hypothesis of leukocyte activation suggests that leukocytes roll along the vessel wall progressively engaging with chemokine signals to reach a global activation threshold. Once achieved, fully activated integrins can then support firm adhesion. However, there is growing support for an alternative hypothesis: leukocyte adhesion induced by immobilized chemokines occurs via local and spatially restricted signaling events to nearby integrins. Our results support the latter hypothesis. In an elegant study, Shamri et al. [84] showed that leukocyte engagement with chemokine locally and reversibly induced the β_2 integrin, LFA-1, into an intermediate affinity state that was essential for interaction with ICAM-1 under flow conditions. Concurrently, engagement with ICAM-1 induced the signaling events needed to fully activate local LFA-1 integrin to the high affinity state that supports firm adhesion. Because of the modeling approach used (providing the ten capabilities, etc.), it will be relatively easy, given appropriate research questions, for future descendents of the ISWBCs to represent such fine-grained, cooperative behaviors and spatially restricted events.

3.4.3 Appraisal of the Model Assumptions

We have simulated human leukocytes of slightly different sizes (neutrophils, lymphocytes, monocytes), however we kept the CONTACT ZONE the same for all simulations. It has been observed in vitro that leukocytes of greater size have a greater area of contact with the surface, and thus can form more bonds that are adhesive. However, biomechanical analysis shows that with increasing leukocyte size there is an increase in the amount of force and torque experienced. This higher magnitude is believed to translate to higher forces experienced by bonds. Cozen-Roberts [Cozen-Roberts '90] presented an analysis that was verified in vitro, which predicts that the disruptive force increases faster than the pro-adhesive effect of increased contact area. Rather than changing the dimensions of the contact area when simulating experiments with different leukocyte types and sizes, we fixed that dimension and compensated by using greater *RearForce* values to represent the same shear force when simulating larger leukocytes (see Table 3.5).

The conceptual model above is widely accepted for neutrophils. However, it is not entirely known how well it applies to other leukocyte types, such as lymphocytes and monocytes. Varying receptor types and densities found on the different leukocyte types may be a factor for differing mechanisms of adhesion. For example, lymphocytes and monocytes express basal levels of VLA-4 integrins sufficient to support rolling [18]. In contrast, it has been shown that transmigration across endothelium or exposure to chemotactic stimuli is necessary to induce expression of VLA-4 integrins on human neutrophils [85]. Therefore, rolling and adhesion through the VLA-4 integrin may require additional or different mechanisms for neutrophils than for lymphocytes and monocytes. Our overall objective was not to come up with a comprehensive model of rolling, activation, and adhesion for all leukocyte types. However,

when simulating monocyte rolling and adhesion, we assumed that monocytes and neutrophils share similar rolling characteristics on P-selectin. Likewise, we assumed that the characteristics of monocyte rolling on VCAM-1 are similar to those for lymphocytes. The only difference was presumed to be the densities of each receptor type found on each leukocyte type. Parameter values representing the densities of the VLA-4 integrins for lymphocytes in experimental condition 2 and monocytes in experimental condition 3 were different to reflect the different VLA-4 density values reported in the literature. Values for PSGL-1 sites/human monocyte were not found in the literature and were assumed to be similar to values reported for human neutrophils.

3.5 Summary

We have constructed a synthetic in silico model for representing the dynamics of leukocyte rolling, activation, and adhesion on substrate-coated flow chambers. Software components were designed, instantiated, verified, plugged together, and then operated in ways that can map concretely to mechanisms believed responsible for leukocyte rolling, activation, and adhesion in vitro using a flow chamber. The experiments using the ISWBC are analogous to those performed using an in vitro system. The SURFACE of the simulated chamber is "coated" with a uniform density of the LIGANDS of interest. While in the FLOW CHAMBER, LEUKOCYTES use their LIGANDS to interact and form BONDS with the SUBSTRATE-COATED SURFACE. Each BOND is an in silico analogue of a single ligand-ligand bond. Those interactions are recorded and measured. Under the influence of simulated flow, BONDS at the rear of the CONTACT ZONE experience a force due to shear.

The ISWBC was able to successfully represent the dynamics of individual leukocytes rolling separately on P-selectin and VCAM-1, along with the transition from rolling to adhesion on P-selectin and VCAM-1 in the presence of GRO-α chemokine. Additionally, the individual in silico and in vitro behavioral similarities translated successfully to population-level measures.

The current ISWBC is an important first step towards our long-term goal of building in silico devices that can simulate leukocyte behaviors in a variety of experimental systems even in the face of considerable uncertainty. The ISWBC are themselves useful objects for experimentation, as are the referent in vitro models. The current ISWBC is capable of mimicking only a few (Table 3.1A-B) of a long list of desired phenotypic attributes of leukocytes observed in vivo and in vitro. The expectation is that ISWBCs can be iteratively refined to become increasingly realistic in terms of both components and behaviors. Because we strove to deliver the ten capabilities listed in the Introduction, any of the above, abstract, low resolution components can be replaced with validated, more realistic, higher resolution composite objects composed of components that map to more detailed biological counterparts, without having to reengineer the whole system, and without having to compromise already validated features and behaviors.

4 Identifying the Rules of Engagement Enabling Leukocyte Rolling, Activation, and Adhesion[2]

4.1 Introduction

Integrin-mediated adhesion is a crucial regulator of cell-cell interactions as well as cell migration, yet its causal mechanisms are still not fully understood. Improved biological insight into how surface component interactions control the distinct steps for leukocyte trafficking, beginning with rolling and adhesion, will enable us to begin precisely manipulating integrin-mediated adhesive interactions between cells [86]. Sustained leukocyte adhesion sufficient to resist blood flow shear forces is a precondition to subsequent trafficking events. There is strong correlative evidence that some degree of LFA-1 integrin clustering as observed in vitro through fluorescence microscopy is essential for efficient, sustained adhesion [22, 34, 40]. Moreover, LFA-1 clustering may facilitate rebinding events, enhancing leukocyte adhesion even further [87, 88].

The use of advanced microscopy techniques have greatly enhanced our understanding of leukocyte trafficking in various tissues by allowing for the visualization of this process at the level of capillaries [47, 89-91]. However, even with current, state-of-the-art wet-lab and intravital microscopy methods, we cannot directly challenge those hypotheses (mentioned above) experimentally because it is infeasible to directly measure molecular level events during the leukocyte adhesion process. By employing relatively new, object-oriented, discrete event simulation methods in which quasi-autonomous components interact within and between nested biomimetic structures, it is feasible to construct, validate, and challenge concrete, working simulations of conceptualized mechanisms. The approach, methods, and objectives are different from those of the familiar inductive approach to modeling and simulation [11]. Upon discovering a system that validated under a variety of experimental conditions, we designed experiments that traced the consequences of specific mechanistic events and thus were able to test mechanistic hypotheses directly. We quantified the role of LFA-1 clustering in leukocyte–surface adhesion, and measured improvements in adhesion efficiency when they occurred. In addition, we determined precisely if and when rebinding events could contribute to sustained adhesion.

To obtain those new mechanistic insights, we needed to create new, multi-level, multi-scale simulation capabilities that could be merged seamlessly with previously developed single cell methods [92]. Object-oriented, software engineering methods were used to implement and iteratively revise biomimetic rolling and adhesion mechanisms [11, 92]. The products of the process were many, extant (actually existing, working, observable) hypothetical mechanisms: these components assembled as specified, will produce observable multi-level mechanisms upon execution that are analogous to those hypothesized to be responsible for leukocyte rolling and sustained adhesion. The objects included leukocyte analogues having multi-level surface components including diffusible LFA-1 analogues capable of clustering. We followed a rigorous, iterative refinement protocol to shrink the set of plausible biomimetic (biologically emulated) mechanisms. Simulation of finalized mechanisms led to validation: multiple, diverse,

phenomena similarities met prespecified similarity criteria for over a dozen different wet-lab experimental conditions, in vitro, ex vivo, and in vivo at both the cell and population levels. Consequently, the mechanisms presented herein stand as a cohesive, concrete, tested and challengeable, working theory about detailed events occurring at the leukocyte–surface interface during rolling and adhesion experiments.

Our simulations enabled us to view how different molecular interaction events on simulated leukocyte surfaces cause behaviors that are unique and diverse at both the molecular and leukocyte levels, and yet—importantly—narrowly constrained at the population level. Within the validated system, CLUSTERING of LFA1 objects was not necessary to achieve ADHESION as long as LFA1 and ICAM1 object densities were above a critical level. However, when LFA1 and ICAM1 object densities were both low and LFA1 CLUSTERING was enabled, ADHESION between LEUKOCYTE and simulated surface exhibited measurable, positive cooperativity. No such cooperativity was evident when densities were high.

Early during simulations, there were no differences in LFA1 REBINDING events with or without having LFA1 CLUSTERING enabled. Thereafter, however, CLUSTERING caused LFA1 REBINDING (to ICAM1) to increase. The situation was somewhat different for ICAM1 REBINDING. As early as 25 seconds into an experiment, significantly more ICAM1 REBINDING (to LFA1) was measured when LFA1 CLUSTERING was enabled.

Class IB phosphoinositide-3 kinase (PI3Kγ) signal transduction molecules play important roles in regulating inflammation. Recruitment of leukocytes lacking PI3Kγ is impaired in several animal models of inflammation. However, details of how PI3Kγ regulates recruitment have not been determined [38, 39]. PI3Kγ is upstream of many signaling pathways and is responsible for many additional leukocyte functions including chemotaxis, secretion, and the neutrophil respiratory burst [93]. To study the role of PI3Kγ in neutrophil adhesion, Smith et al. compared the behaviors of neutrophils from PI3K knockout (KO; PI3Kγ$^{-/-}$) and wild-type (WT) mice in ex vivo flow chambers coated with P-selectin (substrate for rolling), ICAM-1 (substrate for adhesion), and CXCL1 (arrest chemokine for leukocyte activation and subsequent induction of PI3Kγ signaling). Neutrophils from KO mice, compared to WT counterparts, had a reduced ability to adhere to substrate-coated surfaces. Similar experiments were undertaken in vivo in exteriorized cremaster muscle venules of mice injected with CXCL1, and the results were similar. Neutrophils from KO mice, compared to WT counterparts, adhered less to the CXCL1-treated venular surfaces. Interestingly, most neutrophils from KO mice were able to adhere, but only for short intervals [28]. Smith et al., hypothesized that the defects in adhesion observed ex vivo and in vivo were a result of an inability of LFA-1 to redistribute and cluster on the membrane of leukocytes in the PI3Kγ KO mice [28]. We used simulation experiments to directly test this hypothesis. LFA1 objects were designed to cluster upon multivalent binding to multivalent ICAM1 objects, in an analogous fashion to what was observed in vitro by Kim et al [22]. Inhibiting LFA1 CLUSTERING caused simulated neutrophil behaviors that closely mimicked the above adhesion defect results from both ex vivo and in vivo experiments in KO mice across eight different experimental conditions at both the cell- and population-level, including the transient adhesion of simulated KO neutrophils. Thus, the neutrophil–surface interaction model presented herein stands as a tested theory about the mechanistic events that may be occurring in normal and KO mice during neutrophil rolling and adhesion. Experimenting on descendants of these models may help speed discovery and development of critically needed immunotherapeutics [94].

4.1.1 Biological Background

Rolling, activation, and adhesion are critical events in the inflammatory response, as they are required for the proper recruitment of leukocytes to sites of tissue damage. The selectin family of receptors and their respective carbohydrate ligands largely mediate the initial interactions between leukocytes and endothelial cells. Their high frequency rates of association and dissociation allow for transient interactions that slow the speed of travel, enabling leukocytes to roll along the activated endothelial surface and integrate inflammatory signals, such as immobilized chemokines [6].

The transition from rolling to adhesion is exclusively mediated by integrin receptors. They can exist in multiple conformational states each having different ligand binding properties. Low-, intermediate-, and high-affinity states have been identified. Natively, these integrins exist in non-adhesive, low-affinity states to prevent leukocytes from sticking non-specifically to blood vessel surfaces. Upon detection of immobilized chemokines, such as CXCL1, intracellular signaling events can trigger integrin conformational changes to high affinity states that enable a leukocyte to adhere firmly [4]. Post-adhesion events involving integrins are thought to help strengthen the attachment to the endothelium [28, 31].

Earlier studies, in addition to those cited in the Introduction, have provided evidence that LFA-1 clustering is mediated by PI3K and that the process is important for leukocyte adhesion. Constantin et al. showed that chemokines triggered a rapid increase in LFA-1 affinity on lymphocytes. Using immunofluorescently labeled LFA-1 with confocal microscopy, they observed that chemokines also stimulated LFA-1 movement into clusters and large polar patches [34]. Inhibiting PI3K activity blocked LFA-1 mobility but had no effect on LFA-1 affinity change. In separate experiments, PI3K inhibitors prevented lymphocytes from adhering to low densities of immobilized ICAM-1 substrate. At high ICAM-1 densities, inhibiting PI3K had no effect on lymphocyte adhesion. Whether this same phenomena exists in neutrophils remains to be determined.

4.2 Methods

4.2.1 Executable Biology

The simulation system we have constructed is designed to be an experimentally useful analogue of the wet-lab experimental systems used to study leukocyte rolling and adhesion (Figure 4.1). Wet-lab experimental systems provide data that can be used to generate mechanistic hypotheses. We used the synthetic modeling method, an example of what has been referred to as executable biology [12, 13], as a means to instantiate those mechanistic hypotheses so that they can be evaluated and tested. Object-oriented, agent-based software components were designed, instantiated, verified, plugged together, and then operated in ways that can map concretely to mechanisms and processes believed responsible for leukocyte rolling and adhesion. An agent is a quasi-autonomous object capable of scheduling its own actions in much the same way as we imagine cells and some of their components (such as a mitochondrion or modular subsystem) doing. See [92] for details of this approach, the basic framework of the in silico white blood cell (ISWBC), and an iterative refinement protocol for successively developing and validating simulation results. To distinguish the previous version from the current one, we refer to the

former as ISWBC1 (in silico white blood cell) and the latter as ISWBC2. Below we summarize details and the new ISWBC2 capabilities.
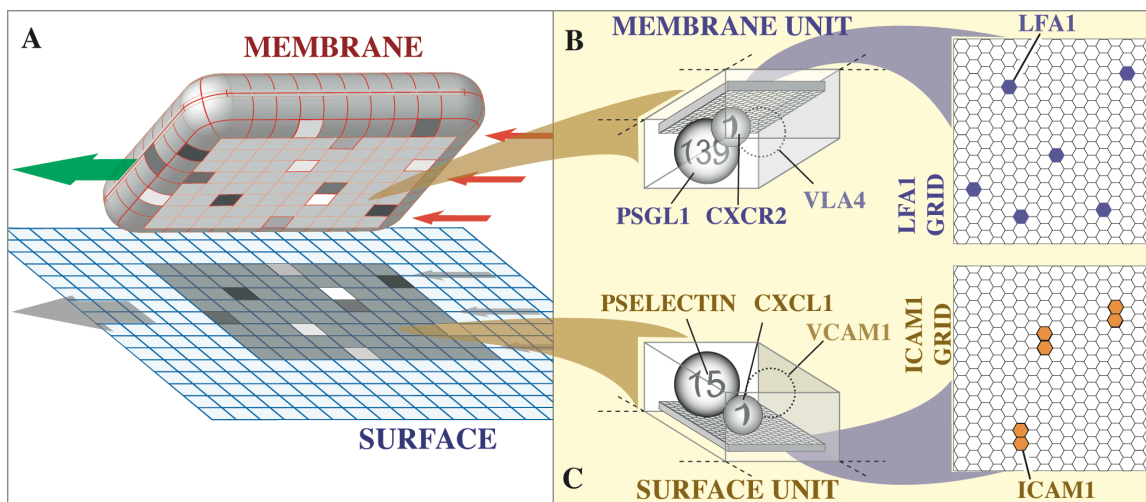
Figure 4.1. **Sketch of the ISWBC2 experimental system components**. (A) A LEUKOCYTE agent is shown pulled away from the simulated surface to which it was attached. The left arrow indicates ROLL direction; the three right arrows indicate SHEAR resulting from the simulated flow. The SURFACE is discretized into independent units of function called SURFACE UNITS. The LEUKOCYTE'S MEMBRANE is similarly discretized into matching units called MEMBRANE UNITS: 600 total (20 x 30). The 8 x10 shaded region on the SURFACE and on the LEUKOCYTE'S underside identifies the CONTACT ZONE. The UNITS within the CONTACT ZONES that are shaded differently indicate that different numbers of BONDS had formed between LIGAND–LIGAND pairs in overlapping UNITS; otherwise, no BONDS formed. ROLLING is the result of a sequence of forward ratchet events. One ratchet event is the result of one row of MEMBRANE UNITS being released at the rear of the CONTACT ZONE along with engagement of a new row of at the front of the CONTACT ZONE. One ratchet event maps to a leukocyte rolling approximately 1 μm (relative to the flow chamber surface). (B) A MEMBRANE UNIT is illustrated. Each is a software object functioning as a container. All leukocyte membrane functionality (relevant to these studies) within each unit of surface on ICAM1GRID is represented by the four objects: PSGL1, VLA4 (not used for most experiments), CXCR2, and LFA1. They map to leukocyte receptors; they are illustrated as spheres. The number on each sphere indicates the number of receptors to which that agent maps. Mobile LFA1 objects reside on a LFA1GRID. Each LFA1 maps to an individual LFA-1 molecule. (C) A SURFACE UNIT is illustrated. Similar to MEMBRANE UNITS, each SURFACE UNIT is simulated using a software object functioning as a container. All flow chamber surface functionality (relevant to these studies) within each SURFACE UNIT is represented by four objects: PSELECTIN, VCAM1 (not used for most experiments), CXCL1, and ICAM1. They map to surface receptors and chemokines. The number on each sphere indicates the number of receptors or chemokines to which that agent maps. Similar to LFA1, an ICAM1 resides on ICAM1GRID, a 2D hexagonal lattice, and maps to an individual ICAM-1 molecule.

50

4.2.2 Iterative Refinement Method

The greater the similarity between the measured behaviors, or phenotype, of an ISWBC2 and corresponding wet-lab attributes of interest, the more useful it will become as a research tool and as an expression of the coalesced, relevant leukocyte knowledge. The expectation has been that increasing phenotype similarity will require, and can be achieved in part through, similarities in design plan and in generative mechanisms. We follow an iterative refinement protocol to systematically and sequentially extend the overlap of the model and referent system phenotypes. This iterative refinement protocol allows us to concatenate in a dynamic fashion new knowledge about the referent systems into the synthetic model, without having to reengineer the whole system, and without having to compromise already validated features and behaviors [92, 95-97]. It is as follows:

- For the wet-lab systems being studied, create a list of attributes to be targeted.
- Design, construct, and enable the analogue to exhibit the targeted phenotypic attributes.
- Iteratively falsify and revise the operating mechanisms until the analogue exhibits the targeted phenotypic attributes within a pre-specified level of similarity, thereby achieving a level of validation.
- The process is then repeated with the addition of more phenotypic attributes to the targeted list.

It is important to note that validity is distinguishable from verity. For this technical context, we define validity as the degree to which an assertion (such as an ISWBC2) can be trusted as true enough or true to within some tolerance (e.g., the similarities discussed herein). In contrast, verity targets ontological truth, regardless of any arguments or belief. One cannot verify a representation such as an ISWBC2 against reality because of the ontological wall. Therefore, we define (http://biosystems.ucsf.edu/research_dictionary.html) verification as the process of determining where two statements agree and disagree, as in comparing a model to its corresponding simulation. One can only validate a representation against reality. Model validation can be achieved at several levels [98]. For example, one level of validation is through the qualitative reproduction of observed behaviors. Another level can be determined through parameter variability and sensitivity analysis. Changes to the values of input and internal parameters should affect model behaviors in a fashion similar to when analogous changes are made to the real system. Additionally, a level of validation can be achieved through the reliable prediction of new data. The most appropriate type and level of validation will depend on the intended model usage. ISWBCs were designed specifically to explain the diverse observations of leukocytes as they interact with endothelial surfaces, which is in contrast to inductive mathematical models that are typically intended for precise prediction [11].

We previously reported progress validating against our initial set of targeted attributes [92]. The ISWBC1 successfully represented the dynamics of individual leukocytes rolling separately on P-selectin and VCAM-1, along with the transition from rolling to adhesion on P-selectin and VCAM-1 in the presence of GRO-a chemokine. Additionally, the individual in silico and in vitro behavioral similarities translated successfully to population-level measures

(Table 4.1A).   Herein we extend the model by also targeting the phenotypic attributes of LFA-1 and ICAM-1 receptor mobility and clustering (Table 4.1B). Doing so allowed us to observe their hypothesized role in initiating adhesion in vitro and sustaining adhesion ex vivo.

Table 4.1 – Revised List of Targeted Phenotypic Attributes of Leukocytes.

ISWBC1 focused primarily on Set A. Once satisfactory simulations began to be achieved, the targeted attributes were expanded to those in Set B. Final validation efforts for ISWBC2 focused on the combined set.

Phenotypic Attribute	Reference
Set A: previously targeted attributes	
Characteristic jerky stop and go movement during rolling	[14]
Highly fluctuating rolling velocities	[15]
Larger rolling velocities observed at higher shear rates	[16]
Smaller rolling velocities at higher ligand substrate densities	[16]
ROLLING velocities on PSELECTIN match reported values	[16]
Small number of bonds within the contact zone, e.g., within 2-20	[17]
Distance-time and velocity-time data for ROLLING on PSELECTIN/VCAM1 are indistinguishable from reported data	[14, 15, 18]
Chemokines induce adhesion within seconds	[19]
Set B: currently targeted attributes	
LFA-1 and ICAM-1 lateral mobility and diffusion	[21]
LFA-1 nanocluster formation upon binding multivalent ligand	[22]
ICAM-1 spatial configurations in vivo	[23-27]
Effect of phosphoinositide 3-kinase inhibitors on adhesion ex vivo	[28]
Effect of phosphoinositide 3-kinase inhibitors on adhesion in vivo	[28]
Set C: future targetable attributes	
Induction of LFA-1-dependent neutrophil rolling on ICAM-1 by engagement of E-selectin	[29]
Synergistic effect observed during neutrophil rolling on P- and E-selectin	[30]
Effect of inhibitors to other signaling molecules on cell arrest (pertussis toxin (PTx)-sensitive G proteins, p38 mitogen-activated protein kinase)	[29]

4.2.3 The In Silico Analogue

We used RePast 3 as our modeling and simulation framework. It is a java-based software toolkit developed at the University of Chicago for creating and exercising agent-based models (http://repast.sourceforge.net/repast_3/index.html). The libraries provided were used to create, run, display, and collect data.

4.2.3.1 Model Components

To avoid confusion and clearly distinguish model components, features, measurements, and events from their *in vitro* or *ex vivo* counterparts, we use SMALL CAPS when referring to those of analogues. The biological aspects of the referent experimental systems and their ISWBC2 counterparts are listed in Table 4.2.

Table 4.2. Table of Biological Aspects from the Experimental System and their ISWBC2 Counterparts. SURFACE maps to either the endothelial cell surface or flow chamber surface depending on the simulation experiment.

Biological Aspects	Model Components	Description or Type
Substrate-Coated Surface	SURFACE	2D Square Lattice (low resolution)
Functional Unit of the Surface	SURFACE UNIT	Grid Unit of the SURFACE
Surface area containing ICAM1	ICAM1GRID	2D Hexagonal Lattice (high resolution)
Leukocyte	LEUKOCYTE	Object
Leukocyte Membrane	MEMBRANE	2D Square Lattice (low resolution)
Functional Unit of Leukocyte Membrane	MEMBRANE UNIT	Grid Unit of the MEMBRANE
Membrane area containing LFA1	LFA1GRID	2D Hexagonal Lattice (high resolution)
Chemokine	CXCL1	Object
Chemokine Receptor	CXCR2	Receptor Object
Adhesion Molecule	ADHESION MOLECULE	Receptor Object
Tensile Force on Rear Bonds	Parameter: *RearForce*	Parameter representing force due to shear
Hypothesized Biological Mechanisms	Operating Mechanisms	Algorithms

The SURFACE with which LEUKOCYTES interact is discretized into independent units of function called SURFACE UNITS. The LEUKOCYTE'S MEMBRANE is similarly discretized into matching units of function called MEMBRANE UNITS. For simplicity, the SURFACE and MEMBRANE are both implemented as 2D toroidal lattices. With current parameter values, one SURFACE UNIT maps to approximately 1 μm^2 and when rolling or adhered, one MEMBRANE UNIT maps to the same amount of surface area on the cell membrane. Contained within each UNIT are RECEPTOR objects, each one mapping to receptors found on the surface or leukocyte membrane. An eight x ten UNIT region shared between the SURFACE and the MEMBRANE identifies the CONTACT ZONE. It determines which SURFACE and MEMBRANE UNITS (and which of their RECEPTORS) can interact.

In ISWBC1s [92], the receptors found at the tips of microvilli (PSGL-1, VLA-4, and CXCR-2) were represented by the RECEPTOR objects PSGL1, VLA4, and CXCR2. Each one mapped to several binding molecules of the same type that may be found within a discrete area within the referent system. For example, a PSGL1 RECEPTOR mapped to several PSGL-1 adhesion molecules. The approximate number to which that object maps is determined by its parameter, *TotalNumber*. In ISWBC2, we have increased granularity (spatial resolution) by adding RECEPTOR objects LFA1 and ICAM1 and placing them within a higher granularity 2D hexagonal grid (LFA1GRID and ICAM1GRID) within some MEMBRANE UNITS and SURFACE UNITS, respectively, as illustrated in Figure 4.1B, C. LFA1 maps to the integrin molecule LFA-1 that is found on leukocyte membranes between microvilli [99, 100], while ICAM1 maps to its ligand-receptor ICAM-1. Distinct from the other RECEPTOR objects, each LFA1 and ICAM1 object maps to single molecules. Each high-resolution hexagonal grid space maps to approximately 100 nm^2 of leukocyte membrane or surface.

4.2.3.2 Behaviors

ISWBC2 experiments are analogous to those performed in vivo or using an ex vivo flow chamber system. While on the SURFACE, LEUKOCYTES use their RECEPTORS and the decisional processes sketched in Appendix Figure A.1 to interact and form BONDS with RECEPTORS on the SURFACE. Those interactions are recorded and measured. The ISWBC2 consists of components having three levels of spatial resolution illustrated in Figure 4.1: LEUKOCYTE-level, MEMBRANE/SURFACE UNIT-level, and LFA1 grid/ICAM1 grid-level. High-level behaviors are dependent upon the collective operation of objects and agents contained within each of the lower levels. For example, the behavior of MEMBRANE and SURFACE UNITS arise from the RECEPTOR objects contained within each. Similarly, the behavior at the LEUKOCYTE-level is dependent upon the collective events that occur within the underlying MEMBRANE/SURFACE UNITS. Conversely, events at the highest level impose constraints upon allowed lower level behaviors. For example, the positioning and movement of the LEUKOCYTE on the SURFACE dictate which MEMBRANE and SURFACE UNITS are overlapping and can interact.

4.2.3.2.1 RECEPTOR Behaviors

Local ACTIVATION of an INTEGRIN within a MEMBRANE UNIT occurs when a CHEMOKINE RECEPTOR detects a CHEMOKINE in an overlapping SURFACE UNIT. When an ACTIVATION SIGNAL is detected, local LFA1 RECEPTORS change from low to high affinity state. They achieve that by changing the parameter values *Pon* (BOND FORMATION rates), BOND b_0, b_1, and b_{Limit} (BOND DISSOCIATION properties), as described in Appendix. Relationships between the parameter

bondforce and probability of BOND DISSOCIATION for each of the four LIGAND pairs included in the ISWBC2 are given in Appendix Figure A.2 along with corresponding in vitro measurements.

The DIFFUSIVE properties of LFA1, specified by the parameter *LFA1MoveNum*, are also dependent on state. LFA1 lateral mobility parameters were specified as described in Appendix A.3 such that they have diffusive properties similar to those observed in vitro. Values are provided in Appendix Table A.1. *LFA1MoveNum* determines the number of attempts that an LFA1 object will take to move to a neighboring space within the LFA1GRID during a single simulation cycle. During lateral movement, LFA1 has an equal probability of moving into any of its six neighboring spaces, but it cannot move into an already occupied space. When simulating the endothelial cell surface, ICAM1 can similarly diffuse on the ICAM1GRID with a rate determined by the parameter *ICAM1MoveNum*. As a simple representation of some LFA-1 trafficking events (removal from endocytosis, deactivation, extraction from the membrane) [101, 102], UNBOUND LFA1 is removed from the MEMBRANE during each simulation cycle with a probability of *LFA1RemovalRate*.

4.2.3.2.2 LEUKOCYTE Movement

The number and location of BONDS at the SURFACE and MEMBRANE UNIT level combined with the decisional processes sketched in Appendix Figure A.1 determine LEUKOCYTE behavior. If there are BONDS between ADHESION MOLECULES within the rear column of the CONTACT ZONE, the LEUKOCYTE pauses, or remains stationary, until the next simulation cycle. If there are no BONDS within the rear column of the CONTACT ZONE, the LEUKOCYTE, influenced by the simulated shear force, performs a forward ROLLING movement. ROLLING is the result of a sequence of forward ratchet events. The process involves removing a column from the rear of the MEMBRANE'S rectangular CONTACT ZONE while a new one is placed at the front of the ZONE above the SURFACE.

4.2.3.2.3 Experimental Behaviors and Similarity Modeling Approach and Strategy

At the beginning of each simulation experiment, Boolean parameters (Table 4.3) determine whether LFA1 CLUSTERING (*LFA1Clustering),* preformed ICAM1 CLUSTERING in ENDOTHELIAL SURFACE UNITS (*ICAM1Pre-Clustered*), or ICAM1 TETRAMER FORMATION (*ICAM1Tetramer)* is allowed to occur.

When mean ISWBC2 results were within the range of mean ± SD of wet-lab results, the two sets of data were declared experimentally indistinguishable.

Table 4.3. Boolean Variables Determining which Rules and Behaviors are Allowed during Simulation

Boolean Parameter Name	Description
LFA1Clustering	Allow LFA1 agents to CLUSTER?
ICAM1Pre-Clustered	Allow ICAM1 agents to be prearranged into CLUSTER?
ICAM1Tetramers	Allow ICAM1 agents to form TETRAMERS upon LIGAND-BINDING?

4.2.3.2.4 LFA1 and ICAM1 CLUSTERING, and TETRAMERS

A LFA1 CLUSTER on the LFA1GRID is specified by the parameter *LFA1ClusterDiameter*. It determines the length and width of the region that LFA1 objects must stay within while DIFFUSING on the LFA1GRID. LFA1 CLUSTERS are formed by randomly choosing non-overlapping regions on the LFA1GRID and then filling each with all LFA1 within that MEMBRANE UNIT (Figure 2B). The number of CLUSTERS per LFA1GRID is specified by the parameter *NumLFA1Clusters*. During a simulation, CLUSTERS with unbound LFA1 randomly move to new and unoccupied locations within the LFA1GRID, a process that maps to molecular diffusion within a membrane region.

Different configurations of ICAM-1 have been reported in the literature. One study suggested that the native state of ICAM-1 is monomeric, because a monomer contains the complete binding site for LFA-1 [103]. Other studies provided evidence that dimeric ICAM-1 is the predominant form expressed by cytokine-activated endothelium [23, 26]. One such study showed that a dramatic conformational change of dimeric ICAM-1 occurs upon binding to LFA-1 such that they form one-dimensional chains of W-tetramers and higher order oligomers [27].

However, more recent studies by Barreiro et al. observed that ICAM-1 is clustered with other adhesion molecules into preformed tetraspanin-enriched microdomains on the surface of activated endothelial cells. They provided convincing evidence that these preformed microdomains might act as specialized endothelial adhesive platforms for leukocytes during adhesion and extravasation [24, 25]. Evidence from immuno-electron microscopy of fixed endothelial cells suggested that these organized microdomains might be smaller than 100 nm in diameter [104]. Scanning electron microscope images of activated endothelial cells stained with anti–ICAM-1 antibodies followed by 40-nm gold immunolabeling showed a cluster size of 2.4 ± 0.1 (mean $\pm$ SE) particles per nanoclusters.

In our simulations of in vivo experiments, we implemented the latter case where ICAM-1 exists preclustered (*ICAM1Pre-Clustered* = true). However, we also implemented the three other hypothesized ICAM-1 spatial configurations in order to observe their relative effects on LEUKOCYTE ADHESION: (1) native monomeric ICAM1 (Figure 4.2C), (2) native dimeric ICAM1 (Figure 4.2D), and (3) in Figure 4.2F, dimeric ICAM-1 forming linear W-tetramers upon ligand binding (*ICAM1Tetramer* = true).

In the simulations, when *ICAM1Tetramer* = true, a BOUND ICAM1 forms a linear TETRAMER structure with a nearby unbound dimeric ICAM1 object (Figure 4.2F). To keep things simple in simulations where *ICAM1Pre-Clustered* = true, preformed ICAM-1 nanoclusters were represented using three ICAM1 MOLECULES held together (Figure 4.2E).
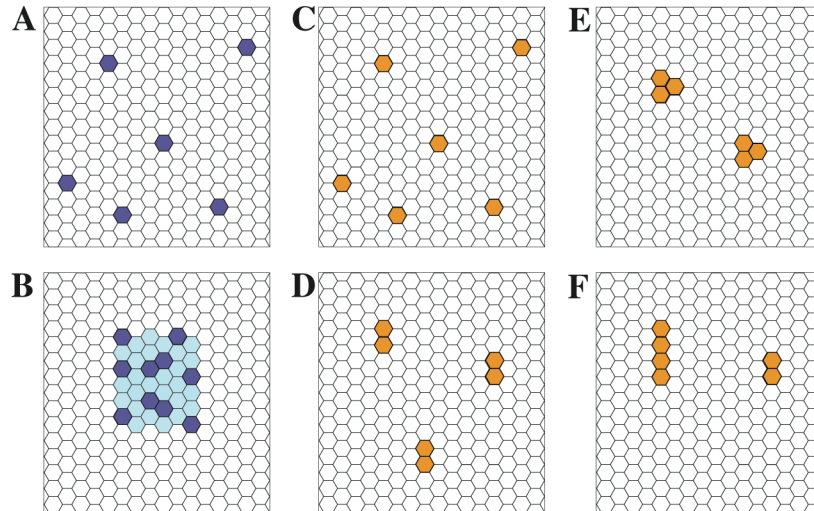
Figure 4.2. Illustrations of the different spatial configurations of LFA1 and ICAM1 ADHESION MOLECULES implemented and tested during simulations. LFA1GRIDS are shown with LFA1 objects labeled dark blue in either (A) a NONCLUSTERED state or (B) a CLUSTERED state. CLUSTERED LFA1 are spatially restricted within the light blue region. ICAM1GRIDS are shown with ICAM1 objects labeled yellow in either a (C) NATIVE MONOMERIC state, (D) a NATIVE DIMERIC state, (E) as preformed CLUSTERS, or (F) as W-TETRAMERS formed after LIGAND-BINDING.

4.2.4 Sensitivity Analysis and REBINDING

Upon achieving LEUKOCYTE behaviors that matched those from ex vivo and in vivo experiments, robustness to changes in a variety of key parameters were measured. Small (5-10%) and large (50%) parameter value changes were made to *Pon* (HIGH AFFINITY LFA1-ICAM1) (BOND FORMATION probabilities for LFA1-ICAM1), *RearForce*, and *LFA1RemovalRate*, while other factors were held constant. For each, ISWBC2 behaviors were recorded.

During a simulation, each LFA1 and ICAM1 object kept track of its BOND event and position history. When needed, that information was transferred to a separate file. Each MEMBRANE UNIT and SURFACE UNIT also kept track of the number of BOND events that involved RECEPTOR objects contained within, including LFA1 and ICAM1 REBINDING events.

4.3 Results

4.3.1 Re-validation Studies of ROLLING on PSELECTIN

Many iterative refinement cycles were performed in order to get from ISWBC1 to ISWBC2. While no code changes were made to the LEUKOCYTE RECEPTORS PSGL1 and VLA4 or to the SUBSTRATES PSELECTIN and VCAM1, software changes were made to manage the simulation output. Therefore, we deemed it necessary to test the ISWBC2's ability to reproduce some of the essential targeted phenotypic attributes from Table 4.1 that were previously used to validate the ISWBC1.

We repeated simulations of in vitro parallel plate flow chamber experiments that observed neutrophils rolling on various densities of P-selectin (9 and 25 sites/mm^2) and under varying wall shear rates (0.5, 1.0, and 2.0 dyn/cm^2), exactly as executed previously [92]. Using analogous in silico experimental conditions, the ISWBC2 LEUKOCYTES produced behaviors (not shown) that were indistinguishable from wet-lab results and from simulation results previously reported. LEUKOCYTES exhibited the characteristic jerky stop-and-go movement with highly fluctuating ROLLING velocities. Average ROLLING velocities were calculated and were still within the ranges reported in the literature. Higher average LEUKOCYTE ROLLING velocities were observed at higher simulated shear rates. At higher PSELECTIN SUBSTRATE densities, LEUKOCYTES ROLLED with smaller average ROLLING velocities. Lastly, comparison of PAUSE TIME distributions revealed no apparent difference between the ISWBC1 and ISWBC2. From these studies, we concluded that the new code introduced to transform ISWBC1 into ISWBC2 did not affect the model's ability to reproduce previously targeted phenotypic attributes.

4.3.2 LFA1 CLUSTERING and LEUKOCYTE ADHESION

To gain insight into the role of PI3Kγ on leukocyte rolling and adhesion under flow conditions, Smith et al. compared the behaviors of leukocytes from PI3Kγ KO and WT mice ex vivo using blood-perfused micro-flow chambers coated with the endothelial cell substrate molecules P-selectin, ICAM-1, and CXCL1 [28]. Nine one-minute recordings of a field of view were taken of the center of each chamber under each experimental condition. Population-level measures of rolling and adhesion were obtained by averaging the number of rolling and adherent cells for each condition. Arrested cells were defined as those that were adherent for at least 30 s. They observed a reduced ability of leukocytes from PI3Kγ KO mice to adhere to the coated surfaces in comparison to leukocytes from WT mice.

We simulated analogous experimental conditions to determine if the addition of a simple LFA1 CLUSTERING mechanism and its INHIBITION would enable the in silico system to mimic that adhesion defect. We used the same combination of substrate analogues. We explored the consequences of changing *LFA1Clustering* in isolation of other variables during each experiment. We chose parameter values based on reported literature values or searched empirically for parameter sets that would provide acceptable matches for all eight experimental conditions. Listed parameters found in the literature were from experiments specifically using murine neutrophils. The LEUKOCYTE parameters from Table 4.4 and the ENVIRONMENT parameters from Table 4.5 (part II) are such a set; they produced the results in Figure 4.3. The data are averages from 20 sets of experiments containing 30 LEUKOCYTES each, with the duration of each run being 600 simulation cycles (maps to 1 minute). The number of ROLLING and ADHERING LEUKOCYTES for each batch were counted and averaged. LEUKOCYTES that remained stationary on the SURFACE for at least 300 simulation cycles (about 30 seconds) were classified ADHERENT. Figure 4.3 shows that for all ligand combinations and genotypic variations simulated, both the LEUKOCYTE ROLLING and ADHESION data matched that from ex vivo experiments: the in silico and wet-lab results were indistinguishable experimentally.

58

	1	2	3	4	5	6	7	8
P-Selectin	+	+	+	+	+	−	+	−
ICAM-1	+	+	+	+	−	+	−	+
CXCL1	−	+	−	+	−	−	+	+
Mouse:	WT	WT	KO	KO	WT	WT	WT	WT
LFA1Clustering:	Yes	Yes	No	No	Yes	Yes	Yes	Yes
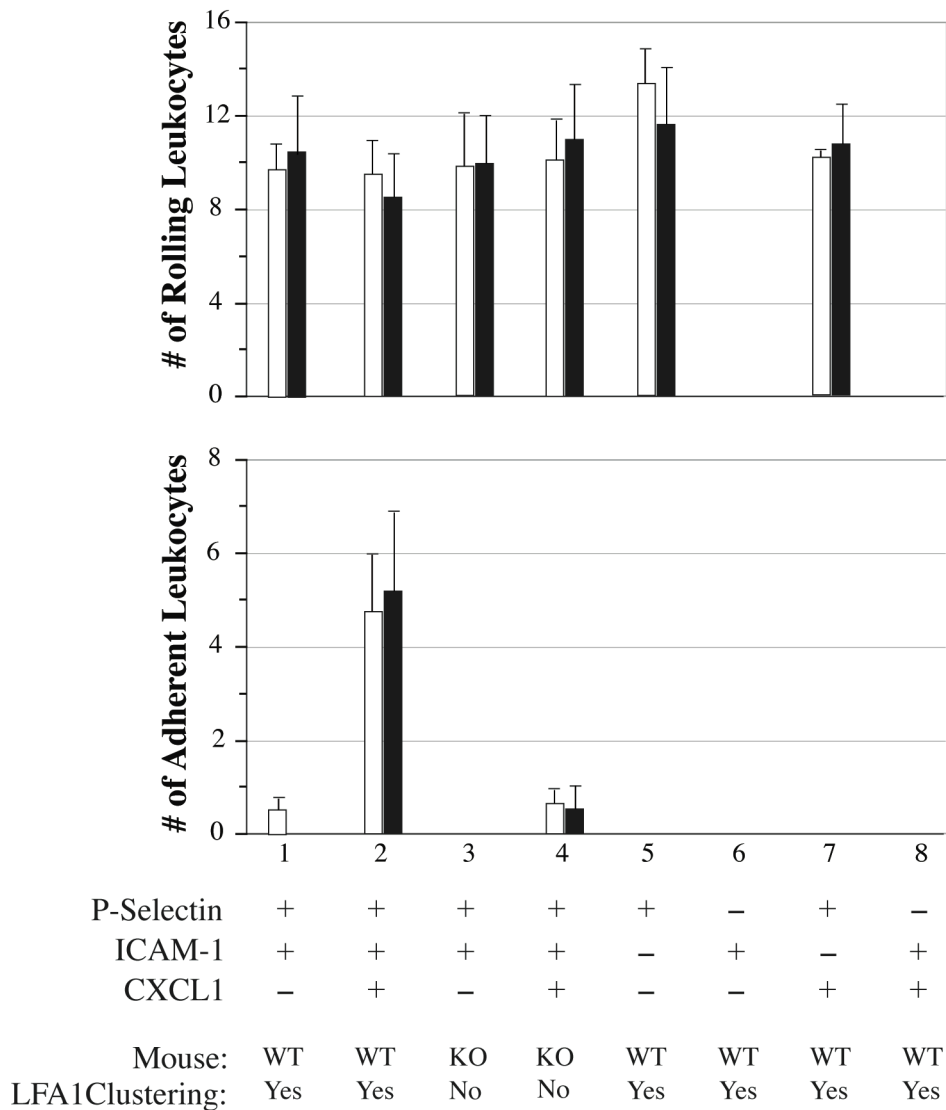
Experimental Condition

Figure 4.3. Ex vivo and in silico results for eight different experimental conditions are compared. Ex vivo conditions (from [28]): the flow chamber surface was coated with P-selectin and/or ICAM-1 with or without immobilized CXCL1 chemokine. Mice were either WT or PI3Kγ knockouts (KO). Leukocytes that rolled and adhered within each of five fields of view were recorded during a 60-second observation interval. White bars are ex vivo means ± 1 SE. The paired black bars are ISWBC2 means ± 1 SD (20 populations containing 30 leukocytes each) for the same condition using the parameter values in Tables 4.4 and 4.5. ISWBC2 experiments that map to WT mouse counterparts used *LFA1Clustering* = true. Simulations of KO mice used the parameter setting *LFA1Clustering* = false.

59

Table 4.4 – Parameter Values for the LEUKOCYTE MEMBRANE and LIGANDS along with Corresponding in Vitro Values.

Parameter Name	Description	Model Parameter Value	Experimental Value	Reference
LeukTotal Width	LEUKOCYTE MEMBRANE width (in the *y* [east-west] dimension)	20 MEMBRANE UNITS	Average murine Neutrophil Diameter: ~7 μm	[105]
LeukTotal Length	LEUKOCYTE MEMBRANE length (in the *x* [north-south] dimension)	30 MEMBRANE UNITS		
LeukExposed Width	CONTACT ZONE width (in the *y* dimension)	8 MEMBRANE UNITS	NA	NA
LeukExposed Length	CONTACT ZONE length (in the *x* dimension)	10 MEMBRANE UNITS	NA	NA
LFA1GridSize ICAM1GridSize	Length/width of LFA1GRID and ICAM1GRID	100 x 100	NA	NA
LFA1Grid Density	Density of LFA1GRID on MEMBRANE exposed to the SURFACE.	0.20	NA	NA
NumLFA1 Clusters	Number of LFA1 CLUSTERS / LFA1GRID formed if CLUSTERING is initiated	2	N/A	N/A
LFA1Cluster Diameter	The length and width of the LFA1 CLUSTER on the LFA1GRID	6	N/A	N/A
PSGL1Density	Mean number of PSGL-1 molecules (± standard deviation) represented by each PSGL1 agent	120 ± 5	~75,000/murine neutrophil[a]	[81]
LFA1Density	Mean number of LFA-1 molecules (± standard deviation) in each MEMBRANE UNIT	25 ± 5	~50,000/murine neutrophil[a]	[106]

LFA1 RemovalRate	Probability that an unbound LFA1 will be removed from the MEMBRANE	0.0025	NA	[101, 102]
CXCR2 Density	Number of CXCR-2 molecules (± standard deviation) represented by each CXCR2 agent	1	NA	NA
Pon (PSGL1-PSELECTIN)	Probability of forming a PSGL1-PSELECTIN BOND	0.001	NA [b]	[82]
Pon (LOW AFFINITY LFA1-ICAM)	Probability of forming a LOW AFFINITY LFA1-ICAM1 BOND	0.01	NA [b]	[107]
Pon (HIGH AFFINITY LFA1-ICAM1)	Probability of forming a HIGH AFFINITY LFA1-ICAM1 BOND	1.0	NA [b]	[108, 109]
Pon (CXCR2-CXCL1)	Probability of CXCR2 interacting with CXCL1	1.0	NA	NA
Poff (CXCR2-CXCL1)	Probability of CXCR2 releasing CXCL1	1.0	NA	NA

[a] Neutrophils were incubated with fluorescence-conjugated mAbs to LFA-1 or PSGL-1 and analyzed by FACScan flow cytometry. LFA-1 receptor number was quantified by comparing the binding of neutrophils to LFA-1-FITC with the binding of receptor-coated microbeads with known binding site densities [106]. PSGL-1 receptor number was determined in a similar fashion [81].

[b] *Pon* and *Kon* are intended to map to aspects of the same in vitro phenomena. However, there is no direct mapping between these parameters because the parent models belong to fundamentally different classes.

Table 4.5. Experimental values for the Blood-Perfused Micro-flow Chamber and the Cremaster Muscle Venule Experiments and the Corresponding ISWBC2 Parameter Values used for the Two Simulated Experimental Conditions.

| Experiment | Experimental Values | | | ISWBC Values | |
	Experimental Parameter	Experimental Value	Reference	PARAMETER	VALUE
I. Blood Perfused Micro-flow chamber					
	P-Selectin	18 μg/mL	[28]	PSELECTIN	15 ± 5
	ICAM-1	15 μg/mL	[28]	ICAM1	25 ± 5
	CXCL1	15 μg/mL	[28]	CXCL1	1
	Shear	2.5 dyn/cm^2	[28]	*RearForce*	0.6
II. In Vivo Neutrophil Adhesion on P-selectin/dICAM-1/CXCL1					
	P-Selectin[a]	1.02x10^7 molecules/cm^2	[110]	PSELECTIN	12 ± 5
	ICAM-1[a]	8.90x10^7 molecules/cm^2	[110]	ICAM1	6 ± 3
	CXCL1	5 μg/mL	[28]	CXCL1	1
	Shear	1-4 dyn/cm^2	[16]	*RearForce*	0.6

[a] Neutrophils were incubated with radiolabelled mAbs to P-Selectin or ICAM-1 and analyzed by laser confocal microscopy. The receptor number is determined by the binding ratio between the fluorescence and immunoglobulin [110].

4.3.2.1 Effect of varying *ICAM1Density* and *LFA1GridDensity*

We varied the values of *ICAM1Density* (density of ICAM1) to determine their impact on simulation outcomes. The results in Figure 4.4 show that at *ICAM1Density* values ≥ 60, disabling CLUSTERING (by changing *LFA1ClusteringAllowed* from true to false) did not change ADHESION. However, at *ICAM1Density* values ≤ 50, disabling CLUSTERING reduced ADHESION. The greatest differences were observed at the lower *ICAM1Density* values, indicating that with CLUSTERING there was cooperative binding between surfaces. We repeated this set of experiments twice (varying *ICAM1Density* values), but *LFA1GridDensity* (the fraction of all MEMBRANE UNITS that contain LFA1GRIDS) values were changed first to 0.1 and then to 0.4. Similar cooperative binding effects were observed at both *LFA1GridDensity* values, but at different ICAM1Density values and with differing magnitudes (Appendix Figs. A.3A and B).

The experimental observations above map well to results of wet-lab experimental studies done by Constantin and co-workers. They demonstrated that PI3K inhibition blocked

lymphocyte adhesion at low densities of ICAM-1. At high ICAM-1 densities, lymphocytes were able to overcome the requirement for PI3K for efficient adhesion [34].

4.3.2.2 Robustness of ISWBC2s to Changes in the *LFA1RemovalRate, Pon,* and *RearForce*

Results of sensitivity analysis experiments for changes in *LFA1RemovalRate*, *Pon* (high affinity LFA1-ICAM1), and *RearForce* are graphed in Figure 4.5. The simulations were repeated using small (5-10%) and large variations (> 50%) in each of these parameters separately, while holding all other parameter values constant. Figure 4.5 shows the ratio of ISWBC2-to-wet-lab results for rolling and adhesion data from both WT and KO mice for four parameter variations selected to show the trends observed. Small variations in all three parameter values resulted in minimal changes in ROLLING and ADHESION both with and without CLUSTERING. The results still matched referent data reasonably well. As was expected, large increases in the *RearForce* (Figure 4.5A) and *LFA1RemovalRate* (Figure 4.5B), or a large decrease in *Pon* values (Figure 4.5C) resulted in a significant decrease in ADHESION both with and without CLUSTERING. Those results failed to match referent data. Results of these and other robustness explorations (not shown) demonstrated that there are many parameter vectors close to the ones in Table 4.4 and Table 4.5 that produce ISWBC2s that validate.
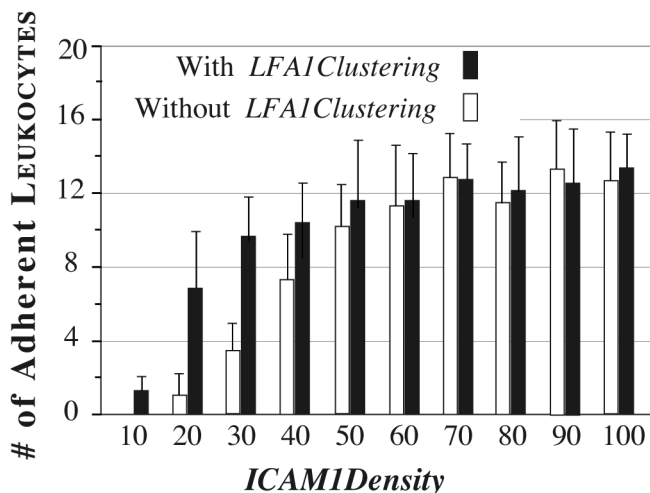
Figure 4.4. Effect of varying *ICAM1Density* parameter values on LEUKOCYTE ADHESION. The effect of Leukocyte *ICAM1Density* was varied from 10 to 100 at intervals of 10. Bar heights are ISWBC2 means ± 1 SD (20 populations containing 30 leukocytes each) for the same condition using the parameter values in Tables 4.4 and 4.5. Black bars indicate simulation experiments when *LFA1Clustering* = true. White bars indicate simulation experiments when *LFA1Clustering* = false.
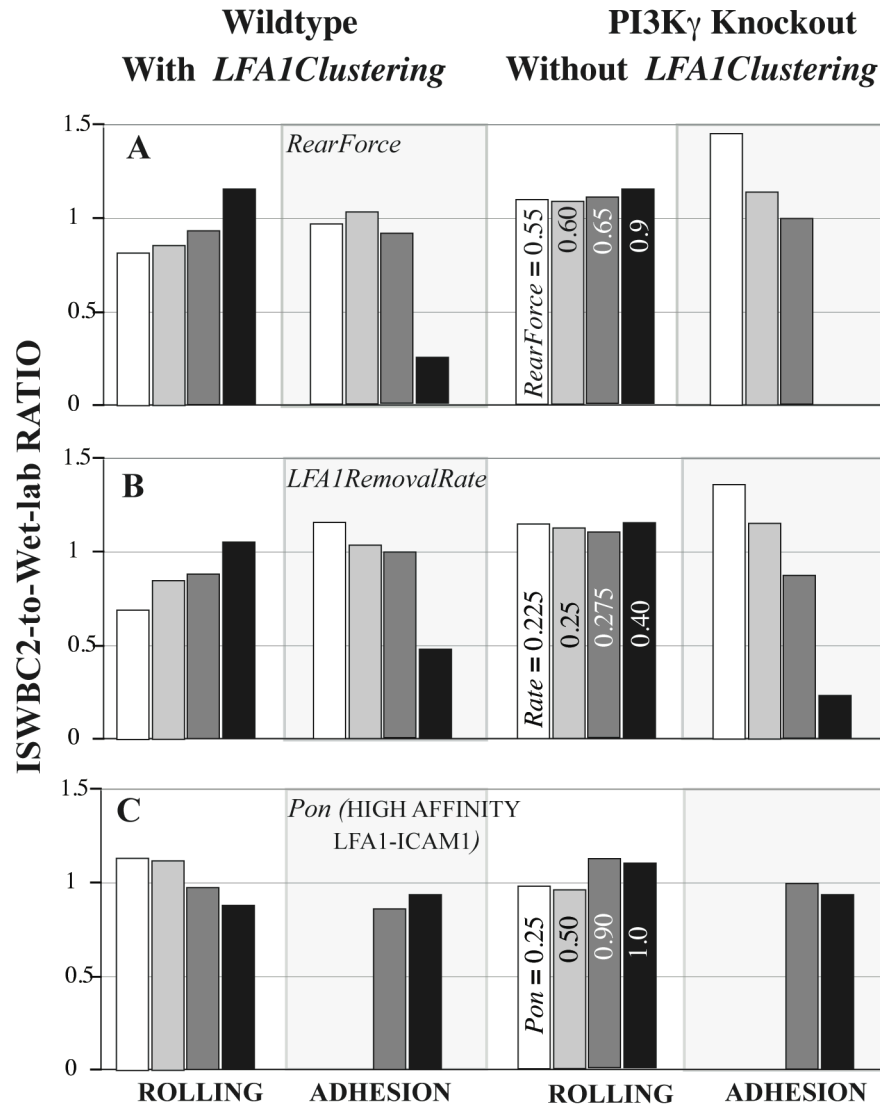
Figure 4.5. Robustness of ISWBC2s to changes in the *LFA1RemovalRate*, *Pon*, and *RearForce*. Separate sets of in silico experiments, using the LEUKOCYTE parameter values in Table 4.4 and ENVIRONMENT parameter values in Table 4.5, were completed while varying either (A) *RearForce*, (B) *LFA1RemovalRate*, or (C) *Pon*(HIGH AFFINITY LFA1-ICAM1) as indicated. Bars heights are ratios of ISWBC2-to-wet-lab results of rolling and adhesion data for both WT and KO mice of the type used for the experiments in Figure 4.3. Comparable adjustments of other parameters caused similar gradual changes in LEUKOCYTE ROLLING and ADHESION data. The listed parameter values for rolling under PI3Kγ Knockout also apply to the similarly shaded bar for the other three conditions.

4.3.3 At low densities, LFA1 CLUSTERING is necessary for sustained LEUKOCYTE ADHESION

Smith et al. observed individual leukocytes in vivo after injection of CXCL1 into the carotid artery of WT and KO mice to determine its role in adhesion. Events in post-capillary venules were recorded using intravital microscopy. Individual cells were tracked in each vessel starting one minute before and ending one minute after CXCL1 injection. After CXCL1 injection, leukocytes rapidly adhered to the vessel wall and remained attached over time in WT mice. However, in KO mice, leukocytes did not attach or attached transiently.

We simulated similar conditions and observed whether disabling LFA1 CLUSTERING would allow the ISWBC2 system to reproduce the observed defect in sustained adhesion. We chose parameter values based on corresponding literature values. When none were available, we searched empirically. LFA1 CLUSTERING was enabled when simulating conditions in WT mice. It was disabled when simulating conditions in KO mice. Figure 4.6A shows that when LFA1 CLUSTERING was enabled, individual LEUKOCYTES initiated ADHESION within SECONDS of exposure to CXCL1 and were able to sustain ADHESION for the duration of the simulation. LEUKOCYTE population level measurements were also similar to those observed in vivo (Figure 4.6B).

When LFA1 CLUSTERING was disabled to simulate conditions in KO mice, LEUKOCYTES exhibited the same transient ADHESION observed in vivo (Figure 4.6C). In the presence of CXCL1 CHEMOKINE, LEUKOCYTES ROLLED for a brief period and then initiated ADHESION to the SURFACE for a brief interval before again initiating ROLLING. Figure 4.6D shows that the similarity in individual LEUKOCYTE behaviors translated successfully to POPULATION level measurements.

In PI3Kγ KO mice during the above-described experiments, a small portion of leukocytes was still able to sustain adhesion. That observation may implicate an additional mechanism. Using ISWBC2, some LEUKOCYTES initiated and maintained ADHESION for long intervals. However, none sustained ADHESION for the entire duration of the simulation. Additionally, in WT mice, some leukocytes were adherent prior to chemokine injection. The intercept values for the wet-lab data in Figure 4.6B show that, at the time of injection, adherent leukocytes were already present. That observation may indicate some leukocyte pre-activation. The ISWBC2 system does not include any pre-activation effects. Consequently, we do not observe any ADHERING LEUKOCYTES at the start of a simulation. Nonetheless, the increases in the number of ADHERENT LEUKOCYTES after CHEMOKINE addition were similar to referent observations.
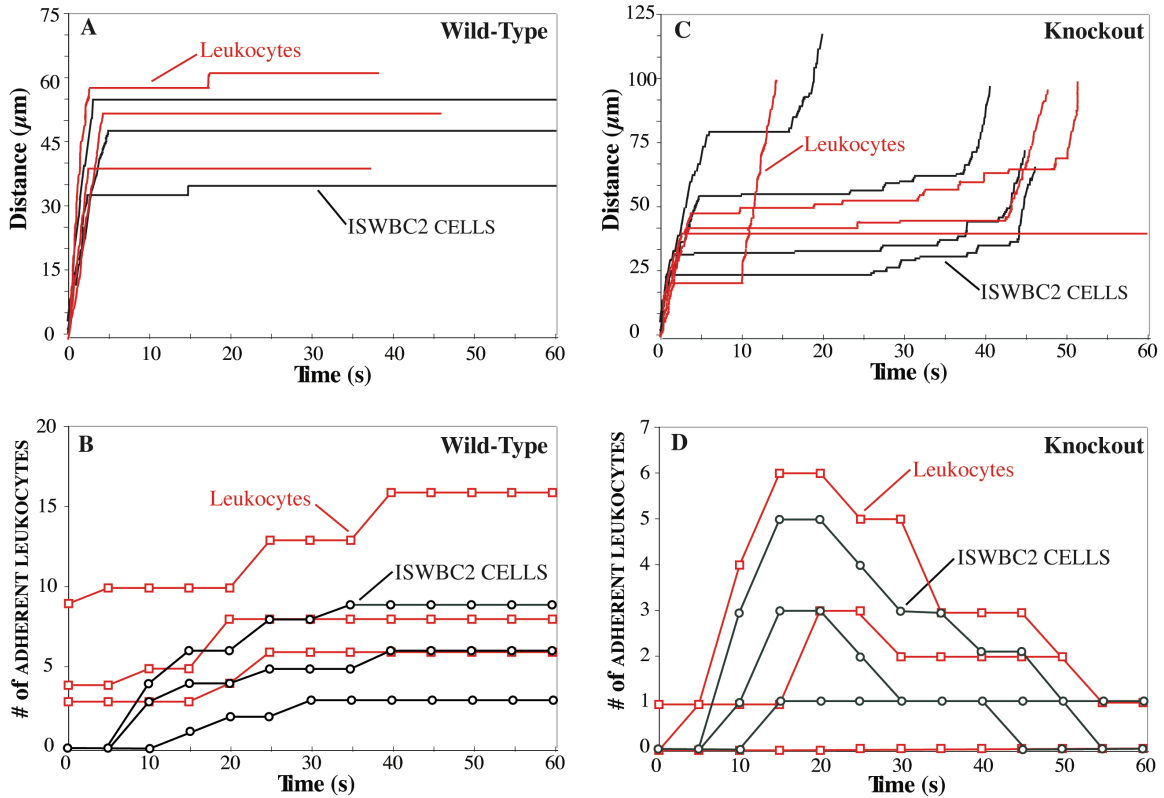
Figure 4.6. Comparison of in vivo and in silico results. In vivo conditions (from [28]): mice were either (A, B) WT or (C, D) KO. Red: wet-lab values; black: ISWBC2 values. Wet-lab experiments: post-capillary venules were observed from one minute before to one minute after CXCL1 injection at $t = 0$. Each simulation ran for 600 simulation cycles (equivalent to about 60 seconds). Individual leukocyte trajectories are plotted for (A) WT and (C) KO mice. (B, D) Individual leukocytes were tracked every 5 s, and those that were adherent during that time were counted. Open squares are adherent leukocyte counts for individual venules. Open circles are corresponding ADHERENT LEUKOCYTE counts for VENULES. Thirty LEUKOCYTES comprised the population within a VENULE. Individual LEUKOCYTES were tracked every 50 simulation cycles (approximately 5 s), and those that were ADHERENT were counted. ISWBC2: parameter values are those listed in Tables 4.4 and 4.5, and LEUKOCYTES are in the presence of CXCL1 beginning at $t = 0$. LFA1 CLUSTERING was either (A, B) enabled or (C, D) disabled.

4.3.4 Influence of LFA1 CLUSTERING on LFA1 and ICAM1 REBINDING events

It has been suggested that integrin clustering may facilitate rebinding events thus enhancing leukocyte adhesion [87, 88]. Rebinding effects are those in which an ICAM-1 that is displaced from one LFA-1 will rapidly bind to a neighboring LFA-1 integrin if it is in sufficiently close proximity. We counted the cumulative number of LFA1 REBINDING events (Figure 4.7A) and ICAM1 REBINDING events (Figure 4.7B) at 50 simulation cycle intervals (every 5 SECONDS) for each LEUKOCYTE. We defined an LFA1 (or ICAM1) REBINDING event as a BOND FORMATION event by an LFA1 (or ICAM1) that had already participated in a BOND FORMATION event during a previous simulation cycle. Averages were taken of 30 LEUKOCYTES from the simulations of the in vivo experiments for each experimental condition (*LFA1Clustering* enabled or disabled). All simulation data for the enabled *LFA1Clustering* experimental condition was generated by LEUKOCYTES that SUSTAINED ADHESION (ROLLING followed by at least 30 simulation cycles of ARREST until the end of the simulation), while all simulation data for the disabled *LFA1Clustering* condition was generated by LEUKOCYTES that exhibited INITIAL and TRANSIENT ADHESION (at least 300 simulation cycles of arrest; average amount of time LEUKOCYTES remained stationary was 39.8 ± 7.2 SECONDS). The average time that LEUKOCYTES detached following transient adhesion was 43.9 ± 7.1 SECONDS for the disabled *LFA1Clustering* condition.

At simulation times prior to 43.9 SECONDS, there were no significant differences in LFA1 REBINDING events for enabled and disabled *LFA1Clustering* condition (Figure 4.7A). A significant difference was observed after 43.9 SECONDS, as expected. LEUKOCYTES with *LFA1Clustering* disabled began to ROLL again after 43.9 SECONDS allowing different LFA1 objects on the MEMBRANE to form new interactions with ICAM1. Those events caused the number of LFA1 REBINDING events to plateau. In contrast, LEUKOCYTES with *LFA1Clustering* enabled continued to SUSTAIN ADHESION enabling the same LFA1 and ICAM1 objects to interact, as evidenced by the rapidly increasing numbers of LFA1 REBINDING events until the end of the simulation.

A different situation was observed with ICAM1 REBINDING. Figure 4.7B shows a significant difference in ICAM1 REBINDING events when LFA1 CLUSTERING is enabled and disabled. As early as 25 SECONDS, the number of ICAM1 REBINDING events was significantly larger for the LFA1 CLUSTERING enabled condition than for the disabled condition. The difference increased throughout the duration of the simulation. These results indicated that when LFA1 was CLUSTERED, more LFA1 objects were REBINDING to the same ICAM1 objects than when LFA1 was randomly distributed and non-CLUSTERED.
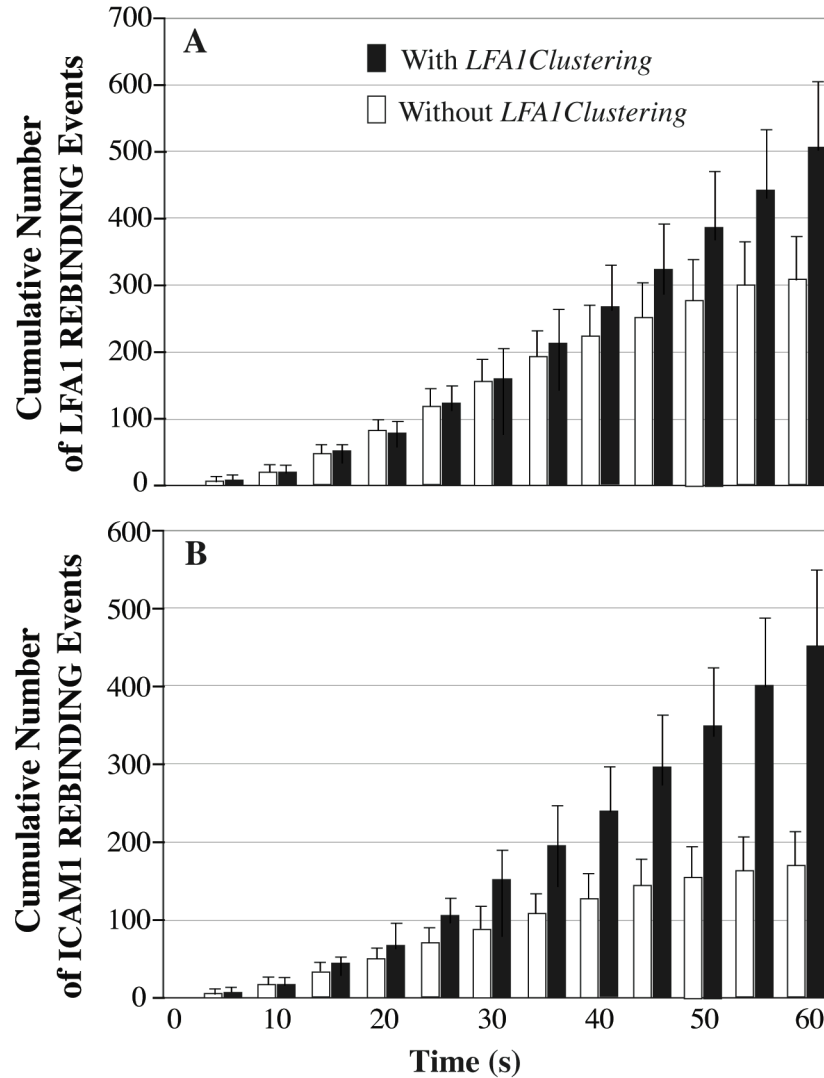
Figure 4.7. Effect of LFA CLUSTERING on LFA1 and ICAM1 RE-BINDING events. The cumulative number of (A) LFA1 RE-BINDING events and (B) ICAM1 RE-BINDING events were counted at 50 simulation cycle intervals (5 SECONDS) for each LEUKOCYTE. A LFA1 (or ICAM1) REBINDING event was defined as a BOND FORMATION event by a LFA1 (or ICAM1) object that had already participated in a BOND FORMATION event in a previous time step. Averages are plotted for 30 LEUKOCYTES per experimental condition (with or without *LFA1Clustering*). Simulation data with *LFA1Clustering* were from LEUKOCYTES that SUSTAINED ADHESION (ROLLING followed by at least 30 simulation cycles of ARREST until the end of the simulation). Simulation data without *LFA1Clustering* were from LEUKOCYTES that exhibited INITIAL and TRANSIENT ADHESION (at least 300 simulation cycles of arrest). Without *LFA1Clustering*, the average ADHESION time was 39.8 ± 7.2 SECONDS before the LEUKOCYTE initiated ROLLING again (average time = 43.9 ± 7.1 SECONDS). Error bars: ± SD.

68

4.3.5 Comparison of the effect of ICAM1 spatial arrangements on sustained ADHESION

ICAM-1 has been reported to arrange itself on endothelial cell membrane surfaces in at least four forms: (1) monomeric, (2) dimeric, (3) dimeric that forms linear tetramers upon ligand binding, and (4) preclustered into tetraspanin enriched microdomains. We implemented each of these spatial configurations in order to compare their effect, in combination with LFA1 CLUSTERING, on LEUKOCYTE's ability to sustain ADHESION. We observed the consequences over a range of *LFA1GRIDDensity* and *ICAM1Density* values. For each ICAM1 configuration, *LFA1Clustering* parameter setting, *LFA1GRIDDensity* value, and *ICAM1Density* value, we performed 450 LEUKOCYTE simulations within LFA1 and ICAM1 density ranges that showed the greatest influence of LFA1 CLUSTERING. We then calculated the percentage of LEUKOCYTES that were able to initiate and sustain ADHESION for the duration of the simulation.

There was no difference in sustained ADHESION between simulations when LFA1 CLUSTERING was either enabled or disabled when ICAM1 existed in a monomeric configuration (not shown). That result was expected because the mechanism is initiated only after a multimeric BOND is formed between multiple LFA1 objects and multiple ICAM1 objects. If ICAM1 is monomeric, the chance of the LFA1 CLUSTERING mechanism being initiated is very small. In contrast, the results in Figure 4.8 show that, for all multimeric configurations tested, significant differences in sustained ADHESION were observed when LFA1 CLUSTERING was either enabled or disabled. Whether ICAM1 existed as a DIMER, a DIMER that formed into linear TETRAMERS upon LIGAND-BINDING, or preclustered produced only slight differences in the percentage of LEUKOCYTES that were able to SUSTAIN ADHESION.
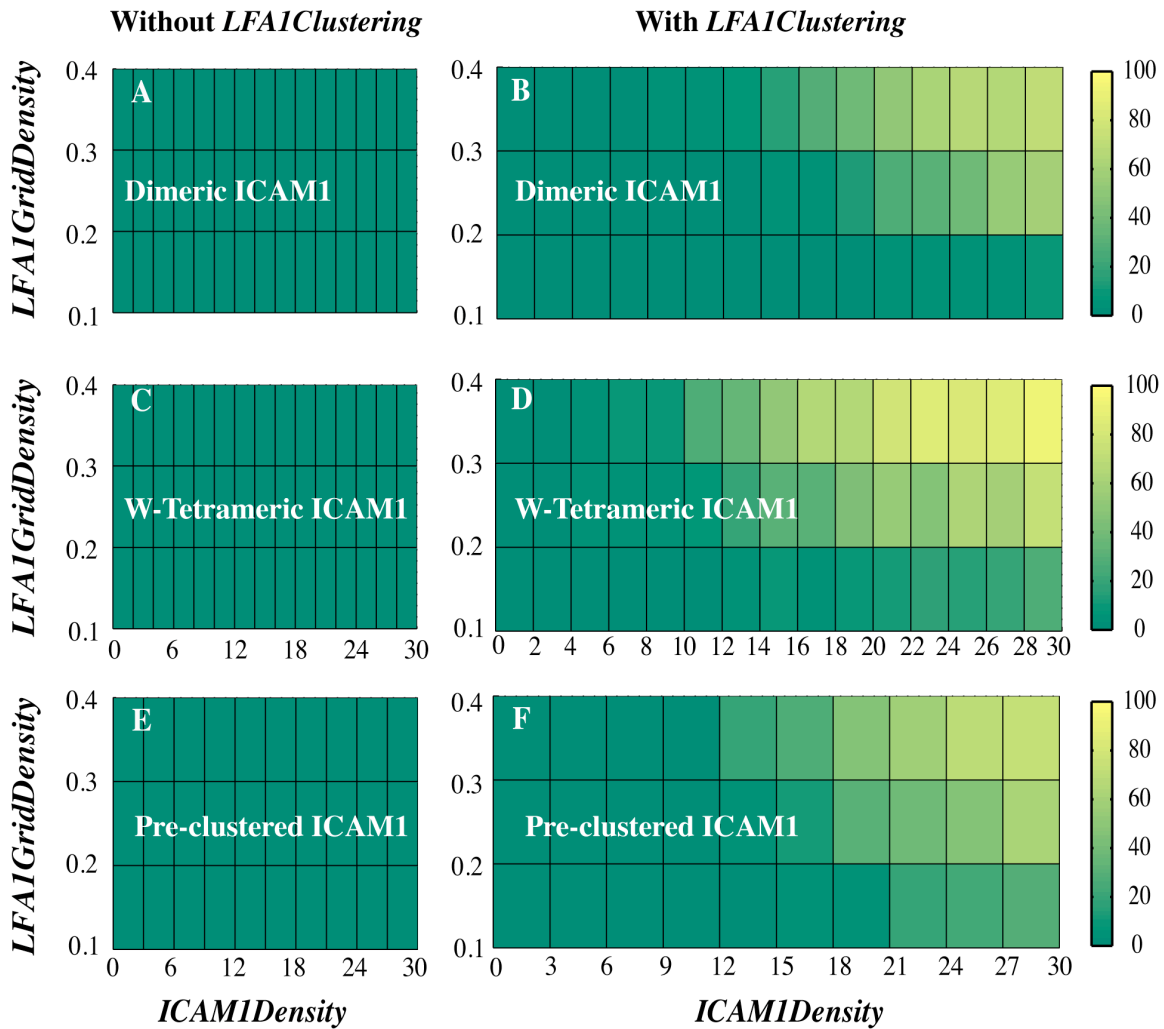
Figure 4.8. Effect on sustained ADHESION of different hypothesized ICAM1 configurations. The percentage of LEUKOCYTES that sustained ADHESION (color scale at right) were calculated for varying *LFA1GridDensity* and *ICAM1Density* values using the different hypothesized ICAM1 configurations discussed in the text. LFA1 CLUSTERING was either disabled (left: A, C, E) or enabled (right: B, D, F). ICAM1 was (A, B) dimeric, (C, D) dimeric and allowed to form linear TETRAMERS upon LIGAND-BINDING, or (E, F) was preformed into NANOCLUSTERS. No sustained ADHESION occurred when ICAM1 was monomeric (not shown).

4.4 Discussion

4.4.1 Achievements

We constructed and validated models of leukocyte rolling, activation, and adhesion. We then experimented on them to test the plausibility of mechanistic hypotheses of how molecular components may interact to cause leukocyte behaviors at the cell and population level. We began with significant leukocyte rolling and adhesion data from ex vivo flow chamber and in vivo mouse cremaster muscle experiments, in which mice lacking functional PI3Kγ exhibited defects in adhesion and sustained adhesion in comparison to leukocytes from WT mice. Smith et al. hypothesized that the adhesion defects were a result of an inability of LFA-1 to redistribute and cluster on the leukocyte membrane in the PI3Kγ KO mice [28].

To challenge that hypothesis, software objects were constructed and assembled according to the mechanistic design in Figure 4.1 using the operating logic in Appendix A.1. The resulting ISWBC2 system was iteratively refined until validation was achieved across multiple experimental conditions and attributes. LFA1 objects were designed to CLUSTER upon LEUKOCYTE activation and post-LIGAND BINDING to multimeric ICAM1. During execution, LEUKOCYTES exhibited behaviors indistinguishable from leukocytes observed in both the ex vivo (Figures 4.3 and 4.5) and in vivo (Figure 4.6) experiments using WT mice. More importantly, inhibiting this mechanism allowed LEUKOCYTE behaviors to mimic the adhesion defects observed both ex vivo and in vivo in KO mice. Thus, ISWBC2 simulations provide a tested theory about the mechanistic events that may be occurring in both WT and KO mice. At higher LFA1 and ICAM1 densities, enabling LFA1 CLUSTERING did not improve ADHESION. However, at low densities, enabling CLUSTERING led to cooperativity at the level of the LEUKOCYTE-SURFACE zone of contact, and that increased ADHESION. Analysis of REBINDING events (Figure 4.7) showed that at later but not earlier times, enabling LFA1 CLUSTERING allowed for an increase in LFA1 REBINDING events in comparison to when LFA1 did not CLUSTER. CLUSTERING enabled increased ICAM1 REBINDING events at early times. Given the multi-attribute validation evidence, it is reasonable to claim that ISWBC2 mechanisms have mouse counterparts.

Though still relatively simple, we have demonstrated that ISWBC2s can achieve a substantial list of targeted attributes under a variety of experimental conditions (Table 4.1A, B). Traditional inductive, equation-based models typically focus on just one or a few different experimental conditions. This observation motivates commentary about the differences between traditional, inductive, equation based models and synthetic, relationally grounded analogues like ISWBC2s. The issues are discussed in detail in [11]. Grounding is defined as the units, dimensions, and/or objects to which a variable or model constituent refers [11]. In models grounded to metric spaces, parameters serve mostly to shift model behavior within a smooth region of the output metric space. In relationally grounded models, like ISWBC2s, in addition to that function, parameters also serve to shift model behavior discontinuously (even abruptly) into an entirely different region of behavior space: they change the analogue's dynamic phenotype. In metrically grounded models, the character of the model is bounded, whereas with relational grounding, model character can change completely with a change in parameters. In the former case, parameters describe one, particular (though abstract) model type. In the latter case, parameters describe families of different yet related models. The ISWBC2s functioning in various experimental conditions are examples of the latter. Relational grounding enables flexible, adaptable analogues, but requires a separate analogue-to-referent mapping model.

The process of discovering a normal ISWBC2 that eventually achieved sustained adhesion typical of WT mouse counterparts, and the process of subsequently discovering modifications that eventually showed defective adhesion indistinguishable from that observed in PI3Kγ KO mice, was the same. It followed the iterative refinement protocol. Each ISWBC2 structure and parameterization was a hypothesis: upon execution, as a consequence of combined micro-mechanisms, measures of leukocyte rolling and adhesion will mimic referent data. Execution and measurement provides data that either support or falsify the hypothesis. Early during iterative refinement, all mechanistic hypotheses were falsified: they failed to achieve the prespecified target attributes. Why one was falsified was often somewhat surprising, reflecting uncertainties about the actual referents' underlying mechanisms. At times it reflected incorrect ideas about how micromechanisms influence ISWBC2 behaviors. The many cycles of iterative refinement that followed required and exercised abductive reasoning, which is essential to achieving new scientific insight [111, 112]. A failure of an early ISWBC2 to achieve one or more prespecified attributes taught us something about those ISWBC2s and improved insight into the referent systems. Failure forced us to think more deeply about plausible mechanistic details, and that in turn forced us to think differently about leukocytes and the process of rolling, activation, and adhesion.

Previous studies by Constantin et al. provided evidence of PI3K mediated LFA-1 clustering in immobilized lymphocytes treated with chemokines [34]. Chemokines triggered a rapid increase in LFA-1 affinity and stimulated LFA-1 movement into clusters and large polar patches. Inhibition of PI3K activity blocked LFA-1 mobility but not LFA-1 affinity changes, and that prevented lymphocytes from adhering to low densities of immobilized ICAM-1. At high densities of immobilized ICAM-1, inhibiting PI3K activity had no effect on lymphocyte adhesion. Because the cell type was different, those observations were not among those originally targeted (Table 4.1). Nevertheless, the validated ISWBC2 that gave the results in Figure 4.4 correctly predicted those results. Whether this same mechanism is operative and influential in murine neutrophils remains to be determined. However, it is noteworthy that our simulation results are consistent. In ISWBC2 experiments, LFA CLUSTERING was important at low ICAM1 densities, but no differences in ADHESION were observed at high ICAM1 densities (Figure 4.4).

Lum et al. used sophisticated in vitro methods to study murine neutrophils after stimulation with IL-8 chemokine [40]. They correlated the dynamics of adhesion with the increased expression of high affinity LFA-1 and membrane redistribution. Using fluorescence microscopy, they observed redistribution of high affinity LFA-1 into small punctate submicron clusters and large polar caps several μm^2 in area within 30 s of IL-8 stimulation. Within 2 min of chemokine stimulation, the polar caps dissipated into numerous smaller clusters. By 10 min, practically all clusters had dispersed and the number of active LFA-1 was observed to have dropped by ~50%. Inhibition of PI3K activity by treatment with wortmannin did not affect the expression of high affinity LFA-1, but significantly inhibited the amount of LFA-1 clustering and formation of polar caps. Treatment with wortmannin after IL-8 stimulation also significantly decreased the amount of adhesion to fluorescent microbeads coated with ICAM-1 in a flow cytometric based assay. They also used a parallel plate flow chamber coated with an ICAM-1 monolayer to observe the strength and stability of neutrophil adhesion over time. Interestingly, the transience of LFA-1 cluster formation and number of active LFA-1 on the membrane correlated with a reversibility of firm adhesion observed in the flow chamber.

We did not target any of the preceding results. One can question whether the observed

behaviors from such in vitro murine neutrophils studies are relevant to those of native cells in the circulation under physiologic conditions [59], such as those used in the ex vivo and in vivo experiments that we targeted. It is recognized that procedures for isolating neutrophils to be studied in vitro can be inefficient and time-consuming. Previous reports have shown that neutrophils become unintentionally modified or activated because of the large number of steps required during isolation [113-115]. For example, in vitro isolated and stained neutrophils do not show normal rolling behavior when injected back in mice [104]. Use of the auto-perfused ex vivo flow chamber system allows one to bypass these cell isolation procedures.

4.4.2 Other Models of Leukocyte Rolling and Adhesion

The discrete-time Adhesive Dynamics (AD) simulations by Hammer and co-workers are the most developed models of leukocyte rolling and adhesion to date [7-10]. In their models, leukocytes are idealized as solid spheres with extensible cylindrical protrusions, to represent microvilli, with receptors located at the tips. Using a Monte Carlo algorithm for the determination of receptor-ligand interactions, they have successfully produced a jerky stop-and-go pattern similar to that observed for rolling leukocytes. Their simulations have also allowed them to explore the molecular properties of adhesion molecules, such as reaction rates and bond elasticity, and how these properties may relate to macroscopic behavior such as rolling and adhesion [8, 9].

At each time step in the Adhesive Dynamics simulation, positions of bonds on the spherical particle are tracked enabling the authors to calculate the forces that each bond experiences. The net force and torque acting on the cell from bonds, fluid shear, steric repulsion, and gravity are calculated assuming the cell is a solid sphere. The position of the cell is then determined for each time step from the net force and torque on the cell using a hydrodynamic mobility function for a sphere near a plane wall in a viscous fluid.

In a recent version of their model, they have simulated the transition from rolling to adhesion upon detection of the IL-8 chemokine [10]. To represent the local G-protein intracellular signaling events, they use a 1D lattice of 1000 units on which a small set of intracellular signaling molecules can diffuse and interact. The bottom end of the lattice represents the microvilli tip. In their model, detection of IL-8 by CXCR1 on a microvilli tip initiates the dissociation of G-protein into two subunits, α and $\beta\gamma$, which can then diffuse along the 1D lattice. Effector molecules become activated when bound to the $\beta\gamma$ subunit. In turn, the activated effector molecule can then diffuse and bind to the intracellular portion of LFA-1 at the bottom end of the lattice, converting it into a high affinity integrin.

They observed a progressive activation of the integrins as cells rolled and interacted with chemokines, leading to a deceleration of the leukocyte before firm adhesion. The slowing of the leukocyte in their model was on a timescale similar to leukocytes from in vitro experiments. In addition, they were able to observe a chemokine density-dependent effect on adhesion time similar to that observed in vitro.

The ISWBC2 differs in many aspects from this recent version of the AD model, which are briefly discussed below. A more detailed comparison of the ISWBCs with the AD models and with other models of leukocyte motility and adhesion can be found in Appendix A.5 and in [92].

In the above AD model, LFA-1 is found at the tips of microvilli. Studies have shown that LFA-1 exists on the cell body surface hidden between the leukocyte microvilli [99, 100].

Therefore, in our ISWBC2 we have specified simply that LFA1 objects are located on sparse regions on the MEMBRANE SURFACE. The fraction of MEMBRANE UNITS containing LFA1GRIDS and LFA1 objects was determined by the parameter *LFA1GridDensity*.

The most recent version of the AD simulations also included a more explicit representation of the signaling events initiated upon chemokine detection. With the ISWBC2, it was not our objective to model the signaling network in detail, and therefore it was not listed as a currently targeted phenotypic attribute in Table 4.1. Our current goal was to test the hypothesized molecular mechanisms at the cell interface of the leukocyte and endothelial substrate surface. However, we have shown previously that synthetic models like ISWBCs can be easily refined to become increasingly realistic in terms of both components and behaviors [92]. As needed, any of the abstract, low-resolution components can be replaced with more realistic, higher resolution composite objects composed of components that map to more detailed biological counterparts. The current ISWBC2 represents the hypothesized mechanisms and processes at a level of detail and resolution that is just sufficient to simulate the currently targeted attributes listed in Table 4.1.

4.5 Summary

The LFA-1 integrin plays a pivotal role in sustained leukocyte adhesion to the endothelial surface, which is a precondition for leukocyte recruitment into inflammation sites. There is strong correlative evidence implicating LFA-1 clustering as being essential to sustained adhesion, and that it may also facilitate rebinding events with its ligand ICAM-1. Smith et al. observed that neutrophils in PI3K KO mice, compared to WT counterparts, had a reduced ability to adhere to P-selectin and ICAM-1 substrate coated flow chamber surfaces in the presence of CXCL1 chemokine. Similar experiments were undertaken in vivo in exteriorized cremaster muscle venules of mice injected with CXCL1, and the results were similar. Neutrophils from KO mice, compared to WT counterparts, adhered less to the CXCL1-treated venular surfaces. Interestingly, most neutrophils from KO mice were able to adhere, but only for short intervals [13]. They hypothesized that LFA-1 clustering following multivalent binding to multivalent ICAM-1 [22] might be the PI3Kγ-mediated mechanism that is responsible for the defect in adhesion

We cannot challenge these hypotheses directly with wet-lab methods because it is infeasible to measure either process in vivo during leukocyte adhesion following rolling. The alternative approach undertaken was to challenge the hypothesized mechanisms by experimenting on validated, working counterparts: simulations in which diffusible, LFA1 objects on the surfaces of quasi-autonomous leukocytes interact with simulated, diffusible, ICAM1 objects on endothelial surfaces during simulated adhesion following rolling. We used object-oriented, agent-based methods to build and execute multi-level, multi-attribute analogues of leukocytes and endothelial surfaces. LFA1 objects were designed to cluster upon LEUKOCYTE activation and post-LIGAND BINDING to multimeric ICAM. During execution, LEUKOCYTES exhibited behaviors indistinguishable from leukocytes observed in both the ex vivo (Figs. 4.3 and 4.5) and in vivo (Figure 4.6) experiments using WT mice. More importantly, disabling the LFA1 CLUSTERING mechanism enabled the ISWBC2 to reproduce the adhesion defects observed with ex vivo and in vivo experiments in KO mice across eight different experimental conditions at both the cell- and population-level, including the transient adhesion of simulated KO

neutrophils. Thus, ISWBC2 simulations provide a tested theory about the mechanistic events that may be occurring in both WT and KO mice.

We quantified rebinding events between individual components under different conditions, and the role of LFA-1 clustering in sustaining leukocyte–surface adhesion and in improving adhesion efficiency. Early during simulations ICAM1 REBINDING (to LFA1) but not LFA1 REBINDING (to ICAM1) was enhanced by CLUSTERING. Later, CLUSTERING caused both types of REBINDING events to increase. We discovered that CLUSTERING was not necessary to achieve ADHESION as long as LFA1 and ICAM1 object densities were above a critical level. Importantly, at low densities LFA1 CLUSTERING enabled improved efficiency: ADHESION exhibited measurable, cell level positive cooperativity.

ICAM-1 has been reported to arrange itself on endothelial cell membrane surfaces in at least four forms: (1) monomeric, (2) dimeric, (3) dimeric that forms linear tetramers upon ligand binding, and (4) preclustered into tetraspanin enriched microdomains. We implemented each of these spatial configurations in order to compare their effect, in combination with LFA1 CLUSTERING, on LEUKOCYTE's ability to sustain ADHESION. With our simulations, we showed no difference in sustained ADHESION between simulations when LFA1 CLUSTERING was either enabled or disabled when ICAM1 existed in a monomeric configuration. In contrast, our simulations show that, for all multimeric configurations tested, significant differences in sustained ADHESION were observed when LFA1 CLUSTERING was either enabled or disabled. Whether ICAM1 existed as a DIMER, a DIMER that formed into linear TETRAMERS upon LIGAND-BINDING, or preclustered produced only slight differences in the percentage of LEUKOCYTES that were able to SUSTAIN ADHESION.

Our simulations enabled us to view how different molecular interaction events on simulated leukocyte surfaces cause behaviors that are unique and diverse at both the molecular and leukocyte levels, and yet—importantly—narrowly constrained at the population level.

5 Conclusion

5.1 Summary

Using the synthetic modeling approach, we have created a set of discrete event, discrete space, and discrete time analogues of the wet-lab experimental systems used to study leukocyte rolling, activation, and adhesion. Object-oriented software components were designed, instantiated, verified, plugged together, and then operated in ways that can map concretely to mechanisms believed responsible for leukocyte rolling, activation, and adhesion. The experimentally measured phenotypic attributes of the ISWBC systems can be compared and contrasted to those of leukocytes from the referent wet-lab systems.

The ISWBCs were designed to be used for testing the plausibility of mechanistic hypotheses of how molecular components may interact to cause leukocyte behaviors during rolling, activation, and adhesion to endothelial surfaces. In this project, we studied the consequences of LFA-1 integrin clustering, or lack thereof, on leukocyte initial adhesion and sustained adhesion. We also sought to determine if LFA-1 integrin clustering could be the PI3Kγ-mediated mechanism responsible for the defect in initial adhesion observed ex vivo and the defect in sustained adhesion observed in vivo in PI3Kγ KO mice by Smith et al. Such questions are impossible to explore using traditional wet-lab models due to the limitations of current experimental techniques.

We first created a foundational analogue of the in vitro parallel plate flow chamber used to study leukocyte rolling, activation, and adhesion in flow conditions. We simulated three different in vitro experiments using flow chambers coated with different combinations of P-selectin, VCAM-1, and GRO-α chemokine [14, 15, 18, 19]. The ISWBC was able to successfully reproduce the dynamics of individual leukocytes rolling separately on P-selectin and VCAM-1, along with the transition from rolling to adhesion on P-selectin and VCAM-1 in the presence of GRO-α chemokine observed in vitro. Additionally, the individual in silico and in vitro behavioral similarities translated successfully to population-level measures.

We then extended the in silico model such that lateral movement and clustering of LFA-1 and its inhibition can be represented in order to test their hypothesized role in adhesion. LFA1 objects were designed to cluster upon LEUKOCYTE activation and post-LIGAND BINDING to multimeric ICAM1. During execution, LEUKOCYTES exhibited behaviors indistinguishable from leukocytes observed in both the ex vivo and in vivo experiments using WT mice. More importantly, disabling the LFA1 CLUSTERING mechanism enabled the ISWBC2 to reproduce the defective adhesion observed ex vivo and the transient adhesion observed in vivo using KO mice. Thus, ISWBC2 simulations provide a tested theory about the mechanistic events that may be occurring in both WT and KO mice.

Within the validated system, we analyzed the effect of varying ICAM1 and LFA1 densities on ADHESION. We observed that clustering of LFA1 was not necessary to achieve initial ADHESION as long as LFA1 and ICAM1 densities were above a critical level. However, when LFA1 and ICAM1 object densities were both low and LFA1 CLUSTERING was enabled, ADHESION between LEUKOCYTE and simulated substrate coated surface exhibited measurable, positive cooperativity. No such cooperativity was evident when densities were high.

We additionally determined if and when REBINDING events as a result from LFA1 CLUSTERING could contribute to sustained ADHESION. Early during simulations, there were no

differences in LFA1 REBINDING events with or without having LFA1 CLUSTERING enabled. Thereafter, however, CLUSTERING caused LFA1 REBINDING (to ICAM1) to increase. The situation was somewhat different for ICAM1 REBINDING. As early as 25 seconds into an experiment, significantly more ICAM1 REBINDING (to LFA1) was measured when LFA1 CLUSTERING was enabled.

ICAM-1 has been reported to arrange itself on endothelial cell membrane surfaces in at least four forms: (1) monomeric, (2) dimeric, (3) dimeric that forms linear tetramers upon ligand binding, and (4) preclustered into tetraspanin enriched microdomains. We implemented each of these spatial configurations in order to compare their effect, in combination with LFA1 CLUSTERING, on LEUKOCYTE's ability to sustain ADHESION. With our simulations, we showed no difference in sustained ADHESION between simulations when LFA1 CLUSTERING was either enabled or disabled when ICAM1 existed in a monomeric configuration. In contrast, our simulations show that, for all multimeric configurations tested, significant differences in sustained ADHESION were observed when LFA1 CLUSTERING was either enabled or disabled. Whether ICAM1 existed as a DIMER, a DIMER that formed into linear TETRAMERS upon LIGAND-BINDING, or preclustered produced only slight differences in the percentage of LEUKOCYTES that were able to SUSTAIN ADHESION.

The results support the feasibility and practicability of using this new class of in silico experimental devices as a tool to expand the experimental options for better understanding the key mechanistic events and interactions between leukocytes and endothelial cells that regulate leukocyte rolling, activation, and adhesion during inflammation.

5.2 Ten Capabilities Achieved and Demonstrated

Our ISWBC system has undergone many cycles of iterative refinement such that they have many behaviors, properties, and characteristics that mimic those of referent wet-lab systems for studying leukocyte rolling, activation, and adhesion. Table 5.1 Set A lists several of those attributes. The greater the similarity between the measured behaviors of our in silico white blood cells and the referent model attributes of interest, the more useful that in silico system will become as a research tool and as an expression of the coalesced, relevant leukocyte knowledge.

Phenotypic Attribute	Reference
Set A: previously targeted attributes	
Characteristic jerky stop and go movement during rolling	[14]
Highly fluctuating rolling velocities	[15]
Larger rolling velocities observed at higher shear rates	[16]
Smaller rolling velocities at higher ligand substrate densities	[16]
ROLLING[a] velocities on PSELECTIN[a] match reported values	[16]
Small number of bonds within the contact zone, e.g., within 2-20	[17]
Distance-time and velocity-time data for ROLLING[a] on [a]PSELECTIN/VCAM1 are indistinguishable from reported data	[14, 15, 18]
Chemokines induce adhesion within seconds	[19]
LFA-1 and ICAM-1 lateral mobility and diffusion	[21]
LFA-1 nanocluster formation upon binding multivalent ligand	[22]
ICAM-1 spatial configurations in vivo	[23-27]
Effect of phosphoinositide 3-kinase inhibitors on adhesion ex vivo	[28]
Effect of phosphoinositide 3-kinase inhibitors on adhesion in vivo	[28]
Set B: future targetable attributes	
Induction of LFA-1-dependent neutrophil rolling on ICAM-1 by engagement of E-selectin	[29]
Synergistic effect observed during neutrophil rolling on P- and E-selectin	[30]
Effect of inhibitors to other signaling molecules on cell arrest (pertussis toxin (PTx)-sensitive G proteins, p38 mitogen-activated protein kinase)	[29]

Table 5.1 – List of Previously and Currently Targeted Phenotypic Attributes of Leukocytes.

ISWBC1 and ISWBC2 focused on Set A. Example leukocyte attributes that may be targeted in the future are listed in Set B.

In Chapter 1 we identified at least ten capabilities that our in silico system should exhibit in order to attain this desired phenotypic attribute overlap between our in silico system and the wet-lab referent systems. With the in silico systems presented in this dissertation we have achieved and demonstrated these ten capabilities:

1. *Individual behavior*: Leukocyte behaviors during rolling and adhesion are by no means deterministic. Rolling, for example, exhibits an irregular, jerky stop-and-go pattern along with highly fluctuating rolling velocities. In Chapters 3 and 4, we showed that the constructed ISWBCs are capable of accurately representing the unique individual behavior patterns typical of leukocytes observed in vitro and in vivo when simulating analogous conditions.

2. *Multilevel*: In order to represent the key mechanisms and features of leukocytes during rolling, activation, and adhesion, it is essential for the model to have multi-level components that can communicate with each other. It should be easy to increase or decrease the number of model levels and alter communications between levels. In Chapter 3 we describe the ISWBC1, which consisted of components having two levels of spatial resolution: LEUKOCYTE-LEVEL and MEMBRANE/SURFACE UNIT-LEVEL. High-level behaviors were dependent upon the collective operation of objects and agents contained within each of the lower levels. For example, the behavior of MEMBRANE and SURFACE UNITS arise from the RECEPTOR objects contained within each. Similarly, the behavior at the LEUKOCYTE-LEVEL is dependent upon the collective events that occur within the underlying MEMBRANE/SURFACE UNITS. CONVERSELY, EVENTS AT THE HIGHEST LEVEL IMPOSE CONSTRAINTS UPON ALLOWED LOWER LEVEL BEHAVIORS. FOR EXAMPLE, THE Positioning and movement of the LEUKOCYTE on the SURFACE dictate which MEMBRANE and SURFACE UNITS are overlapping and can interact. In Chapter 4, we showed with the ISWBC2 that it was relatively easy to increase the number of model levels by adding a third level: the LFA1 GRID/ICAM1 GRID-LEVEL. Importantly, this was achieved without significant re-engineering of the system and without affecting the ISWBC2's ability to reproduce some of the essential targeted phenotypic attributes that were previously used to validate the ISWBC1.

3. *Mapping:* In the ISWBCs, there are clear mappings between in silico components and leukocyte components and their interactions because in silico observables have been designed to be consistent with those of the referent wet-lab experimental systems. Each in silico receptor component maps to a distinct molecular receptor found in the referent wet-lab experimental system (See Table 3.2 and Table 4.2). Additionally, all mechanisms that were implemented in the ISWBCs were based on wet-lab experimental observations or were hypothesized events supported by the literature.

4. *Turing test:* When an ISWBC and the simulated flow chamber are each endowed with a specified set of ligands, the measures of ISWBC behaviors during simulations should be, to a domain expert (in a type of Turing test), experimentally indistinguishable from the wet-lab experimental measurements. We showed in Chapter 3 that the ISWBC was able to reproduce the dynamics of leukocytes rolling separately on a P-selectin or VCAM-1 substrate under flow conditions. The ISWBC was able to mimic the transition from rolling to adhesion on P-selectin and VCAM-1 in the presence of GRO-α chemokine.

When simulating populations of leukocytes under different experimental conditions (combinations of substrate molecules), the in silico system generated quantitative population-level data that were indistinguishable from in vitro data. Similarly, in Chapter 4, we showed that shows that for all ligand combinations (P-selectin, ICAM-1, and CXCL1) and genotypic variations (WT and KO) simulated, both the LEUKOCYTE ROLLING and ADHESION data matched those from ex vivo experiments: the in silico and wet-lab results were indistinguishable experimentally.

5. *Transparent*: The details of ISWBC components and their interactions as the simulation progresses need to be visualizable, measurable, and accessible to intervention. In Chapter 4, we illustrated this capability with the analysis of RECEPTOR REBINDING events with and without LFA1 CLUSTERING. We demonstrated that LFA1 CLUSTERING after multivalent BINDING to multimeric ICAM1 led to an increase in ICAM1, and not LFA1, REBINDING events, which enabled the LEUKOCYTE to sustain ADHESION. Such measurements are inaccessible when studying leukocyte rolling and adhesion in vivo, and thus highlights a key advantage of synthetic models like ISWBCs.

6. *Articulate:* It both Chapters 3 and 4, we showed that the ISWBC components are easy to join, disconnect, and be replaced within and between levels, including the simulated experimental context. In Chapter 3, we simulated flow chamber experiments that used six different combinations of three types of substrate molecules. Similarly, in Chapter 4, we simulated flow chamber experiments that used 8 different combinations of three types of substrate molecules and two mouse genotypic variations. By adding or removing ISWBC components during a simulation, the in silico system was able to successfully represent each experimental condition. Importantly, this was achieved without having to significantly re-engineer the system each time.

7. *Granular*: Throughout the development of the ISWBCs, we followed a parsimony guideline. The level of granularity chosen for the model and its components was, at the margin, fine enough to exhibit the list of currently targeted attributes, but not so detailed or complicated that a component could be eliminated without significantly degrading behavior similarities for the full set of targeted attributes. At each stage of iterative refinement, in which new attributes are added to the targeted list, it may be determined that a change in the level of granularity is needed to achieve the new targeted list. Because of the *Multi-level* and *Articulate* capabilities (listed above), any of the abstract, low resolution components can be replaced with validated, more realistic, higher resolution composite objects composed of components that map to more detailed biological counterparts, without having to reengineer the whole system, and without having to compromise already validated features and behaviors. In the development of the ISWBC2, we determined that the level of granularity of the ISWBC1 needed to be increased in order to explore the hypothesized mechanism of LFA1 CLUSTERING and its effect on ADHESION. In Chapter 4, with the addition of LFA1, LFA1GRID, ICAM1 and ICAM1GRID objects into the ISWBC2, we illustrated how it is relatively simple to increase detail in order to meet the particular needs of an experiment, without requiring significant re-engineering of the in silico system.

8. *Reusable:* We showed in Chapters 3 and 4 that ISWBC components were reusable for simulating behaviors in different experimental conditions. In Chapter 3, the ISWBC1

components were reused for the three different in vitro experiments simulated. In Chapter 4, many ISWBC1 components (PSELECTIN, PSGL1, and CXCR2) were similarly reused in the ISWBC2 in order to simulate the ex vivo and in vivo experiments. Again, this was achieved without significant re-engineering of the system and without affecting the ISWBC2's ability to reproduce some of the essential targeted phenotypic attributes that were previously used to validate the ISWBC1.

9. *Embeddable*: We demonstrated that the ISWBCs can function as components of larger, whole organism or tissue models, so that they may eventually represent the full range of trafficking attributes. In Chapter 3, we began by simulating in vitro parallel plate flow chamber experiments. In Chapter 4, we extended the model to first represent ex vivo experiments that used an autoperfused flow chamber system. In Chapter 4, we also show how we extended the ISWBC to represent experiments using an in vivo model of inflammation in the murine cremaster muscle venule. While the current ISWBC2 may appear to be a relatively simple representation of a complex in vivo model, we have demonstrated that any of the abstract, low resolution ISWBC components can be replaced with validated, more realistic, higher resolution objects consisting of components that map to more detailed biological counterparts.

10. *Discrete interactions:* The ISWBCs are discrete event, discrete time, and discrete space models. Discrete models offer many advantages because they facilitate achieving the preceding nine capabilities. In cases where a continuous model is advantageous, a discrete model can approximate it with desirable precision (Zeigler BP 2000).

With these ten capabilities, ISWBCs will be flexible and adaptable enough such that they can be continually expanded and updated as new data and knowledge of leukocyte rolling and adhesion becomes available.

5.3 Perspectives

There are many directions to which we can refine the model. Our current representation of the intracellular signaling events initiated by CHEMOKINE detection leading to INTEGRIN ACTIVATION and LFA1 CLUSTERING is significantly coarse grained. In the ISWBC2, when a CXCR2 CHEMOKINE RECEPTOR detects a CHEMOKINE it deterministically ACTIVATES all INTEGRINS within the MEMBRANE UNIT and puts all LFA1 objects into CLUSTERS when simulating wild type mice. It was not our objective to model the signaling network in detail, and therefore it was not listed as a currently targeted phenotypic attribute. Our current goal was to test the hypothesized molecular mechanisms at the cell interface of the leukocyte and endothelial substrate surface. A future goal might be to explicitly represent the intracellular signaling network initiated upon chemokine detection in order to gain insight into the signaling dynamics and to assess the consequences of therapeutic interventions. PI3Kγ is thought to be an attractive therapeutic target for the treatment of many autoimmune and inflammatory disorders because expression of the PI3Kγ isoform is limited to the haematopoietic system [116]. Despite the fact that PI3K is upstream of many signaling networks that regulate several fundamental biological processes, such as cell survival and proliferation, mice lacking PI3Kγ are still able to develop normally while show defects in adaptive immunity [116].

In Chapter 4, we described how we iteratively refined the ISWBC to represent leukocyte rolling, activation, and adhesion in a section of a mouse cremaster muscle venule. Although the current representation is very simplistic and rudimentary, many of the essential details of the in vivo tissue (such as additional key adhesion molecules and chemokine receptors) can be incorporated into future versions of the model when deemed necessary. For example, E-selectin expression is induced in both acutely and chronically inflamed endothelial beds. In many of these settings, P- and E-selectin appear to have redundant functions. Inclusion of these key adhesion molecule receptors will allow the ISWBC to become increasingly realistic, and therefore more useful for studying the key events mediating leukocyte rolling, activation, and adhesion in vivo.

With the iterative refinement protocol, we have also established an efficient, systematic, and scientific method to deal with the iterative nature of the modeling and validation process. With the ten capabilities of the ISWBC, we can also easily continually refine our models without having to reengineer the whole system, and without having to compromise already validated features and behaviors. Together, these tools will provide a means to explore the space of reasonably realistic, biomimetic mechanisms that can cause the emergence of leukocyte behaviors at various system levels during inflammation. By selecting those mechanistic hypotheses that survive the falsification process we can shrink the space of biomimetically plausible mechanisms, thereby providing insights into directions of future research and help speed development and discovery of critically needed immunotherapeutics.

6 References

1. Ulbrich H, Eriksson EE, Lindbom L (2003) Leukocyte and endothelial cell adhesion molecules as targets for therapeutic interventions in inflammatory disease. Trends Pharmacol Sci 24: 640-647.

2. Springer TA (1994) Traffic signals for lymphocyte recirculation and leukocyte emigration: the multistep paradigm. Cell 76: 301-314.

3. Ley K, Laudanna C, Cybulsky M, Nourshargh S (2007) Getting to the site of inflammation: the leukocyte adhesion cascade updated. Nat Rev Immunol 7: 678-689.

4. Simon SI, Green CE (2005) Molecular mechanics and dynamics of leukocyte recruitment during inflammation. Annu Rev Biomed Eng 7: 151-185.

5. Laudanna C (2005) Integrin activation under flow: a local affair. Nat Immunol 6: 429-430.

6. Ley K (2002) Integration of inflammatory signals by rolling neutrophils. Immunol Rev 186: 8-18.

7. Hammer DA, Apte SM (1992) Simulation of cell rolling and adhesion on surfaces in shear flow: general results and analysis of selectin-mediated neutrophil adhesion. Biophys J 63: 35-57.

8. Chang KC, Tees DF, Hammer DA (2000) The state diagram for cell adhesion under flow: leukocyte rolling and firm adhesion. Proc Natl Acad Sci USA 97: 11262-11267.

9. Bhatia SK, King MR, Hammer DA (2003) The state diagram for cell adhesion mediated by two receptors. Biophys J 84: 2671-2690.

10. Caputo KE, Hammer DA (2009) Adhesive dynamics simulation of G-protein-mediated chemokine-activated neutrophil adhesion. Biophys J 96: 2989-3004.

11. Hunt CA, Ropella GE, Lam TE, Tang J, Kim SH, et al. (2009) At the biological modeling and simulation frontier. Pharm Res. DOI 10.1007/s11095-009-9958-3.

12. Fisher J, Henzinger TA (2007) Executable cell biology. Nature Biotechnology 25: 1239-1249.

13. Hunt CA, Ropella GE, Park S, Engelberg J (2008) Dichotomies between computational and mathematical models. Nature Biotechnology 26: 737-738.

14. Smith MJ, Berg EL, Lawrence MB (1999) A direct comparison of selectin-mediated transient, adhesive events using high temporal resolution. Biophys J 77: 3371-3383.

15. Park EY, Smith MJ, Stropp ES, Snapp KR, DiVietro JA, et al. (2002) Comparison of PSGL-1 microbead and neutrophil rolling: microvillus elongation stabilizes P-selectin bond clusters. Biophys J 82: 1835-1847.

16. Lawrence MB, Kansas GS, Kunkel EJ, Ley K (1997) Threshold levels of fluid shear promote leukocyte adhesion through selectins (CD62L P, E). J Cell Biol 136: 717-727.

17. Chen S, Springer TA (1999) An automatic braking system that stabilizes leukocyte rolling by an increase in selectin bond number with shear. J Cell Biol 144: 185-200.

18. Alon R, Kassner PD, Carr MW, Finger EB, Hemler ME, et al. (1995) The integrin VLA-4 supports tethering and rolling in flow on VCAM-1. J Cell Biol 128: 1243-1253.

19. Smith DF, Galkina E, Ley K, Huo Y (2005) GRO family chemokines are specialized for monocyte arrest from flow. Am J Physiol Heart Circ Physiol 289: H1976-1984.

20. Granger DN, Kubes P (1994) The microcirculation and inflammation: modulation of leukocyte-endothelial cell adhesion. J Leukoc Biol 55: 662-675.

21. Cairo CW, Mirchev R, Golan DE (2006) Cytoskeletal regulation couples LFA-1 conformational changes to receptor lateral mobility and clustering. Immunity 25: 297-208.

22. Kim M, Carman CV, Yang W, Salas A, Springer TA (2004) The primacy of affinity over clustering in regulation of adhesiveness of the integrin {alpha}L{beta}2. J Cell Biol 167: 1241-1253.

23. Miller J, Knorr R, Ferrone M, Houdei R, Carron CP, et al. (1995) Intercellular adhesion molecule-1 dimerization and its consequences for adhesion mediated by lymphocyte function associated-1. J Exp med 172: 1231-1241.

24. Barreiro O, Yanez-Mo M, Sala-Valdes M, Gutierrez-Lopez MD, Ovalle S, et al. (2005) Endothelial tetraspanin microdomains regulate leukocyte firm adhesion during extravasation. Blood 105: 2852-2861.

25. Barreiro O, Zamai M, Yanez-Mo M, Tejera E, Lopez-Romero P, et al. (2008) Endothelial adhesion receptors are recruited to adherent leukocytes by inclusion in preformed tetraspanin nanoplatforms. J Cell Biol 183: 527-542.

26. Reilly PL, Woska JR, Jr., Jeanfavre DD, McNally E, Rothlein R, et al. (1995) The native structure of intercellular adhesion molecule-1 (ICAM-1) is a dimer. Correlation with binding to LFA-1. Journal of Immunology 155: 529-532.

27. Jun CD, Carman CV, Redick SD, Shimaoka M, Erickson HP, et al. (2001) Ultrastructure and function of dimeric, soluble intercellular adhesion molecule (ICAM-1). J Biol Chem 276: 29027.

28. Smith DF, Deem TL, Bruce AC, Reutershan J, Wu D, et al. (2006) Leukocyte phosphoinositide-3 kinase {gamma} is required for chemokine-induced, sustained adhesion under flow in vivo. Journal of Leukocyte Biology 80: 1491-1499.

29. Chesnutt BC, Smith DF, Raffler NA, Smith ML, White EJ, et al. (2006) Induction of LFA-1-dependent neutrophil rolling on ICAM-1 by engagement of E-selectin. Microcirculation 13: 99-109.

30. Smith ML, Sperandio M, Galkina EV, Ley K (2004) Autoperfused mouse flow chamber reveals synergistic neutrophil accumulation through P-selectin and E-selectin. J Leukoc Biol 76: 985-993.

31. Gakidis MA, Cullere X, Olson T, Wilsbacher JL, Zhang B, et al. (2004) Vav GEFs are required for beta2 integrin-dependent functions of neutrophils. J Cell Biol 166: 273-282.

32. van Kooyk Y, van Vliet SJ, Figdor CG (1999) The actin cytoskeleton regulates LFA-1 ligand binding through avidity rather than affinity changes. J Biol Chem 274: 26869-26877.

33. van Kooyk Y, Weder P, Heije K, Figdor CG (1994) Extracellular Ca2+ modulates LFA-1 cell surface distribution on T lymphocytes and consequently affects adhesion. J Cell Biol 124: 1061-1070.

34. Constantin G, Majeed M, Giagulli C, Piccio L, Kim JY, et al. (2000) Chemokines trigger immediate beta2 integrin affinity and mobility changes: differential regulation and roles in lymphocyte arrest under flow. Immunity 13: 759-769.

35. Myou S, Zhu X, Boetticher E, Qin Y, Myo S, et al. (2002) Regulation of adhesion of AML14.3D10 cells by surface clustering of Beta2-integrin caused by ERK-independent activation of cPLA2. Immunology 107: 77-85.

36. Katagiri K, Maeda A, Shimonaka M, Kinashi T (2003) RAPL, a novel Rap1-binding molecule, mediates Rap1-induced adhesion through spatial regulation of LFA-1. Nat Immunol 4: 741-748.

37. Carman CV, Springer TA (2003) Integrin avidity regulation: Are changes in affinity and conformation underemphasized. Curr Opin Cell Biol 15: 547-556.

38. Rommel C, Camps M, Ji H (2007) PI3K delta and PI3K gamma: partners in crime in inflammation in rheumatoid arthritis and beyond? Nat Rev Immunol 7: 191-201.

39. Hawkins PT, Stephens LR (2007) PI3Kgamma is a key regulator of inflammatory responses and cardiovascular homeostasis. Science 18: 64-66.

40. Lum AFH, Green CE, Lee GR, Staunton DE, Simon SI (2002) Dynamic regulation of LFA-1 activation and neutrophil arrest on intercellular adhesion molecule 1 (ICAM-1) in shear flow. J Biol Chem 277: 20660-20670.

41. Ley K, Mestas J, Pospieszalska MK, Sundd P, Groisman A, et al. (2008) Chapter 11. Intravital microscopic investigation of leukocyte interactions with the blood vessel wall. Methods Enzymol 445: 255-279.

42. Miura S, Asakura H, Tsuchiya M (1987) Dynamic analysis of lymphocyte migration into Peyer's patches of rat small intestine. Lymphology 20: 252-256.

43. Liu L, Kubes P (2003) Molecular mechanisms of leukocyte recruitment: Organ-specific mechanisms of action. Thromb Haemost 89: 213-220.

44. Tabuchi A, Mertens M, Kuppe H, Pries AR, Kuebler WM (2008) Intravital microscopy of the murine pulmonary microcirculation. J Appl Physiol 104: 338-346.

45. von Andrian UH (1996) Intravital microscopy of the peripheral lymph node microcirculation in mice. Microcirculation 3: 287-300.

46. Saetzler RK, Jallo J, Lehr HA, Philips CM, Vasthare U, et al. (1997) Intravital Fluorescence Microscopy: Impact of Light-induced Phototoxicity on Adhesion of Fluorescently Labeled Leukocytes. J Histochem Cytochem 45: 503-513.

47. Mempel TR, Henrickson SE, von Andrian UH (2004) T-cell priming by dendritic cells in lymph nodes occurs in three distinct phases. Nature 427: 154-159.

48. Acton ST, Wethmar K, Ley K (2002) Automatic tracking of rolling leukocytes in vivo. Microvasc Res 63: 139-148.

49. Warnock RA, Campbell JJ, Dorf ME, Matsuzawa A, McEvoy LM, et al. (2000) The Role of Chemokines in the Microenvironmental Control of T versus B Cell Arrest in Peyer's Patch High Endothelial Venules. JExpMed 191: 77-88.

50. Cara DC, Kubes P (2004) Intravital microscopy as a tool for studying recruitment and chemotaxis. Methods Mol Biol 239: 123-132.

51. Vaporciyan AA, Jones ML, Ward PA (1993) Rapid analysis of leukocyte-endothelial adhesion. J Immunol Methods 159: 93-100.

52. Siegelman M (2001) More than the sum of the parts: cooperation between leukocyte adhesion receptors during extravasation. J Clin Invest 107: 159-160.

53. Ellies LG, Sperandio M, Underhill GH, Yousif J, Smith M, et al. (2002) Sialyltransferase specificity in selectin ligand formation. Blood 100: 3618-3636-3625.

54. Smith ML, Olson TS, Ley K (2004) CXCR2- and E-selectin-induced neutrophil arrest during inflammation in vivo. J Exp Med 7: 935-939.

55. Spessotto P, Giacomello E, Perris R (2000) Fluorescence assays to study cell adhesion and migration. Methods in Molecular Biology 139: 321-343.

56. Finger EB, Puri KD, Alon R, Lawrence MB, Von Andrian UH, et al. (1996) Adhesion through L-selectin requires a threshold hydrodynamic shear. Nature 379: 266-269.

57. Cuvelier SL, Patel KD (2004) Studying leukocyte rolling and adhesion in vitro under flow conditions. Basic Cell Culture Protocols. Totowa, NJ: Humana Press Inc. pp. 331-342.

58. Frow EK, Reckless J, Grainger DJ (2004) Tools for anti-inflammatory drug design: In vitro models of leukocyte migration. Med Res Rev 24: 276-298.

59. Hafezi-Moghadam A, Thomas KL, Cornelssen C (2004) A novel mouse-driven ex vivo flow chamber for the study of leukocyte and platelet function. Am J Physiol Cell Physiol 286: C876-C892.

60. Goldman AJ, Cox RG, Brenner H (1967) Slow viscous motion of a sphere parallel to a plane wall. II. Chem Eng Sci 22: 635-660.

61. Zhu C, Bao G, Wang N (2000) Cell mechanics: mechanical response, cell adhesion, and molecular deformation. Annu Rev Biomed Eng 2: 189-226.

62. Yago T, Leppanen A, Qiu H, Marcus WD, Nollert MU, et al. (2002) Distinct molecular and cellular contributions to stabilizing selectin-mediated rolling under flow. J Cell Biol 158: 787-799.

63. Firrell JC, Lipowsky HH (1989) Leukocyte margination and deformation in mesenteric venules of rat. Am J Physiol 256: H1667-1674.

64. Dong C, Cao J, Struble EJ, Lipowsky HH (1999) Mechanics of leukocyte deformation and adhesion to endothelium in shear flow. Ann Biomed Eng 27: 298-312.

65. N'Dri NA, Shyy W, Tran-Son-Tay R (2003) Computational modeling of cell adhesion and movement using a continuum-kinetics approach. Biophys J 85: 2273-2286.

66. Jadhav S, Eggleton CD, Konstantopoulos K (2005) A 3-D computational model predicts that cell deformation affects selectin-mediated leukocyte rolling. Biophys J 88: 96-104.

86

67. Bailey AM, Thorne BC, Peirce SM (2007) Multi-cell agent-based simulation of the microvasculature to study the dynamics of circulating inflammatory cell trafficking. Ann Biomed Eng 35: 916-936.

68. Steels L (1995) In: Steels L, Brooks R, editors. The artifical life route to artificial intelligence. New Jersey: Larence Earlbaum Associates, Inc. pp. 83-121.

69. Czarnecki K, Eisenecker U (2000) Generative programming: methods, tools, and applications. New York: Addison-Wesley. pp. 10, 251-254.

70. Liu Y, Hunt CA (2005) Studies of intestinal drug transport using an in silico epithelio-mimetic device. Biosystems 82: 154-167.

71. Liu Y, Hunt CA (2006) Mechanistic study of the cellular interplay of transport and metabolism. Pharm Res 23: 493-505.

72. Brenner S (1998) Biological computation. In: Bock G, Goode JA, editors. The limits of reductionism in biology. Chichester (United Kingdom): Wiley. pp. 106-116.

73. Noble D (2003) The future: putting Humpty-Dumpty together again. Biochem Soc Trans 31: 156-158.

74. Huo Y, Weber C, Forlow SB, Sperandio M, Thatte J, et al. (2001) The chemokine KC, but not monocyte chemoattractant protein-1 triggers monocyte arrest on early atherosclerotic endothelium. J Clin Invest 108: 1307-1314.

75. Ramachandran V, Williams M, Yago T, Schmidtke DW, McEver RP (2004) Dynamic alterations of membrane tethers stabilize leukocyte rolling on P-selectin. Proc Natl Acad Sci USA 101: 13519-13524.

76. Tozeren A, Ley K (1992) How do selectins mediate leukocyte rolling in venules. Biophys J 63: 700-709.

77. Schmid-Schonbein GW, Usami S, Skalak R, Chien S (1980) The interaction of leukocytes and erythrocytes in capillary and postcapillary vessels. Microvascular Research 19: 45-70.

78. Zhang X, Craig SE, Kirby H, Humphries MJ, Moy VT (2004) Molecular basis for the dynamic strength of the integrin a4b1/VCAM-1 interaction. Biophys J 87: 3470-3478.

79. Zwartz G, Chigaev A, Foutz T, Larson RS, Posner R, et al. (2004) Relationship between molecular and cellular dissociation rates for VLA-4/VCAM-1 interactions in the absence of shear stress. Biophys J 86: 1243-1252.

80. Diamond MS, Springer TA (1993) A subpopulation of Mac-1 (CD11b/CD18) molecules mediates neutrophil adhesion to ICAM-1 and fibrinogen. J Cell Biol 120: 545-556.

81. Norman KE, Katopodis AG, Thoma G, Kolbinger F, Hicks AE, et al. (2000) P-selectin glycoprotein ligand-1 supports rolling on E- and P-selectin in vivo. Blood 96: 3585-3591.

82. Chigaev A, Blenc AM, Braaten JV, Kumaraswamy N, Kepley CL, et al. (2001) Real time analysis of the affinity regulation of alpha 4-integrin. The physiologically activated receptor is intermediate in affinity between resting and Mn(2+) or antibody activation. J Biol Chem 276: 48670-48678.

83. Mehta P, Cummings RD, McEver RP (1998) Affinity and kinetic analysis of P-selectin binding to P-selectin glycoprotein ligand-1. J Biol Chem 273: 32506-32513.

84. Shamri R, Grabovsky V, Gauguet JM, Feigelson S, Manevich E, et al. (2005) Lymphocyte arrest requires instantaneous induction of an extended LFA-1 conformation mediated by endothelium-bound chemokines. Nat Immunol 6: 497-506.

85. Kubes P, Niu XF, Smith CW, Kehrli MEJ, Reinhardt PH, et al. (1995) A novel beta 1-dependent adhesion pathway on neutrophils: a mechanism invoked by dihydrocytochalasin B or endothelial transmigration. FASEB J 9: 1103-1111.

86. Kinashi T (2005) Intracellular Signalling Controlling Integrin Activation in Lymphocytes. Nat Rev Immunol 5: 546-59.

87. Sarantos MR, Raychaudhuri S, Lum AFH, Staunton DE, Simon SI (2005) Leukocyte function-associated antigen 1-mediated adhesion stability is dynamically regulated through affinity and valency during bond formation with intercellular adhesion molecule-1. J Biol Chem 280: 28290-28298.

88. Roca-Cusachs P, Gauthier NC, del Rio A, Sheetz MP (2009) Clustering of a5B1 integrins determines adhesion strength wheras avB3 and talin enable mechanotransduction. PNAS 106: 16245-16250.

89. Norman MU, Hulliger S, Colarusso P, Kubes P (2008) Multichannel fluorescence spinning disk microscopy reveals early endogenous CD4 T cell recruitment in contact sensitivity via complement. J Immunol 180: 510-521.

90. Zarbock A, Ley K (2009) New insights into leukocyte recruitment by intravital microscopy. Curr Top Microbiol Immunol 334: 129-152.

91. McDonald B, McAvoy EF, Lam F, Gill V, de la Motte C, et al. (2008) Interaction of CD44 and hyaluronan is the dominant mechanism for neutrophil sequestration in inflamed liver sinusoids. J Exp Med 205: 915-927.

92. Tang J, Ley KF, Hunt CA (2007) Dynamics of in silico leukocyte rolling, activation, and adhesion. BMC Syst Biol 1:14.

93. Andrews S, Stephens LR, Hawkins PT (2007) PI3K Class IB Pathway in Neutrophils. Sci STKE 2007: cm3.

94. Vodovotz Y, Csete M, Bartels J, Chang S, An G (2008) Translational systems biology of inflammation. PLoS Comput Biol 4: e1000014.

95. Grant MR, Mostov KE, Tlsty TD, Hunt CA (2006) Simulating properties of in vitro epithelial cell morphogenesis. PLoS Comput Biol 2: e129.

96. Kim SH, Debnath J, Mostov KE, Sunwoo P, Hunt CA (2009) A computational approach to resolve cell level contributions to early glandular epithelial cancer progression. BMC Syst Biol 3: 122.

97. Kim SH, Yu W, Mostov KE, Matthay MA, Hunt CA (2009) A computational approach to understand in vitro alveolar morphogenesis. PLoS One 4: e4819.

98. Xiang X, Kennedy R, Madey G (2005) Verification and validation of agent-based scientific simulation models. Agent-Directed Simulation Conference. San Diego, CA. pp. 47-55.

99. Hocde SA, Hyrien O, Waugh RE (2009) Cell adhesion molecule distribution relative to neutrophil surface topography assessed by TIRFM. Biophys J 97: 379-387.

100. Laudanna C, Kim JY, Constantin G, Butcher EC (2002) Rapid leukocyte integrin activation by chemokines. Immunol Rev 186: 37-46.

101. Tohyama Y, Katagiri K, Pardi R, Lu C, Springer TA, et al. (2003) The critical cytoplasmic regions of the alphaL/beta2 integrin in Rap1-induced adhesion and migration. Mol Biol Cell 14: 2570-2582.

102. Shao JY, Hochmuth RM (1999) Mechanical anchoring strength of L-selectin, beta2 integrins, and CD45 to neutrophil cytoskeleton and membrane. Biophys J 77: 587-596.

103. Jun CD, Shimaoka M, Carman CV, Takagi J, Springer TA (2001) Dimerization and the effectiveness of ICAM-1 in mediating LFA-1 dependent adhesion. Proc Natl Acad Sci U S A 98: 6830-6835.

104. Ley K, Zhang H (2008) Dances with leukocytes: how tetraspanin-enriched microdomains assemble to form endothelial adhesive platforms. J Cell Biol 183: 375-376.

105. Frommhold D, Mannigel I, Schymeinsky J, Mocsai A, Poeschl J, et al. (2007) Spleen tyrosine kinase Syk is critical for sustained leukocyte adhesion during inflammation in vivo. BMC Immunol 8: 31.

106. Ding ZM, Babensee JE, Simon SI, Lu H, Perrard JL, et al. (1999) Relative contribution of LFA-1 and Mac-1 to neutrophil adhesion and migration. J Immunol 163: 5029-5038.

107. Shimaoka M, Lu C, Palframan RT, von Andrian UH, McCormack A, et al. (2001) Reversibly locking a protein fold in an active conformation with a disulfide bond: Integrin alphaL I domains with high affinity and antagonist activity in vivo. Proc Natl Acad Sci U S A 98: 6009-6014.

108. Lupher ML, Jr., Harris EA, Beals CR, Sui LM, Liddington RC, et al. (2001) Cellular activation of leukocyte function-associated antigen-1 and its affinity are regulated at the I domain allosteric site. J Immunol 167: 1431-1439.

109. Tominaga YK, Satoh A, Asai S, Kato K, Ishikawa K, et al. (1998) Affinity and kinetic analysis of the molecular interaction of ICAM-1 and leukocyte function-associated antigen-1. J Immunol 4016.

110. Granger DN, Stokes KY (2005) Differential regulation of leukocyte-endothelial cell interactions. In: Aird WC, editor. Boca Raton, FL: Taylor and Francis Group. pp. 229-243.

111. Magnani L (2000) Abduction, reason and science - processes of discovery and explanation. New York, NY: Kluwer Academic/Plenum Publishers.

112. Gabbay DM, Woods J (2005) A Practical Logic of Cognitive Systems, Volume 2: The reach of abduction: insight and trial: Elsevier Science. 496 p.

113. Kuijpers TW, Tool AT, van der Schoot CE, Ginsel LA, Onderwater JJ, et al. (1991) Membrane surface antigen expression on neutrophils: a reappraisal of the use of surface markers for neutrophil activation. Blood 78: 1105-1111.

114. Forsyth KD, Levinsky RJ (1990) Preparative procedures of cooling and re-warming increase leukocyte integrin expression and function on neutrophils. J Immunol Methods 128: 159-163.

115. Glasser L, Fiederlein RL (1990) The effect of various cell separation procedures on assays of neutrophil function. A critical appraisal. Am J Clin Pathol 93: 662-669.

116. Barton S (2005) Cooling the inflammatory response. Nature Rev Drug Discov 4: 811-811.

117. Zhang X, Wojcikiewicz E, Moy VT (2002) Force spectroscopy of the leukocyte function-associated antigen-1/intercellular adhesion molecule-1 interaction. Biophysical Journal 83: 2270-2279.

118. Melder RJ, Munn LL, Yamada S, Ohkubo C, Jain RK (1995) Selectin- and integrin-mediated T-lymphocyte rolling and arrest on TNF-activated endothelium: Augmentation by erythrocytes. Biophys J 69: 2131-2138.

119. King MR, Hammer DA (2001) Multiparticle adhesive dynamics. Interaction between stably rolling cells. Biophys J 81: 799-813.

120. Krasik EF, Hammer DA (2004) A semianalytic model of leukocyte rolling. Biophys J 87: 2919-2930.

121. Alon R, Chen S, Puri KD, Finger EB, Springer TA (1997) The kinetics of L-selectin tethers and the mechanics of selectin-mediated rolling. J Cell Biol 138: 1169-1180.

7 Appendices

A.1 Decisional Processes for LFA1, PSELECTIN, MEMBRANE UNIT, LEUKOCYTE MEMBRANE, and ICAM1

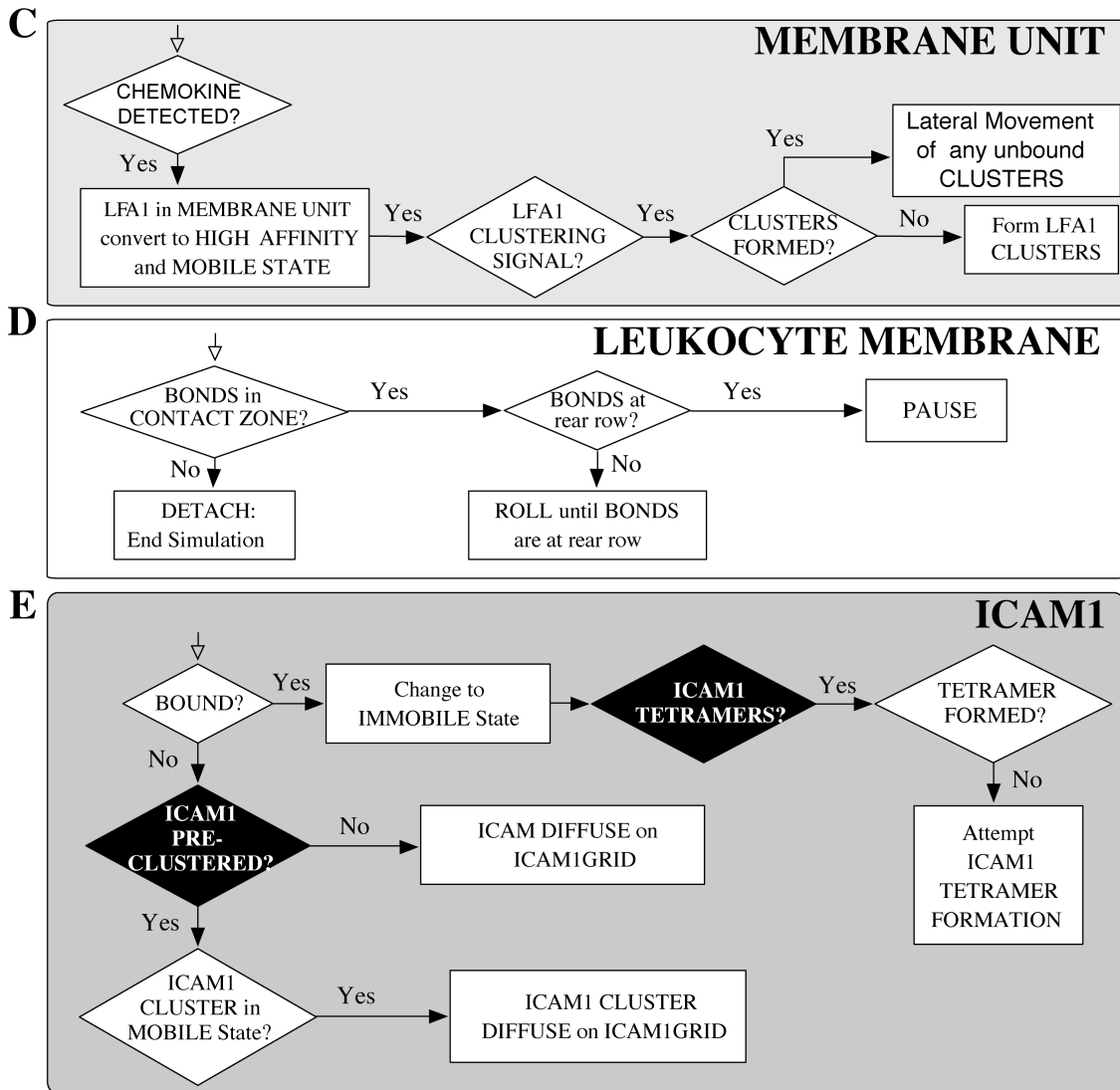Figure A.1 was referred in section 4.2.3.2.
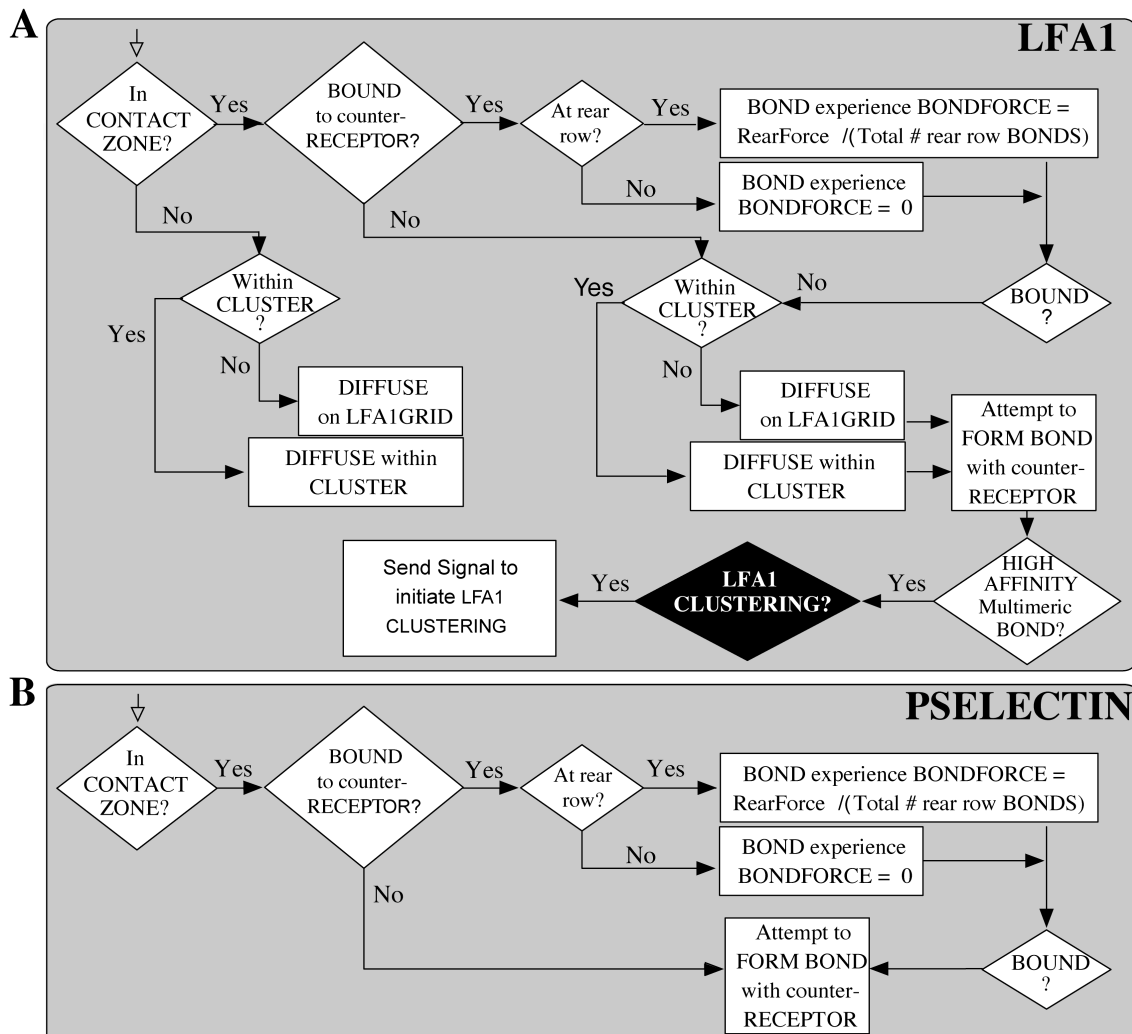
Figure A.1. **Decisional processes for LFA1, PSELECTIN, MEMBRANE UNIT, LEUKOCYTE MEMBRANE, AND ICAM1.** Sketched is the decisional process for the (A) LFA1, (B) PSELECTIN, (C) LEUKOCYTE MEMBRANE UNIT, (D) LEUKOCYTE MEMBRANE, and (E) ICAM1 during a simulation cycle. Black diamonds are Boolean variables that determine which behaviors are allowed during a simulation experiment, allowing us to manipulate them individually, or in combination, and to observe the overall emergent effect on LEUKOCYTES and LEUKOCYTE populations. White arrows indicate the starting point for each agent in their decisional process.

A.2   BOND Formation and Dissociation

BOND formation, dissociation, and Figure A.2 are mentioned in the Section 4.2.3.2.1. The effect of shear on the rear of a leukocyte is represented by the variable *RearForce*. BONDS at the rear experience a *bondforce* that is calculated each simulation cycle by dividing the *RearForce* value by the total number of BONDS in the rear row of the CONTACT ZONE. BONDS within the rest of the CONTACT ZONE experience no *bondforce*. Drawing from in vitro data, we have assumed simple linear relationships between *bondforce* and the probability of BOND dissociation for each of the receptor-ligand pairs in our model (Figure A.2). It is calculated as (probability of dissociation) = b0 + (*bondforce*) x b1, where b1 and b0 are the slope and intercept, respectively, of the line segment associated with a specific *bondforce*. Each type of simulated adhesion molecule pair uses a unique set of b0 and b1 values.

Park et al. calculated PSGL-1/P-selectin dissociation rates as a function of force experienced by the bond by observing PSGL-1 covered microbeads rolling on P-selectin substrate in a parallel plate flow chamber. For the range of dissociation rate constants relevant to this report (*Koff* values < 10/s), the in vitro data, as shown in Figure A.2B, is close to linear (the values in Figure A.2B were calculated from the reported, best-fit values [15]). The unstressed dissociation constant, K^0off, for PSGL-1/P-selectin bonds was calculated to be 1.6/s.

Zhang et al. used atomic force spectroscopy to determine the strength of the LFA-1/ICAM-1 complex [117], and single-molecule dynamic force spectroscopy to investigate the strength of the VLA-4/VCAM-1 complex [78]. The experimental conditions for both studies were not the same as ex vivo or in vivo. Nevertheless, the relative behaviors they observed for LFA-1/ICAM-1 and VLA-4/VCAM-1 complexes are expected to be similar to that in the flow chamber. Measurements revealed two activation barriers in the dissociation of the LFA-1/ICAM-1 complex. The outer barrier is the rate-limiting step in the dissociation of the unstressed complex. The K^0off values for the outer energy barriers for the low- and high-affinity LFA-1/ICAM-1 complexes were 4/s and 0.17/s, respectively. The dissociation of the VLA-4/VCAM-1 complex was also determined to involve overcoming two activation energy barriers. Under pulling forces < ~50 pN, dissociation rates were governed principally by the properties of the outer activation energy barrier. The K^0off values for the outer energy barriers for the low- and high-affinity complexes were 1.4/s and 0.0035/s, respectively. The high affinity LFA-1/ICAM-1, low affinity LFA-1/ICAM-1, and high affinity VLA-4/VCAM-1 data in Figure A.1B were converted from the reported semi-log plots [78, 117]. The force dependence of dissociation rate for low affinity VLA-4/VCAM-1 was not reported. We assumed that it is similar to PSGL-1/P-selectin, and represented it so in Figure A.2A.
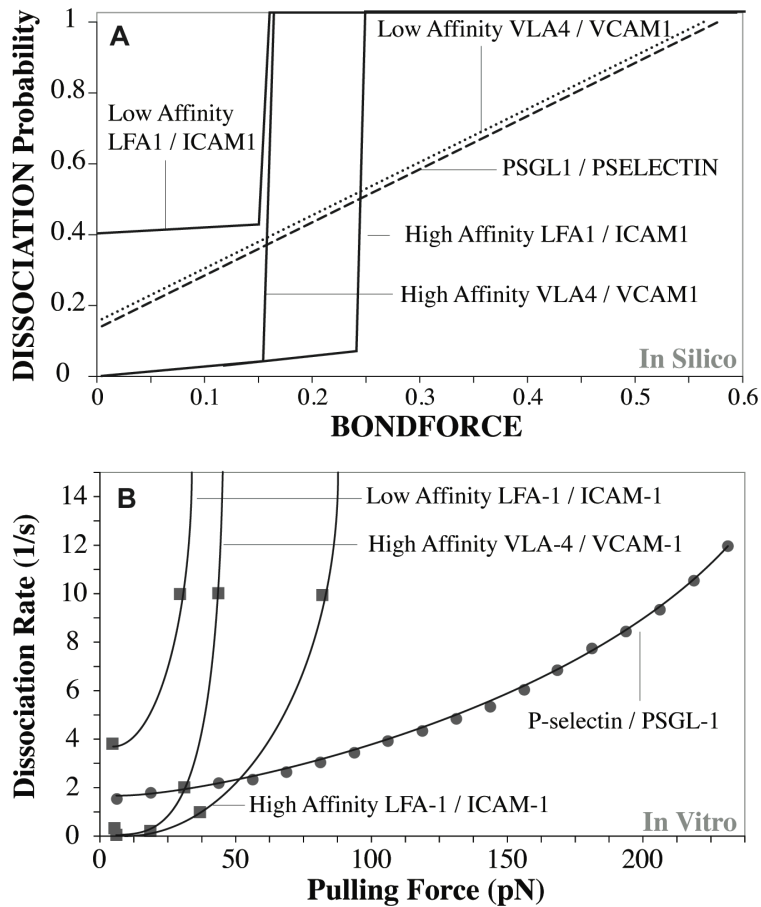
Figure A.2. FORCE dependence on BOND DISSOCIATION probability and force dependence on bond dissociation rates. (A) Shown is the relationship between *bondforce* and probability of BOND DISSOCIATION for each of the four LIGAND pairs included in the ISWBC2. The effects of shear on the ligand-ligand bonds that form at the rear of the leukocyte are simulated using *bondforce*. BONDS within the rear row of the CONTACT ZONE experience a *bondforce* that is calculated by dividing the *RearForce*, a unitless parameter representing the effects of shear, by the total number of BONDS within the rear row. During a simulation cycle, each MEMBRANE UNIT in the rear row uses the current value of *bondforce* and the graphed relationship to calculate a probability that each BOND will be broken during that cycle. All BONDS elsewhere within the CONTACT ZONE experience a *bondforce* value of 0. UNSTRESSED (*bondforce* value of 0) DISSOCIATION probabilities for PSGL1/PSELECTIN, LOW-AFFINITY VLA4/VCAM1, HIGH-AFFINITY VLA4/VCAM1, LOW-AFFINITY LFA1/ICAM1, and HIGH-AFFINITY LFA1/ICAM1 were specified to be 0.14, 0.16, and 0.0035, 0.4, and 0.017 respectively. (B) The in vitro force dependence of dissociation rates for P-selectin/PSGL-1 bonds (as reported in [15]) and the high affinity VLA-4/VCAM-1 bonds (as reported in [78]) are plotted for comparison to the analogue relationships in **A**. The plotted values were taken from the fitted in vitro data: see Methods for details. The relationships in **A** are analogues of these experimentally determined relationships and are not meant to either match or fit that data. The dissociation rates of the PSGL-1/P-selectin bonds as a function of force were determined by experiments using PSGL-1-coated microbeads rolling on a P-selectin substrate in a parallel plate flow chamber [15]. The

dissociation rates for the LFA-1/ICAM-1 complex were calculated from data obtained using atomic force spectroscopy [117]. The dissociation rates for the VLA-4/VCAM-1 complex were calculated from data obtained using single-molecule dynamic force spectroscopy [3]. The force dependence of dissociation rates for low affinity VLA-4/VCAM-1 data was not reported. We assumed that it is similar to PSGL-1/P-selectin relationship in **A**.

A.3   LFA1 Diffusion

LFA1 DIFFUSION and Table A1 are mentioned in the Section 4.2.3.2.1. LFA1 lateral mobility parameters were determined such that they have similar relative diffusive properties as observed in vitro. At each time step, each LFA1 object is allowed to randomly move to any of the 6 neighboring hexagonal grid sections on the LFA1GRID, for a specific number of times determined by the parameter *LFA1MoveNum*.   We explored several parameter values for *LFA1MoveNum* and calculated the diffusion coefficients using Eq 1. $<r^2>$ is the MSD, t is the time interval, D is the time-dependent diffusion coefficient, and the α coefficient classifies the mode of anomalous diffusion.

$$< r^2> = 4Dt^\alpha \qquad \text{[Eq. 1]}$$

Cairo et al. used single-particle tracking to determine the diffusion coefficients of LFA-1 on peripheral blood lymphocytes prior to and after activation with phorbol-12-myristate-13-acetate [21].   They observed in all cells before and after activation the existence of two subpopulations of LFA-1, immobile and mobile, distinguished by their diffusive properties. Diffusion coefficients have not been determined for neutrophils. We assumed neutrophil LFA-1 had similar diffusive properties. We first sought *LFA1MoveNum* parameter values that would allow our LFA1 objects to exhibit similar diffusive properties as those in the mobile and immobile subpopulations. In their calculations of diffusion coefficients, Cairo et al. observed values of α that were consistent with Brownian diffusion ($0.7 < \alpha < 1.2$), and therefore we calculated D values using a α value of 1. We determined that a *LFA1MoveNum* of 10 gave similar diffusive properties to those of the immobile subpopulation, while a *LFA1MoveNum* of 120 yielded similar diffusive properties to the mobile subpopulation (Table A.1).

	In Vitro		In Silico	
	Diffusion Coefficient (Untreated) [10^{-10} cm^{2}s^{-1}]	**Diffusion Coefficient (PMA Treated) [10^{-10} cm^{2}s^{-1}]**	*LFA1MoveNum*	**Diffusion Coefficient (maps to) [10^{-10} cm^{2}s^{-1}]**
Immobile LFA-1	0.14 ± 0.73	0.11 ± 0.71	10	0.19 ± 0.05
Mobile LFA-1	3.8 ± 1.9	1.3 ± 1.0	120	2.1 ± 0.3

Table A.1. Comparison of In Vitro and In Silico Diffusion Coefficients of Immobile and Mobile LFA-1

A.4   Effect of varying *ICAM1Density* and *LFA1GridDensity* on LEUKOCYTE ADHESION

This section and Figure A.3 are mentioned in section 4.3.2.1. We repeated the experiments aimed at identifying the effect of *ICAM1Density* on LEUKOCYTE ADHESION, but changed the *LFA1GridDensity* parameter value (the fraction of all MEMBRANE UNITS that contain LFA1GRIDS) from 0.2 to 0.1. When *LFA1GridDensity* was decreased to 0.1 (Figure A.3A), the *ICAM1Density* below which the influence of CLUSTERING became significant shifted from 50 to 70. The magnitude of the clustering effect increased at lower *ICAM1Density* values. On the other hand, when *LFA1GridDensity* was increased, for example from 0.2 to 0.4 (Figure A.3B), the *ICAM1Density* below which the influence of CLUSTERING became significant shifted from 50 to 30. That trend continued at larger *LFAGridDensity* values. However, in both cases, cooperative binding effects were still observed.
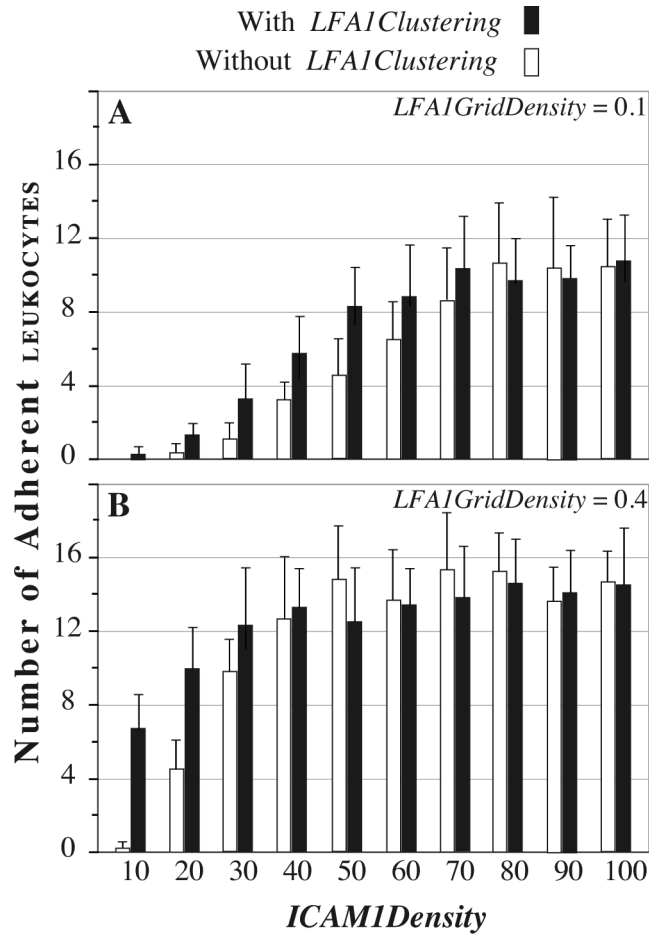
Figure A.3. Effect of varying *ICAM1Density* and *LFA1GridDensity* parameter values on LEUKOCYTE ADHESION. The effect of Leukocyte *ICAM1Density* was varied from 10 to 100 at intervals of 10. LFA1GridDensity was set to (A) 0.1 or (B) 0.4. Bar heights are ISWBC2 means ± 1 SD (20 populations containing 30 leukocytes each) for the same condition using the parameter values in Tables 4 and 5. Black bars indicate simulation experiments when *LFA1Clustering* = true. White bars indicate simulation experiments when *LFA1Clustering* = false. Cooperative binding effects were observed both at *LFA1GridDensity* values of (A) 0.1 and (B) 0.4, but at different ranges of ICAM1Density values and with differing magnitudes.

A.5 Appraisal of Model Specifications

This section was cited in section 4.4.2. Following the parsimony guideline, we strove to assemble a system of interacting components that would, at the margin, be complicated enough to exhibit multiple, different targeted attributes under different experimental conditions, but not so complicated that a component could be eliminated without significantly degrading behavioral similarities for the full set of targeted attributes. Some ISWBC2 components map to a conflated set of leukocyte features. Some leukocyte features have no ISWBC2 counterparts. The latter does not mean that those features were ignored or assumed unimportant. At each stage of iterative refinement, a goal was to determine the degree of biomimicry (level of biological emulation) that could be accomplished with a few components before concluding that others may be needed.

Both wet-lab experimental systems used whole blood containing red blood cells in addition to leukocytes. It is well known that smaller red blood cells can enhance leukocyte-substratum interactions by pushing the larger leukocytes from the axial flow to the vessel wall [63, 77, 118]. We do not discount the significance of such interactions under some conditions, however we chose specifically to focus on the interactions between an already attached leukocyte and its surface. At the beginning of each simulation, LEUKOCYTES were placed on the surface where interactions were allowed to form (or not). We posited that red blood cell—leukocyte interactions were similar in WT and KO mice, contributing equally to differences in wet-lab results, and so could be ignored.

The flow chamber system was perfused by murine blood. The dynamics of leukocyte rolling and adhesion may have been influenced by the pulsatile blood flow. A rheological evaluation of the autoperfused flow chamber system was undertaken and reported stable flow conditions and tolerable changes in blood-flow velocity and wall shear stress. Flow through the chamber was essentially laminar and quasi-steady, as reflected by a Reynolds number less than three and a Womersley number of 0.5 [30]. In vivo, wall shear stress varies along the venular tree as vessel diameter and flow rate change. We started by specifying a constant SHEAR STRESS (REARFORCE) at all locations and times within in silico experiments. Our protocol called for retaining that parsimonious specification until falsification of a particular ISWBC2 required adopting a more fine-grained specification, which it did not. Varying REARFORCE can be implemented, as done earlier [92], when that is needed. Adhering to the parsimony guideline within the iterative refinement protocol has proven an effective tool in preventing ISWBC2s from becoming unnecessarily complicated.

With their Adhesive Dynamics (AD) model of leukocyte rolling and adhesion, King and Hammer demonstrated that only bonds at the trailing edge of the contact zone were under stress and that increases in instantaneous velocity correlated with breakage of trailing edge bonds [119]. They state that it is reasonable to simplify the force and torque balances such that only bonds at the trailing edge of the contact zone experience force [120]. Therefore, we have implemented the model specification that only bonds at the rear of the leukocyte experiences force, and that this is shared equally among all bonds at the rear.

Our approach has been focused on simulating a targeted set of system-level properties. It was not our intention to discover ISWBC parameterizations that would yield simulation results that tightly fit specific sets of experimental data. Therefore, we did not, for example, attempt an explicit mapping between the shear force and the amount of force experienced by bonds at the rear of the leukocyte. Leukocytes are notoriously deformable and therefore we elected to avoid a

mapping such as the Goldman equation [60], which has been used in the AD models to calculate the amount of force a sphere experiences from an applied shear force by assuming that the sphere is solid. In addition, the mapping from the force on the cell to the force on the rear bonds can be quite complex as PSGL-1 and VLA-4 are both ligands that are concentrated at the tips of stretchy and heterogeneous microvilli. It should be noted that an estimate of 124.4 ± 26.1 pN per dyn/cm^2 wall shear stress for selectin tethers at the rear of neutrophils has been calculated previously using the Goldman equation [121].

To account for the effect of an applied force on the kinetics of bond dissociation in their AD simulations, Hammer and co-workers employed both the Bell model and Dembo Hookean Spring model (see [61]). The Bell Model predicts the bond dissociation rate as a function of applied force, whereas the Dembo model treats bonds as Hookean springs and relates bond dissociation rate to the length of the stretched bond. Use of a similar fine-grained representation of bond dissociation may have yielded more precise simulation results, but that level of resolution and precision was not needed to meet the simulation objectives in Table 4.1. We used a simple model to relate the probability of bond dissociation with bond force (Figure A.2A); it was motivated by in vitro experiments by Park et al. [15], and Zhang et al. [78, 117]. We previously determined that this implementation was sufficient [92].

Many molecular level details are believed to impact effective bond formation and breakage within small portions of a leukocyte membrane and the corresponding portion of the surface. Examples include contact irregularities, local dynamics and ligand relocation within the membrane, force history of bond loading, and bond compliance. All of these factors are aggregated and controlled in the ISWBC by an event probability. When explanation of system level behaviors requires a more detailed representation, one or more of these factors can be specifically represented, without compromising the function of other ISWBC components. The probability parameters will remain, but their values and explanation will have changed.

There are many adhesion molecules present on the endothelial surface with varying site densities. Additionally, there is an endothelial surface layer. Studies have shown that the endothelial surface layer may slow plasma flow and may limit the exposure of adhesion molecules [30]. We specified two classes of ENDOTHELIAL ADHESION objects. One maps to P-selectin and any other molecules that behave similarly under the referent wet-lab conditions. The other maps to ICAM-1 and any similarly behaving molecules. We also specified two classes of LEUKOCYTE ADHESION objects. One maps to PSGL-1 and any other molecules that behave similarly under the referent wet-lab conditions. The other maps to LFA-1 and any similarly behaving molecules. We specified one class of CHEMOKINE RECEPTOR objects. It maps to CXCR2 and any other chemokine receptors behaving similarly under the referent wet-lab conditions.

We started by specifying simply that LEUKOCYTES would interact with a layer of randomly distributed RECEPTOR and CHEMOKINE objects. The nature of the actual surface to which those objects are attached was not specified. The RECEPTOR and CHEMOKINE objects map to reactive counterparts that are sufficiently exposed to react. We did not encounter non-matching simulation results that would have triggered revising that specification. Consequently, ISWBC2 systems map equally well to those having engineered and endothelial surfaces.

CXCL1 is not a proinflammatory chemokine. We can therefore posit that ISWBC2 system surfaces map to inactive endothelial cells having a basal expression of adhesion molecules [28]. Again, when it is needed, it is straightforward to add objects that map to endothelial surface features without having to reengineer other features of the ISWB2 system.

100